Swansea University
Prifysgol Abertawe

Understanding the sanitising efficacy of a new, environmentally friendly hot tub water treatment product, eco3spa

A thesis submitted to Swansea University College of Engineering in fulfilment of the requirements for the degree of Master of Science by Research in Materials Engineering

By Michael Si-Hom Chau, BSc

April 2023

II. Abstract

Infrequent cleaning increases the risk of biofilms being formed on hot tub surfaces and pipes by *Escherichia coli* and *Pseudomonas aeruginosa*. This is aided by inappropriate use of biofilm control agents which promote antimicrobial resistance. This presents a challenge for water sanitation using biofilm prevention and removal products.

This study analysed the efficacy of an environmentally friendly 3-step biofilm prevention and removal product designed for hot tubs called eco3spa. Eco3spa contains Active Oxygen and a water conditioner which was assessed for growth and biofilm prevention properties. Eco3spa biofilm remover was tested in combination with Active Oxygen for biofilm removal properties.

E. coli K12 and *P. aeruginosa* PA01 cultures were grown and biofilms formed under static conditions at 37^{o}C, normal operating temperature and maintenance temperatures of 25^{o}C. Various product concentrations were tested for growth and biofilm prevention from pH 5.2-8. Pre-formed biofilms were treated with biofilm removal products before subjection to dynamic forces to mimic the flushing of water and function of jets in hot tubs.

Results revealed that recommended concentrations of Active Oxygen prevent growth and biofilm formation of *E. coli* and *P. aeruginosa* without losing efficacy from pH 5.2 to 8. Addition of the water conditioner does not enhance Active Oxygen activity in preventing growth and biofilm formation. Furthermore, Active Oxygen kills *E. coli* within 5 minutes and chemical stability is maintained for at least 7 days. Light and fluorescent microscopy illustrated that Active Oxygen in combination with the water conditioner may lead to viable but non-culturable cells.

This study demonstrates the sanitising efficacy of eco3spa in hot tub environments where efficacy of Active Oxygen is maintained over a defined pH range. Therefore, the industrial sponsor has been provided with more insights into the sanitising efficacy of eco3spa which promotes a water treatment product with benefits over chlorine.

III. Declaration

This work has not previously been accepted in substance for any degree and is not being concurrently submitted in candidature for any degree.

Signed 

Date: 13/04/23

This thesis is the result of my own investigations, except where otherwise stated. Other sources are acknowledged by footnotes giving explicit references. A bibliography is appended.

Signed 

Date: 13/04/23

I hereby give consent for my thesis, if accepted, to be available for photocopying and for inter-library loan, and for the title and summary to be made available to outside organisations.

Signed 

Date: 13/04/23

The University's ethical procedures have been followed and, where appropriate, that ethical approval has been granted.

Signed 

Date: 13/04/23

IV. Table of Contents

Chapter 2: Materials and Methods

Chapter 3: Optimisation, calibration and benchmarking

Chapter 4: Efficacy of Active Oxygen, water conditioner and product combinations on growth and biofilm prevention under static conditions including effects on cell viability and cell morphology

Chapter 5: Dynamic biofilm removal using Active Oxygen, biofilm remover and Eco3spa product combinations

Chapter 6: Analytical assessment of components in Product 2 (Water conditioner), Product 3 (Active Oxygen tablets) and chlorine granules

Chapter 7: General Discussion and Conclusions

V. Acknowledgements

I would like to thank Dr Geertje van Keulen, Professor Chedly Tizaoui and Dr Christopher Phillips for all their guidance and supervision during this project. Furthermore, I would like to personally thank Craig Allan, Joe Coombes and colleagues working on floor 5 in ILS1, Joe Bater-Davies and Benjamin Harrison for their help in Bay Campus including the staff at M2A for their assistance throughout the project.

Also, I would like to thank my family for their love and support during the pandemic.

Engineering and Physical Sciences Research Council

VI. List of Figures

Chapter 1: Introduction

Chapter 2: Materials and Methods

Chapter 3: Optimisation, calibration and benchmarking

Chapter 4: Static biofilm prevention assays using active oxygen, water conditioner and product combinations including effect of Active Oxygen on cell viability and cell morphology

VII. List of Tables

VIII. List of abbreviations

Abbreviation	Definition
AMR	antimicrobial resistance
ATR	acid-tolerance response
BAC	benzalkonium chloride
BCA	Bicinchoninic acid
BSA	bovine serum albumin
CA	colanic acid
CAT	catalase
c-di-GMP	cyclic diguanosine monophosphate
CFU	colony forming units
DBP	disinfection by-product
DPD	N,N-diethyl-p-phenylenediamine
eDNA	extracellular DNA
EPS	extracellular polymeric substances
FAC	free available chlorine
HOBr	hypobromous acid
HOCl	hypochlorous acid
IC	ion chromatography
IEC	ion-exchange chromatography
KMPS	pentapotassium peroxymonosulphate
LB	Luria-Bertani
MRSA	methicillin-resistant *Staphylococcus aureus*
NaDCC	sodium dichloroisocyanurate
OCl	hypochlorite ion
OD	optical density
PBS	Phosphate buffered saline
PDS	peroxydisulfate
PMS	peroxymonosulphate
QS	quorum sensing
SDS	Sodium dodecyl sulphate
SEM	Standard error of the mean
SOD	Superoxide dismutase
SOP	standard operating procedure
TCA	Trichloroacetic acid
THM	Trihalomethane
VBNC	viable but non-culturable
WTA	wall teichoic acids

Chapter 1: Introduction

1.1 Hot tubs and infections associated with regular hot tub use

During the outbreak of COVID-19 and the enforcement of lockdown restrictions, figures have shown a sharp increase in hot tub sales by 1080% (Gausden, 2020) with online searches for hot tubs rising by 57% (van Gelder, 2020). It is estimated that approximately 100,000 hot tubs are in current use in the UK alone with Britain itself ranking in the top 10 of the hot tub world market (BISHTA, 2015). However, frequent cleaning regimes are an essential part of sanitising hot tub water, which, if not adhered to on a regular basis leads to the presence of bacterial biofilms causing water to adopt changes in colour as well as further growth of biofilms attached to pipes and corrosion (Camper, 2014; Hambsch et al., 2014; van der Kooij et al., 2003). Recreational waters including spas, hot tubs and pools are known to be associated with fecal water contamination due to irregular water sanitation and management (Cosgrove and Loucks, 2015). A diverse range of microorganisms have been found in these environments such as *Escherichia coli*, *Legionella* spp, *Cryptosporidium* spp., *Giardia* spp, *Shigella* spp., *Vibrio cholerae*, *Salmonella* spp., *Campylobacter jejuni* and *Pseudomonas aeruginosa* which are commonly linked with infections (Leoni et al., 2018; Lugo et al., 2021; Tirodimos et al., 2018). Other sources of contamination include faeces from individuals, animals e.g. pet dogs and wild birds and bodily secretions such as vomit, mucus and saliva (Thorolfsdottir and Marteinsson, 2013). Hot tubs pose a potential health risk because they can be a breeding ground for bacteria which can cause infections. In particular, elderly individuals that have damaged immune systems and suffer from anatomical and functional defects are more susceptible to infections (Beeson, 1985; Schneider, 1983; Yoshikawa, Norman and Grahn, 1985).

Escherichia coli is a gram negative and rod-shaped bacterium linked with urinary tract infections, sepsis and food poisoning. Previous research has identified 54% of *E. coli* strains in recreational waters which have originated from a human source (Meyer et al., 2005). Recent data has shown 19 pathogenic outbreaks of *E. coli* and high prevalence of Shiga-toxin producing *E. coli* in specific regions of the United States where four strains were discovered to be closely linked through whole genome sequencing (Vanden Esschert et al., 2020; Graciaa et al., 2018). Butler et al (2021) discovered that high levels of *E. coli* found in recreational waters was correlated with the detection of *Salmonella* and *Cryptosporidium*. This led to the conclusion that *E. coli* is a good indicator of contamination and pathogen load. *E. coli* may also confer resistance to antibiotics such as β-lactams by having genes that code for enzymes that inactivate antibiotics from exhibiting their function (Poirel et al., 2018). Tocut et al (2022) investigated mortalities in sepsis patients in response to cephalosporins, a class of β-lactam antibiotic. Results revealed that altogether, 97 out of 118 patients with sepsis caused by *E. coli* resistant to cephalosporins died within 1 year. This emphasises the need for routine inspection of water for microorganisms that can cause infections and be fatal if not maintained regularly.

Pseudomonas aeruginosa is a gram-negative bacterium found in water and soil which is commonly associated with lung infections in cystic fibrosis patients as well as bloodstream, respiratory and urinary tract infections (Bhagirath et al., 2016; CDC, 2012; Newman et al., 2022; Zhao et al., 2020). There has also been a marked increase in the prevalence of skin infections caused by *P. aeruginosa* such as hot tub folliculitis, a skin infection that occurs around the lower parts of hair follicles. Previously, water samples taken from a hot tub party have been identified to contain *P. aeruginosa* with genetic analysis showing a banding pattern similarity index of 98.9% between patient and hot tub isolates (Yu et al., 2007). Swabbed samples from a male patient using a hot tub led to the growth of *P. aeruginosa* and further physical examination led to the diagnosis of hot tub folliculitis. It was later discovered that the hot tub was not cleaned thoroughly leading to residual water being contained within the systems of the hot tub (Osborne et al., 2021). Other cases of *P. aeruginosa* have been reported in hot tubs after microbiological analysis. One study investigated samples using pulsed-field gel electrophoresis and found identical bands between *P. aeruginosa* strains found in the patient's sputum and hot tub filter (Crnich, Gordon and Andes, 2003). Huhulescu et al (2011) analysed water samples taken from a hot tub and detected 37,000 colony-forming units of *P. aeruginosa*/100 ml. This suggested a high degree of biofilm formation in the bath circulation and lack of hygienic maintenance. In addition to the problems created by irregular sanitation, the rise in multidrug-resistant strains of *P. aeruginosa* are responsible for 32,600 infections documented in the United States with 2,700 mortalities highlighting the significance of sanitation procedures (CDC, 2019).

1.2 Biofilm formation

The process of biofilm formation consists of five stages: primary adhesion, secondary/irreversible adhesion, proliferation, maturation and dispersion of cells from the biofilm. Figure 1.1 shows a schematic of the biofilm formation process.

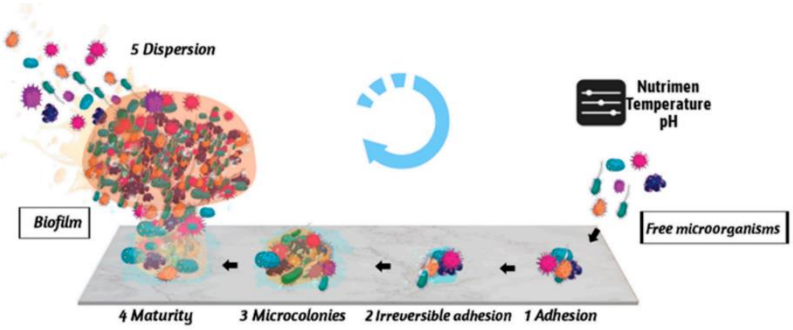

Figure 1.1. Stages of biofilm formation (Zhou et al., 2022).

1.2.1 Conditioning films

Prior to biofilm formation, conditioning films are a structure by which adsorption of macromolecules influences the physicochemical properties of a surface (Lorite et al., 2011). Conditioning films are known to contain polysaccharides, proteins, lipids, humic acids, nucleic acids and aromatic amino acids which facilitate the attachment of bacteria to a surface (Bakker et al., 2004). Analysis of organic carbon, nitrogen and amino acid content shows that conditioning films are primarily composed of degraded organic matter which provides a source of nutrients which bacteria can feed on to encourage attachment in the initial stages of biofilm formation (Bhosle et al., 2005).

1.2.2 Primary adhesion

Initial attachment of cells to a particular surface can be abiotic (e.g. plastic, glass and metal implants) as well as biotic (e.g. human skin). A range of environmental factors such as temperature, pH, repulsive electrostatic and hydrodynamic forces in a liquid medium can impede biofilms from forming (Liu, Zhang and Ji, 2020). However, bacteria such as *E. coli* possess peritrichous flagella which enables them to surpass these barriers acting as a foundation in which it provides motility and frequent interactions between the bacterium and the surface (Pratt and Kolter, 1998). This is the first time where cell-to-surface contact occurs resulting in adhesion to the surface (Sharma et al., 2016). Additionally, chemotaxis which involves directional movement in response to concentration gradients drives the biofilm formation process. Previous research illustrates that *P. aeruginosa* PA01 biofilms grown in glucose minimal medium can be produced by mechanisms involving non-motile and motile bacterial populations. The proposed method of biofilm formation by motile bacteria is attributed to their build-up on the top of caps by climbing mushroom stalks which is facilitated by the action of pili (Klausen et al., 2003). Chemotaxis mutants of *P. aeruginosa* PA01 are unable to form the typical mushroom-like structures conveying links between biofilm formation, chemotaxis and motility (Sheraton et al, 2018). The ability of *E. coli* mixed-species populations to form biofilms suggests that there are similar profiles of biofilm formation between motile and non-motile cells which is based on the actions of flagellar motility (Benyoussef et al., 2022).

1.2.3 Secondary adhesion

Following primary adhesion, bacteria enter secondary adhesion where synthesis of the flagella is inhibited by signalling molecules such as cyclic diguanosine monophosphate (c-di-GMP) which increases in concentration during the biofilm formation process. Biofilm quantitation assessed by crystal violet assays displays significantly higher levels of biofilm in *P. aeruginosa* PA01 strains in comparison to strains deficient in c-di-GMP (Zhang et al., 2020). These results support data obtained by Cole and Lee (2016) where PA14 strains mutated to confer overexpression of diguanylate cyclases

revealed colony counts similar to control strains. It is now known that type 1 fimbriae and curli fimbriae are the organelles responsible for irreversible attachment of *E. coli* (Prüß et al., 2006). Type 1 fimbriae encoded by the *fim* gene participates in reversible and irreversible attachment while curli fimbriae encoded by *csg* genes play an important role in attachment to surfaces by facilitating cell-to-surface interactions as well as cell-to-cell communication (Carter et al., 2016).

1.2.4 Maturation

During the maturation phase, cells adapt a formation where they accumulate through cell-to-cell interactions and begin to construct the extracellular matrix which gives the biofilm its three-dimensional structure (Flemming and Wingender, 2010). The key elements which are essential for biofilm maturation are autotransporters and extracellular polymeric substances (EPS).

Autotransporter proteins are able to translocate themselves to the outer membrane without the requirement for accessory proteins. Antigen 43 is a well-known autotransporter protein encoded by the *flu* gene which contributes to the aggregation process and three-dimensional structure of the biofilm. Biofilm assays conducted by Taghadosi et al (2017) show that antigen 43 plays a role in *E. coli* biofilm formation. In addition, transporter proteins such as AidA and TibA have been identified in some strains of *E. coli* which participate in the aggregation process (Klemm et al., 2006).

The EPS is a gel-like matrix which enhances cell-to-cell and cell-to-surface interactions creating a support medium which aids in the three-dimensional structure of the biofilm. Water comprises a large proportion of the EPS but other components include proteins, nucleic acids, lipids and extrapolymeric compounds (Flemming and Wingender, 2010). Previous work carried out by Dogsa et al (2005) isolated EPS by trichloroacetic acid/ethanol extraction techniques and investigated components of the EPS using chromatography methods. Analysis of EPS structure found that it contained the monosaccharides glucose and galactose and that the influence of pH caused alterations in the EPS structure.

Bacteria also carry out a chemical signalling system called quorum sensing (QS), which results in the release of signalling molecules known as autoinducers. Autoinducers facilitate cell-to-cell communication and regulate gene expression during the biofilm formation process (Waters and Bassler, 2005). The presence of high concentrations of autoinducer leads to interactions with other proteins which in turn can influence gene, motility and fimbriae expression (Sturbelle et al., 2015).

1.2.5 Dispersal

In the final stage of biofilm formation, bacteria detach from the biofilm and revert to a planktonic phase from which the process can repeat again. Single amino acid changes from glutamate to

glutamine at position 50 in the protein BdcA isolated from *E. coli* enhances biofilm dispersal of *P. aeruginosa* through binding of c-di-GMP leading to increased motility and lower rates of extracellular polysaccharide production (Ma et al., 2011; Ma et al., 2011). Certain stimuli can encourage the detachment of bacteria from the mature biofilm such as enzymatic degradation and as a direct consequence of QS signalling pathways because of fluctuations in nutrition content and oxygen depletion (Sawyer and Hermanowicz, 1998).

1.3 Structural components of biofilms

The composition of biofilm matrices comprises of three typical structures: exopolysaccharides, extracellular proteins and extracellular DNA (eDNA).

1.3.1 Exopolysaccharides

Biofilms formed by opportunistic pathogens such as *P. aeruginosa* have been discovered to contain three polysaccharides that have been well characterised: alginate, Psl and Pel. Previous research shows that through creating mutant constructs deficient in these polysaccharides, alginate has a functional role in the viability of cells in biofilms and is dependent on the presence of Psl and Pel as constructs which only produce alginate were unable to form biofilms (Ghafoor et al., 2011). Additionally, *E. coli* biofilms contain the exopolysaccharides cellulose, β-1,6-N-acetyl-D-glucosamine polymer and colanic acid (CA). CA has previously been shown to have an essential role in formation of the three-dimensional structure of biofilms through transposon mutagenesis experiments disrupting the *wcaF* gene needed to produce colonic acid (Stevenson et al., 1996). By comparing CA positive and negative strains grown in Luria-Bertani broth in polyvinylchloride wells, macroscopic analysis illustrated clear differences in the appearance of biofilms through a 45-hour period between the wild type and CA defective strain. These results confirm that colonic acid production contributes to biofilm formation and when absent affects surface attachment (Danese et al., 2000).

1.3.2 Extracellular proteins

In vitro models demonstrate that curli in *E. coli* can interfere with the classical complement pathway in the immune system by binding to proteins and inhibiting their functions (Biesecker et al., 2018). Additionally, extracellular proteins such as aminopeptidase in *P. aeruginosa* PA01 is known to contribute significantly to biofilm architecture. Deletion of aminopeptidases leads to increased cell death which is consistent with biofilm dispersal through degradative activity of the exopolysaccharide matrix by glycosyl hydrolases released from dead bacteria into the biofilm matrix environment (Yu et al., 2015; Zhao et al., 2018).

1.3.3 eDNA

Many studies have indicated that eDNA is an essential component required for biofilm formation. Whitchurch et al (2002) employed a flow chamber system where fluorescently tagged *P. aeruginosa* was added in combination with minimal media with or without the addition of DNase I. After 3 days, channels without DNAase I were covered with high levels of bacteria whereas only a small amount was observed with the presence of DNase I. Confocal microscopy results indicated that when medium was changed to that containing DNase I at 12, 36 and 60 hours, *P. aeruginosa* biofilms were dissolved. These results confirm that eDNA is required for biofilm formation. Qin et al (2007) showed that *the atlE* gene which codes for an autolysin AtlE in *Staphylococcus epidermis* is responsible for producing a large proportion of eDNA which promotes biofilm formation. Furthermore, studies have demonstrated that eDNA generation requires acylhomoserine lactone and *Pseudomonas* quinolone signalling, flagella and type IV pili (Allesen-Holm et al., 2006). There is also evidence that eDNA generation during biofilm formation cross-links single cells present in microcolonies contributing to mechanical stability (Lappann et al, 2010; Schlafer et al., 2017).

1.4 Role of horizontal gene transfer in biofilm formation

Horizontal gene transfer is the exchange of genetic material which has been linked to biofilm formation in bacteria. Generally, the rate of horizontal gene transfer is increased in biofilms in comparison to planktonic cells (Madsen et al., 2012). Previous data supports this concept by indicating that high rates of conjugation between *E. coli* are observed in biofilms (Hausner and Wuertz, 1999). Results obtained by May et al (2010) indicate that the transfer of plasmids during conjugation of pili in *E. coli* K12 act as a mechanism of cell-to-cell interaction. Following conjugation, it is suggested that pili are replaced by adhesion factors which aid in preserving biofilm integrity.

1.5 Effect of shear stress on biofilm formation in dynamic and static environments

Hydrodynamic forces generated by pumps and water jets in hot tubs produce dynamic environments which assist in biofilm formation. Biofilm viability is significantly reduced in static compared to dynamic environments at 37^{o}C as observed by Santos et al (2019). Other studies demonstrate that *E. coli* K12 strains subjected to shear stress encourage colonisation and contain less flagella providing a foundation for which more cells can adhere to the surface (Thomen et al., 2017; Wang and Li, 2022). This is supported by epifluorescence results obtained by Saur et al (2017) where increases in shear stress from 0.09 Pa to 7.3 Pa encourage a higher degree of bacterial attachment with cells aggregating as clusters.

1.6 Role of phenazines in biofilm formation

There are several Gram-positive and Gram-negative strains of bacteria including *P. aeruginosa* which can produce nitrogen-containing compounds called phenazines. Phenazines are redox-active molecules that participate in electron transport through redox-active reactions which are commonly known to influence gene expression, increase biofilm formation and promote bacterial survival (Pierson and Pierson, 2010). The most widely studied phenazines in *Pseudomonas* spp. are pyocyanin, pyoverdine and phenazine-1-carboxylic acid. Confocal laser scanning microscopy of *P. aeruginosa* PA01 strains mutated in genes that code for production of phenazines demonstrate that biofilm structure is drastically affected and is highly dependent on autoinducer and QS molecules such as acyl-homoserine lactones (Díaz-Pérez et al., 2022).

1.7 Biocide tolerance in gram negative bacteria

Biocides are classed as chemical substances which kill or control the growth of microorganisms (Unamuno, van de Plassche and van der Wal, 2022). Examples of biocides include the use of disinfectants for water disinfection (refer to section 1.11). The use of biocides in water disinfection has shown increasing concern due to the development of biocide tolerance mechanisms in bacteria. This allows bacteria to grow and proliferate contributing further to the spread of antimicrobial resistance (AMR) with a higher chance of infection. The number of AMR-related deaths is expected to rise exponentially from 700,000 to 10 million by 2050 which surpasses the number of deaths due to cancer (O'Neill, 2016). This highlights the importance of relevant studies to elucidate these mechanisms and understand how bacteria are able to survive in the presence of biocides.

Repeated exposure with chloramines which are produced in swimming pools when chlorine reacts with ammonia results is linked with increased tolerance in *E. coli* (Daer et al., 2022). Wastewater effluents treated with chlorine at a concentration of 0.5 mg/L show low efficacy in the inactivation of *E. coli* demonstrating high levels of tolerance (Owoseni, Olaniran and Okoh, 2017). In addition, tetracycline-resistant *E. coli* shows higher tolerance to chlorination as the hemi-inhibitory concentration which is a measure of survival in the bacterial population increased compared to ultraviolet disinfection (Huang et al., 2013). Montagnin et al (2022) tested different disinfectants against *E. coli* and *P. aeruginosa* to validate the recommended concentrations documented by the UK Department for Environment, Food and Rural Affairs' disinfectant-approval scheme. Differences between bacterial strains were observed where *P. aeruginosa* was more tolerant to chlorine containing disinfectants. Therefore, it is necessary to assess the effectiveness of biocides against different bacterial strains. Common mechanisms responsible for biocide tolerance include changes in gene

expression, horizontal gene transfer and alterations in the structure of the cell membrane (Chen et al., 2021).

1.7.1 Changes in gene expression and horizontal gene transfer

Gram negative bacteria exhibit higher tolerance to biocides due to the presence of an outer membrane rich in lipopolysaccharide material which lowers membrane permeability (Slipski, Zhanel and Bay, 2018). Efflux pump genes such as *cepA*, *qacEΔ1* and *qacE* have been found to be associated with reduced susceptibility to biocides containing quaternary ammonium compounds, dimethanol and isopropanol alcohol in multidrug resistant strains of *P. aeruginosa* (Goodarzi et al., 2021). Amsalu et al (2020) showed that there is a link between biocide use and AMR in benzalkonium chloride (BAC) tolerant strains of *P. aeruginosa* resulting in higher levels of the MexAB-OprM efflux pump due to mutations in the amino acid residues of regulators MexR, NalC, or NalD. Previous research illustrates that mutant strains of *E. coli* deficient in the *fabI* gene have lower binding affinity for triclosan leading to higher tolerance. This occurs through the activation of enoyl-ACP reductase isoenzymes which have functional roles in lipid biosynthesis (Sivaraman et al., 2003). Furthermore, the expression of the *fabI* gene can be increased by 40-fold in triclosan-resistant *E. coli* strains including efflux pump genes *ydcV, ydcU, ydcS, ydcT, cysP, yihV, acrB, acrD and mdfA* as shown by Zeng et al (2020) in qRT-PCR experiments. This is consistent with studies conducted in other gram negative bacteria such as *Acinetobacter baumannii* where *fabI* and the efflux pump genes *adeG, adeJ and adeM* displayed a 5-fold and 2-fold increase in expression following treatment with triclosan (Yu et al., 2020). *P. aeruginosa* are able to survive in the presence of high concentrations of BAC due to changes in gene expression of spermidine synthase gene *PA4774* which encode for polyamines which bind lipopolysaccharide material as a protective mechanism to stabilise the charge on the cell membrane preventing oxidative damage (Johnson et al., 2012; Kim et al., 2018). Tolerance to hypochlorous acid (HOCl) has been attributed to the presence of the *rcsA* gene in *P. aeruginosa* PA01 which encodes an alkyl hydroperoxidase D-like protein which functions as an antioxidant. Protein sequence analysis showed that amino acid residues such as Cys60, Cys63 and His67 are needed for the degradation of HOCl leading to tolerance. The expression of vectors containing the *rcsA* gene derived from *P. aeruginosa* also results in increased tolerance to HOCl in *E. coli* K12 suggesting that the transfer of genetic material between bacterial strains by horizontal gene transfer promotes bacterial tolerance to HOCl (Nontaleerak et al., 2020). Jin et al (2020) discovered that the transformation frequency of plasmids in chlorine-injured *E. coli* and *P. aeruginosa* can be increased by more than 200-fold. This led to higher bacterial survival and facilitated the exchange of genetic elements such as antibiotic resistance genes promoting the re-emergence of antibiotic resistant bacteria. Therefore, it can be deduced that chlorine

disinfection can increase the rate of horizontal gene transfer within a bacterial population in response to oxidative stress. Other literature shows that 3010 complete or fragmented plasmids have been found in *P. aeruginosa* populations which may contain resistance or virulence genes highlighting the pivotal role of horizontal gene transfer in biocide tolerance (Freschi et al., 2019).

1.7.2 Modified structure of the cell membrane

Gundlach and Winter (2014) showed increased levels of outer membrane protein A and antioxidant proteins such as KatG, AhpC and F in *E. coli* cells treated with HOCl. Further analysis of gene transcript levels by qRT-PCR revealed that *oxyS* and *dps* genes which are part of the OxyR regulon are highly expressed. Interestingly, the oxidation state of the OxyR regulon assessed by thiol trapping needed to be partially oxidised. Therefore, induction of the OxyR regulon is responsible for the elevated levels of outer membrane and antioxidant proteins leading to HOCl tolerance. Elevated levels of the outer membrane porin OmpC have been identified in *E. coli* suggest that changes in the lipid content limit the rate of diffusion of biocides into the cell (Fernández and Hancock, 2012; Ishikawa et al., 2002). Further evidence demonstrates that the inner membrane protein YejM in *E. coli* exhibits phosphatase activity with a 100-fold increase in activity in the presence of Mg^{2+}. This suggests that YejM plays a role in membrane alteration through direct involvement in the biosynthesis of lipopolysaccharides (Gabale et al., 2020).

1.8 Structural differences in the cell wall of gram positive bacteria

Gram positive bacteria contain wall teichoic acids (WTA) which are defined as glycopolymers containing phosphodiester linked units which are attached covalently to peptidoglycan present in the cell wall (van Dalen, Peschel and van Sorge, 2020). The typical structure of WTAs consists of a polymer backbone containing a variety of side chain moieties such as D-alanine, glycans or phosphorylcholine groups which contributes greatly to structural diversity in WTA structure (Mistretta et al., 2019; van Dalen, Peschel and van Sorge, 2020; Waldow et al., 2018). WTAs are known to play essential roles in cell metabolism, maintenance of cell shape, biofilm formation, cell division, resistance to antimicrobial agents and horizontal gene transfer (Brown, Santa Maria and Walker, 2013; van Dalen, Peschel and van Sorge, 2020). Together, the different structural adaptations that WTAs can have and its functional roles highlights that gram positive bacteria have evolved over time and are acquiring new mechanisms to maintain bacterial survival in response to antimicrobial agents.

1.8.1 D-alanylation

Previously, it has been shown that *dltA* mutants which are deficient in D-alanine esters attached to WTAs result in a 3-fold higher susceptibility to vancomycin treatment. Tolerance to vancomycin can only be observed when *S. aureus* strains undergo complementation with plasmids containing the active *dltABCD* operon which plays an essential role in D-alanine transfer to WTAs in the cell wall of *S. aureus*. The binding capacity of vancomycin to *S. aureus* was also assessed by reverse phase high performance liquid chromatography. Results revealed that in wild type *S. aureus*, 46% of the added vancomycin was bound to cells whereas 61% was bound to *dlt* mutant strains (Peschel et al., 2000). Tolerance to vancomycin and polymyxin B is also shown by other gram positive bacteria such as *Clostridium difficile* which is also attributed to the *dlt* operon. This was consistent with findings that the D-alanine content in the cell walls of *dltD* mutants are 100-times lower than wild type strains with normal levels being restored through complementation with plasmids containing the active *dltDABC* operon (McBride and Sonenshein, 2011).

1.8.2 Glycosylation

In methicillin-resistant *S. aureus* (MRSA), WTAs can be modified by β-O-GlcNAcylation, α-O-GlcNAcylation or D-alanylation. Brown et al (2012) previously identified a glycosyltransferase enzyme which adds β-*O*-GlcNAc residues to WTAs labelled TarS. High performance liquid chromatography showed that when TarS is incubated with poly (RboP)-WTA and UDP-GlcNAC or UDP-Glc, the most dominant peak observed is for UDP-Glc. This demonstrated that UDP-Glc is the preferred donor substrate used by TarS during the glycosylation process. Further experiments revealed that TarS is only able to glycosylate substrates which contain multiple RboP units as polyacrylamide gels showed that other intermediates such as CDP-ribitol, ribitol phosphate and lipoteichoic acid could not undergo glycosylation under the action of TarS. Complementation using plasmids containing an active form of TarS in mutant constructs of MRSA and quadruple time-of-flight mass spectrometry provided additional evidence that *tarS* mutants lack the glycosyltransferase enzyme required to glycosylate the WTA where lower m/z ratios were detected. Also, quantitative real-time PCR demonstrated that there was 4-fold increase in gene expression levels of *tarS.* The structure of TarS has been found to exist as a trimer with a molecular weight of 200kDa identified through size exclusion chromatography-multiangle light scattering along with many carbohydrate binding motifs (Sobhanifar et al., 2016). Further evidence indicates that MRSA can produce alternative glycosyltransferase enzymes such as TarP which are involved in the catalysis of GlcNAc residues onto the hydroxyl group of WTAs which decreases immunoglobulin G levels by up to 40-fold in mice (Gerlach et al., 2018). Therefore, the

development of TarS and TarP inhibitors is important to prevent the re-emergence of resistance or protection against infection.

1.9 Strains for analysis

1.9.1 *Escherichia coli* K12 (*E. coli* K12)

E. coli is a fecal indicator of contamination in water distribution systems. In addition, *E. coli* K12 has the ability to form biofilms on pipe walls which are a reservoir for pathogens in hot tub systems highlighting the importance of regular sanitation (Liu et al., 2014). Proteomic and spectrometry methods have proposed mechanisms by which *E. coli* K12 confer tolerance to disinfectants. This occurs as a result of upregulation of outer membrane proteins involved in membrane permeability and structural integrity conveying that changes in protein expression lead to export of biocides and reduced permeability in the outer membrane for subsequent uptake into bacterial cells (Zhang et al., 2011). Q-PCR experiments conducted by Lu et al (2014) reveal a method for detection of *E. coli* K12 on pipe biofilms. This provides increasing concern that *E. coli* K12 may form biofilms in the pipes of hot tubs. Therefore, the use of the *E. coli* K12 strain in this study was of great importance.

1.9.2 *Pseudomonas aeruginosa* PA01 (*P. aeruginosa* PA01)

Pseudomonas aeruginosa is a gram-negative bacterium found in water and soil which is commonly associated with lung infections in cystic fibrosis patients as well as bloodstream, respiratory and urinary tract infections (Bhagirath et al., 2016; CDC, 2012; Newman et al., 2022; Zhao et al., 2020). Specific locations in hot tubs where high levels of biofilm are found include gutter drains, jets and strainer baskets. Regardless of high disinfection levels, 96% of *P. aeruginosa* strains resistant to common antimicrobial agents and antipseudomonal drugs have been found in hot tubs and swimming pools (Lutz and Lee, 2011). In addition, exposure to chlorine disinfectants has been shown to cause resistance in *Pseudomonas* populations by the activation of oxidative stress responses in which antioxidant enzymes are upregulated, limiting the extent to which oxidative damage can occur (Jin et al., 2020; Tong et al., 2021). This highlights the demand for sanitation products which can overcome problems associated with AMR. As a result, *P. aeruginosa* PA01 is a relevant bacterium of study.

1.10 Enzymes in water sanitation and biofilm removal

Enzymes are the catalysts of chemical reactions in biological systems which are commonly used within the water treatment industry due to their ability to degrade organic pollutants. The basis of enzyme action revolves around the induced fit model where upon binding of a substrate, the shape of the active site present on enzymes is altered to adopt a complementary formation allowing cleavage of

chemical bonds within molecules (Berg et al., 2015). The rate at which enzymes can speed up a chemical reaction is dependent on pH and temperature where optimum conditions enhance enzyme activity (Robinson, 2015). Therefore, enzymes are an attractive option for use in water treatment systems for sanitation and biofilm removal. Enzymes have been produced with optimal protease, amylase and lipase activity at pH 6 at 37°C and have been reported to cause removal 99% of pathogens making them useful tools in water treatment applications (Arun and Sivashanmugam, 2015; Arun and Sivashanmugam, 2017).

1.10.1 Proteases

Proteases digest proteins by hydrolytic reactions using the additional of water to cleave peptide bonds in molecules. Most proteolytic enzymes are sourced from *Bacillus* spp. and their sanitising potential as single enzyme preparations is known to be effective (Puspitasari, 2010). Alkaline proteases have pH stability at values from 7 to 12 with 135.8% of residual activity maintained at optimum pH of 11 and are stable at temperatures from -10 to 80°C where activity is not hindered by the presence of surfactants or detergents (Beena et al., 2012; Beena, 2014). In addition, Zhang et al (2022) illustrate that exposure to a protease containing enzyme preparation causes lower molecular weight of proteins detected by gel electrophoresis in the presence of water-softening agents.

1.10.2 Amylases

The functional role of α-amylases is to catalyse the cleavage of α-1,4-glycosidic linkages in starch and glycogen. α-amylases are derived from *Bacillus* and *Aspergillus* spp and have been known to be effective in water treatment applications. Using combination enzyme treatments of protease and α-amylase can successfully remove *E. coli* biofilms by 78% after treatment for 2h at 37°C (Jee et al., 2020). Furthermore, the effect of α-amylases on *P. aeruginosa* causes dispersal of biofilms by degrading carbohydrates present in the EPS leading to significantly reduced thickness of biofilms by more than 56% (Kalpana et al., 2012).

1.10.3 Lipases

Lipases comprise of a group of enzymes which degrade triacylglycerols into free fatty acids and glycerol. Various sources of lipases include *Aspergillus* and *Penicillium* spp. Lipase activity can be detected in samples containing ethyl butyrate as a substrate with a water activity of 0.33-0.75, a term used to describe the level of unbound water which determines the reaction rate of an enzyme (Chowdary and Prapulla, 2002). Lipases transferred onto polymer surfaces containing *E. coli* revealed a 7 times and 5 times reduction in carbohydrate and biofilm protein content which was supported by changes in the amount of lactate dehydrogenase being released (Prabhawathi et al., 2014).

1.11 Typical water sanitation products and their detection

1.11.1 Chlorine

The hot tub chlorine granules used in this project contain the active compound sodium dichloroisocyanurate (NaDCC) shown in Fig. 1.2A. NaDCC is the sodium salt of a chlorinated cyanurate frequently used as a source of HOCl and free available chlorine (FAC) for water disinfection (Wahman, 2018). FAC is defined as the oxidising power of chlorine in a compound and is reported as a percentage (Pinto and Rohrig, 2003). The level of FAC in the dihydrate form of sodium dichloroisocyanurate recorded by the manufacturer of the chlorine granules is 55.10%. In comparison to sodium hypochlorite, the active component in bleach, NaDCC is advantageous in terms of stability since previous data shows that the level of available chlorine can be maintained for up to 40 months when stored in a dry environment (Coates, 1987).

When NaDCC comes into contact with water, it undergoes a hydrolysis reaction which leads to the liberation of FAC where various equilibrium reactions exist between six chlorinated and four non-chlorinated compounds (Fig. 1.2B).

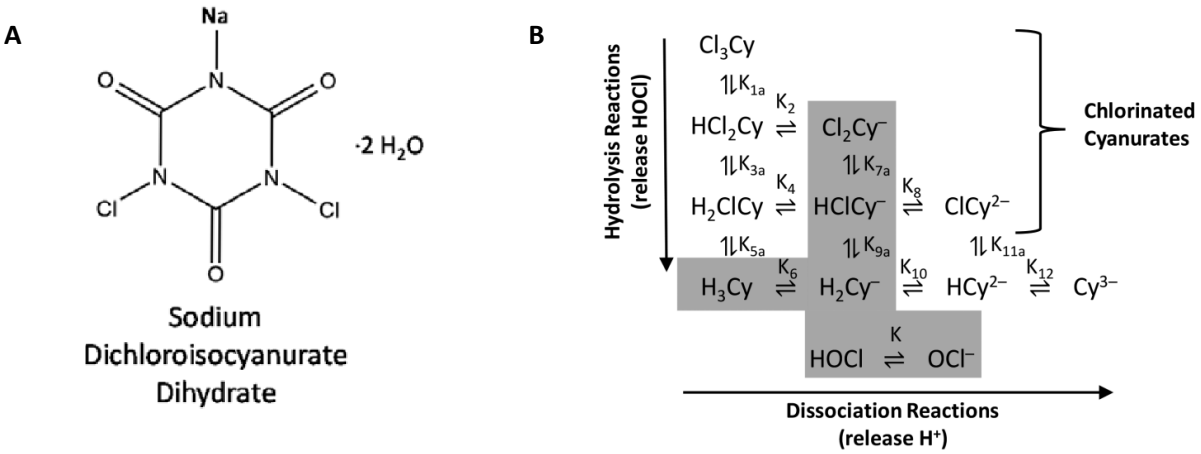

Figure 1.2. Chemical structure of sodium dichloroisocyanurate shown in A (Wahman, 2018) and model for hydrolysis of chlorinated cyanurates in drinking water (B). Equilibrium reactions are observed between six chlorinated and four non-chlorinated compounds with chlorine being released as hypochlorous acid (HOCl) or hypochlorite ions (OCl^-). Highlighted in grey are typical cyanurate containing species expected in drinking water conditions (Wahman et al., 2019).

The levels of total available chlorine, temperature, pH and equilibrium constant values are determining factors in the concentration of each species (Kuznesof, 2004). Figure 1.3 illustrates the effect of pH on

the level of different chlorine species. Low pH values result in hydrolysis of nearly all Cl_2 whereas raising the pH higher than 4 causes degradation of HOCl into OCl^- (Deborde and Gunten, 2008).

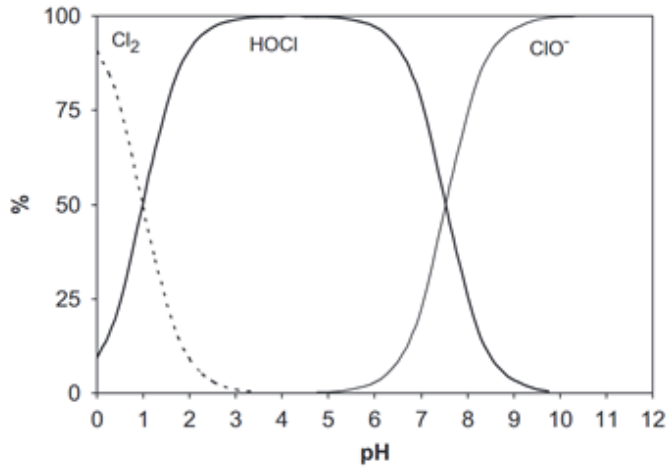

Figure 1.3. Distribution of chlorine species as a function of pH at 25°C (B). Optimal activity is observed around pH 7.4 where deviations in pH lead to subsequent breakdown of chlorine species (Deborde and Gunten, 2008).

Clasen et al (2007) carried out randomised controlled trials giving half of households NaDCC tablets to treat drinking water and the other half a placebo. Routine sampling of water illustrated a considerable difference between the coliforms of bacteria found between treatment groups where no bacteria was detected in 61.7% of samples taken from households using NaDCC tablets. The use of NaDCC at a concentration of 200ppm has been shown to cause a log reduction greater than 1.95 in coliforms of *E. coli* after 15 minutes of exposure (Nascimento et al., 2003). Zhang and Hu (2012) used a combination treatment of *P. aeruginosa* phages and sodium hypochlorite to investigate their effects on biofilms and found that 88% of biofilms were removed. Chlorine disinfection has also proven effective against *Legionella* biofilms developed on galvanised steel and polyvinyl chloride with a reduction rate of 2.8 log_{10} after exposure to 150 mg/L of chlorine (Assaidi et al., 2020). String et al (2020) revealed that higher reductions in levels of bacteria were observed when surfaces were sprayed with chlorine in comparison to wiping highlighting the need for surfaces to be wetted to obtain optimal disinfection.

There are various methods used to measure the levels of FAC in water samples. The simplest method is the use of test strips which are placed into water samples and compared against a standard colour chart. Test tube kits are also used where vials are filled with sample and reagents followed by comparison to standard charts. Murray and Lantagne (2015) examined different methods of measuring FAC using colorimeters, test tube kits and test strips. Results found that test strips are associated with

high probability of error accounting for 32% of false negatives and 43% of false positive outcomes. Using test strips is disadvantageous since they can be difficult to read by eye and are subject to interpretation making them a less reliable option for measuring FAC in water samples. Another option is to use electronic meters such as colorimeters to measure absorbance at specific wavelengths dependent on colour intensity. *N,N*–diethyl–*p*–phenylenediamine (DPD) testing and amperometric titration is applied in routine water testing since there is a direct reaction with free chlorine (Wahman, Alexander and Dugan, 2019). DPD testing is colorimetric where a coloured reagent is indicative of the concentration of FAC (Moberg and Karlberg, 2000) whereas amperometric titration utilises phenylarsine oxide which undergoes a chemical reaction with the sample and is measured by reductions in current (Hernlem and Tsai, 2000). Iodometric titration utilises potassium iodide and an indicator such as starch solution which absorbs any iodine that is released. This results in a colour change from dark blue to colourless following titration with sodium thiosulphate which resembles the end point of the titration. As a result, the level of iodine released is indicative of the FAC levels present (Rajachar et al., 2021; Saberi et al., 2019).

There is no set equation used to calculate FAC levels since each method uses a different detection method such as changes in current or through colorimetric methods. However, the way in which FAC can be calculated as shown in the following equation:

FAC = TC – CAC

where TC represents total chlorine and CAC represents combined available chlorine. Total chlorine is defined as the sum of free chlorine and combined available chlorine. Combined available chlorine is the amount of chlorine available following the disinfection process (Patterson, 2020).

Furthermore, addition of disinfecting agents to water also leads to the possible formation of disinfection by-products (DBP) of which the most prevalent class are trihalomethanes (THMs). THMs include chloroform, bromodichloromethane, dibromochloromethane and bromoform. There are major concerns regarding the formation of THMs since previous research has linked exposure to THMs with heightened risk of rectal cancer, bladder cancer and negatively impacts on the male reproductive system (Bove et al., 2007; Villanueva et al., 2004; Zeng et al., 2016). THMs are known to be associated with the addition of chlorinated disinfectants (Kristensen et al., 2010) with chloroform being found in 80% of samples isolated from recreational waters. This suggests that regular dosing of chlorine results in increasing levels of THM formation (Stack et al., 2000). Therefore, it is important to monitor the levels of chlorine present in water systems.

Determination and quantitation of cations and anions in water samples is routinely performed using ion-exchange chromatography (IEC). IEC quantifies ionic species in response to interactions with an analytical column which is composed of a polymeric resin. Cations and anions are separated based on their retention time, a term used to describe the amount of time taken for an analyte to pass through a column. Common anions detected are chloride, fluoride, bromide, nitrate, sulphate and phosphate as well as oxyhalide anions chlorite and chlorate (Paun et al., 2020). As previously described, the use of chlorine containing disinfectants can lead to DBPs such as chlorite and chlorate of which anion levels must be monitored. Chlorite and chlorate are generated following disinfection with chlorine dioxide and sodium hypochlorite (Veschetti et al., 2005) with studies showing an association of chlorite exposure with haemolytic anaemia (Hulshof et al., 2019).

Figure 1.4 illustrates a schematic of the apparatus which make up the ion chromatography system. The first component of IEC is the eluent, a liquid which aids the separation of ions which is pushed through the system by a pump which operates at high pressure. Then, the sample of interest is injected manually with a syringe or through automated controls. The pump is able to push the eluent and sample through an analytical column where ion exchange occurs. Often, guard columns are fitted in order to eliminate contaminants that could interfere with measurements. As sample ions migrate through the analytical column, they are separated due to their contact with ion exchange sites before passing through a suppressor. Suppressors are advantageous since they increase analyte response and reduce background signals significantly. The final stage involves electrical conductance of sample ions by a conductivity detector which generates a signal on a chromatogram which is relayed to a data collection system for data visualisation.

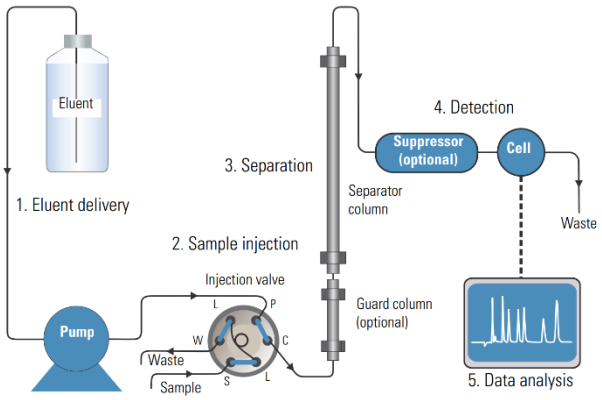

Figure 1.4. Components of ion chromatography systems. The eluent and sample is pushed through the system by pumps operating at high pressures before being separated on analytical columns and being detected by a data analysis software to create a chromatogram (Thermo Scientific, 2016).

1.11.2 Bromine

Bromine is an alternative option to using chlorine which does not exhibit a strong smell, is less irritant to skin and is effective at a wider range of pH levels. However, it has higher costs compared to chlorine and is broken down at a faster rate on exposure to sunlight requiring the addition of more product to compensate for its breakdown (Patterson, 2019).

When bromine is added to hot tubs and swimming pools it exhibits a similar process to the reactions described with using chlorine. Instead, hypobromous acid (HOBr) and bromide is formed as products of the reaction. Ammonia can react with HOBr resulting in bromamines. Bromamines are known to have a higher sanitation efficacy due to its hydrolysis equilibrium being favoured more towards the formation of HOBr than that of chloramines which results in low levels of HOCl. In addition, bromine is more effective at higher pH levels as HOBr ionises to a lower extent compared to HOCl at pH 8.7 (Water Technology, 2015).

El-Athman et al (2021) showed that HOBr and HOCl exhibits similar disinfection efficacy against *E. coli, P. aeruginosa, S. aureus and E. faeceium*. Schmidt et al (2012) employed a wash method by spraying HOBr at concentrations of 220ppm and 500ppm on cattle hides obtained after slaughtering. At the concentrations tested, the prevalence of *E. coli* O157:H7 was reduced by more than 10% whereas this value was greater than 20% for *Salmonella*. Plate counts illustrated that applying 500ppm of HOBr to cattle hides can cause a 3.3 log reduction in colony forming units. These findings have been replicated in other literature described by Owens (2011) where the high efficacy of hypobromous acid on pathogen reduction has been shown. Lim et al (2012) treated lettuce inoculated with *E. coli, Salmonella typhimurium and Staphylococcus aureus* with sodium hypochlorite alone and in combination with HOBr. Their findings demonstrate that HOBr treatment can extend biocidal activity for longer periods of time since sodium hypochlorite treatment alone showed increased populations of bacteria which was suggested to be due to chlorine loss over the study period of 10 days.

1. 12 Active Oxygen

Since there are health risks associated with both chlorine and bromine, the use of Active Oxygen substances for sanitation has been a field that has been gaining attention in a variety of research areas. It is an attractive option as it is odourless and does not cause irritation to the eyes and skin. Active Oxygen species is a term used to describe chemical species that originate from oxygen molecules but exhibit more reactive characteristics (Murphy et al., 2022). Often such compounds are also referred to as reactive oxygen species. Several Active Oxygen species have been identified such as singlet oxygen, superoxide anion, hydroxyl radicals and sulphate radicals (Fig. 1.5). Common examples of active oxygen-containing substances include hydrogen peroxide and ozone.

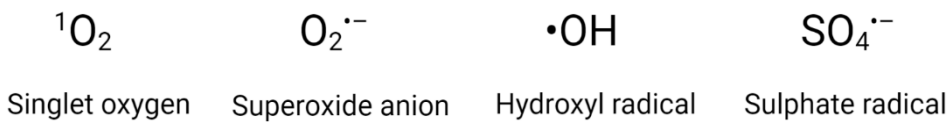

Figure 1.5. Overview of Active Oxygen species. Created with BioRender.com.

Ozone contains an additional oxygen atom in its chemical structure which allows it to react with other organic compounds making it a strong oxidant. In response to reacting with an organic compound, it can facilitate breakdown and exhibit biocidal activity. The use of ozone generators has proven successful in the eradication of *E. coli and P. aeruginosa* levels as evidence has showed no colony forming units detected after ozone treatment (Fontes et al., 2012). As a result, Active Oxygen has widespread applications in refrigerators, washing machines and dental applications (Cunha et al., 2019; Sheridan, 2016).

1.12.1 Singlet oxygen

Proposed mechanisms regarding inactivation of planktonic *E. coli* cells in the dark have been previously documented using photoactivated singlet oxygen. A method known as singlet oxygen priming has been put forward which involves reactions with an alkene surfactant leading to the formation of hydrogen peroxides and subsequent production of peroxide radicals which encourage disinfection. *E. coli* cells pre-treated with singlet oxygen are positively correlated with biocidal activity and increasing levels of hydrogen peroxides being detected over a 1h period. This gave speculation that there may be interactions between the light and dark processes where the presence of singlet oxygen leads to the priming which occurs through removal of hydrogen ions and radical formation (Jabeen et al., 2020). Photosensitisers which absorb visible light and induce the formation of Active Oxygen species via the movement of electrons also play a role in the loss of viability of *P. aeruginosa* PA01 cells grown in glucose minimal media. *P. aeruginosa* stains harbouring a mutation in the *phzA1* gene involved in phenazine synthesis have been found to exhibit higher levels of viable bacteria compared to other mutant strains and controls in response to photosensitisers. This indicates a possible role of phenazine pigments in adopting a protective mechanism against singlet oxygen leading to survival (Orlandi et al., 2015).

1.12.2 Superoxide anion

The antibacterial activity of the antioxidant astaxanthin has been demonstrated against *E. coli* and *P. aeruginosa* strains grown in Mueller-Hinton broth. Measurement of superoxide anions indicated that astaxanthin caused elevated levels of superoxide anions in comparison to cells treated with dimethyl sulfoxide which resembled the same effect in cells treated with common antibiotics (Aribisala et al.,

2021). Sviridova et al (2021) utilised two luminescent biosensors based on *E. coli* K12 which contain a recombinant plasmid with the *lux* operon fused with promoters of the *soxS* and colicin *colD* gene. Results found that the antimicrobial compound dioxidine was able to stimulate the SOS response in relation to DNA damage as high levels of luminescence were detected which is reliant on the concentration of superoxide anion in cells. Electrophoretic analysis revealed that DNA degradation is positively correlated with increasing dioxidine concentration which was reduced when cells were treated with antioxidants. This illustrated that superoxide anion radical formation was responsible for loss of viability in response to increasing concentrations of dioxidine since antioxidants dampen the induction of the SOS response leading to fewer superoxide anion radicals being generated. Similar results have been replicated by Ajiboye et al (2017) showing consistent decreases in optical density, viability of *E. coli* and *P. aeruginosa* and higher levels of DNA degradation following exposure to protocatechuic acid. Treatment also caused levels of superoxide anions of both strains to rise by 12.44 and 27.34-fold as well as inhibition of components of the electron transport chain. Therefore, these results indicate that protocatechuic acid stimulates the formation of superoxide anions in *E. coli* and *P. aeruginosa* by mechanisms involving DNA fragmentation and lipid peroxidation which results in bacterial cell death.

1.12.3 Hydroxyl radicals

Hydroxyl radicals can be formed from hydrogen peroxide via catalytic reactions with transition metal ions (e.g. Fe^{2+} and Fe^{3+}) or as a result of radiation (Halliwell et al., 2021). Wang et al (2022) concluded that hydrogen peroxide exhibits antibacterial activity against *E. coli* by undergoing a radical propagation reaction generating hydroxyl radicals. The ability to oxidise methylene blue was strongly associated with levels of Fe^{3+} due to reduction reactions to Fe^{2+}. This suggested that the change in oxidation state from Fe^{3+} to Fe^{2+} was attributed to oxidation of *E. coli* cells which caused reductions in viability and cell damage. Interestingly, mutational defects in the superoxide dismutase enzyme (SOD) which converts superoxide anions into peroxide show that *E. coli* have protective mechanisms which allow them to evade cell death when treated with quinolone antibiotics. This indicated that due to the inability of SOD to convert superoxide anions in peroxides, accumulation of superoxide anions dominated the protective effects which are observed in response to mutations in the SOD enzyme (Wang and Zhao, 2009). Suspension tests conducted by Boateng et al (2011) demonstrate potent antibacterial activity of hydrogen peroxide against *E. coli* and *P. aeruginosa* in the presence of iron catalysts achieving log reductions of 4.76 and 5.59 following treatment after 1h. Additionally, exposing *E. coli* to hydrogen peroxide and incubating for 24h displays antibacterial activity (Khurshid et al., 2019). Recent literature has investigated the effects of hydroxyl radicals on bacterial gene expression of PA01 strains of *P. aeruginosa*. Ultraviolet induced activation of hydrogen peroxide caused a 33.914-

fold change in expression level of the *PA3237* gene in comparison to controls. Further experiments using a radical scavenger tert-butanol to inhibit oxidation processes revealed that higher expression levels of the *PA3237* gene were linked to hydroxyl radical formation since its presence diminished expression levels (Aharoni et al., 2018).

1.12.4 Sulphate radicals

The antibacterial effect of sulphate radicals on *E. coli* has been widely investigated. Peroxydisulfate (PDS) is effective at inactivating *E. coli* K12 through sulphate radical formation in the presence of Fe^{2+} when applied at concentrations with a molar ratio 1:5 of Fe^{2+} to PDS. Supporting evidence shows that addition of PDS at a concentration of 9.10^{-5} M combined with light, heat and Fe^{2+} activator significantly enhances complete killing of *E. coli* which was achieved within 1h (Marjanovic et al., 2018). In PDS systems combined with ultraviolet in PBS solutions at pH 7, sulphate radicals are one of the most dominant species produced which has been shown to cause a 5-log reduction in *E. coli* (Sun et al., 2016). Further evidence demonstrates that sulphate radicals lead to the loss of *E. coli* cell viability five times faster than that seen with hydroxyl radicals. This suggests that sulphate radicals may react with components located on the surface of *E. coli* cell membranes in order to elicit their killing action (Wordofa et al., 2017). Optimal antibacterial activity of peroxymonosulphate (PMS) against *E. coli* and *P. aeruginosa* following exposure to ultraviolet radiation is observed at 0.5 mmol/L causing 5-log reduction within 15 minutes of treatment (Berruti et al., 2021). This adds further evidence of the biocidal activity of PMS due to the generation of sulphate radicals. Activation of PDS following exposure to visible light causes a 4.5-log reduction in *P. aeruginosa* and complete inactivation of *E. coli* within 120 minutes. Mechanistic studies involving measurement of SOD and catalase (CAT) levels show that at the start of bacterial inactivation, biocidal activity progresses slowly whereas SOD and CAT activity sharply increases which acts as a host bacterial cell defence system against damage. Towards the later stages of bacterial inactivation, there is a decline in SOD and CAT activity which is concurrent with enhanced disinfection indicating that the high levels of sulphate radicals being produced surpass the protective mechanisms exhibited by the defence system leading to subsequent death of cells (Wang et al., 2019). Recent development of synthetic gels in the presence of PMS and visible light has led to loss of viability of *E. coli* which is attributed to the generation of Active Oxygen species confirmed by radical scavenger assays (Karbasi et al., 2020).

1.13 Pentapotassium peroxymonosulphate

The Active Oxygen sanitiser tablets used in this project contain the active compound pentapotassium peroxymonosulphate (KMPS) which is shown in Fig. 1.6.

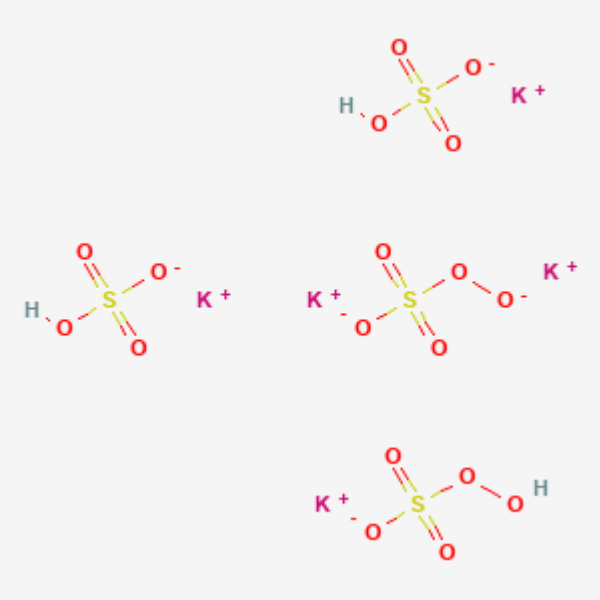

Figure 1.6. Chemical structure of KMPS (Kim et al., 2021).

When KMPS comes into contact with water, it causes a peroxymonosulphate ion to generate a hydroxy radical and sulphate ion radical which is shown in equations 1-4 (Fig. 1.7). These radicals can be formed from other Active Oxygen species such as organic peroxyacids, hydrogen peroxide or PDS (Kennedy and Stock, 1960).

$$HOOSO_3^- \longrightarrow HO\cdot + \cdot OSO_3^- \qquad (1)$$

$$RCOOOH \longrightarrow RCOO\cdot + \cdot OH \qquad (2)$$

$$HOOH \longrightarrow 2HO\cdot \qquad (3)$$

$$(O_3SOOSO_3)^{-2} \longrightarrow 2\cdot OSO_3^- \qquad (4)$$

Figure 1.7. Formation of hydroxyl and sulphate radicals following the use of KMPS (Kennedy and Stock, 1960).

KMPS is the active antimicrobial agent in the common disinfectant Virkon. Virkon at 1% concentrations are effective against *E. coli and P. aeruginosa* after 5 minutes of exposure causing log reductions greater than 5 (Hernndez et al., 2000). Previous literature shows that Virkon solutions at 1% are able to eradicate *E. coli* and *P. aeruginosa* within 30 seconds whereas at 0.5% concentration, 15 minutes is

required to kill both bacteria (Chakraborty et al., 2014). *E. coli* and *P. aeruginosa* have been identified in over 95% of water samples in a study conducted by Kamal et al (2019) which have been discovered to express chlorine resistance. Results showed that the addition of KMPS was able to kill *E. coli* and *P. aeruginosa* within 15 minutes of exposure in comparison to other disinfecting agents such as quaternary ammonium compounds where only 3 out of 19 chlorine resistant strains were killed. KMPS causes a 2-log reduction and 4-log reduction in *E. coli* colony counts in combination with cobalt after 1h of exposure (Anipsitakis et al., 2008). In addition, at recommended concentrations and at concentrations down to 0.125x more dilute, Kunanusont et al (2020) revealed that although there were no marked differences in *E. coli* colony counts, longer incubation times were required in order to achieve the same killing effect. Moslehifard et al (2015) inoculated dental stone casts with bacteria and after exposure to 1% Virkon, demonstrated complete killing of *P. aeruginosa*.

There are a limited number of studies that discuss the effect of temperature on the ability of PMS to remove organic contaminants. Ji et al (2016) revealed that addition of PMS in the presence of tetracycline was not able to facilitate breakdown. This was only observed when heat was applied at a temperature of 50^{o}C with aqueous solutions at pH 4 and 7. This suggests that subjecting PMS to higher temperatures stimulates the generation of sulphate radicals. Similarly, Zhou et al (2019) used a temperature range of 30-60^{o}C and showed that the effect of increasing temperature promotes the decomposition of PMS leading to higher levels of sulphate radicals being formed. The influence of pH on PMS has not been discussed widely in research. Available literature gives insight that increasing pH from 8 to 10 causes increased degradation of chemical pollutants due to elevated rates of PMS photolysis leading to marked increases in hydroxyl and sulphate radical levels (Guan et al., 2011).

1.14 Aims and objectives

Eco3spa has designed an environmentally friendly water treatment product for the hot tub sector which is a 3-step product consisting of a hot tub cleaner for biofilm remover as well as Active Oxygen sanitiser tablets and water conditioner which are to be used in combination with each other. The manufacturer instructions state using the hot tub cleaner first to remove biofilms followed by two sanitiser tablets with the water conditioner for optimal sanitation. For subsequent sanitation of the hot tub, one tablet of Active Oxygen is added to the water.

Previous research has revealed that the Active Oxygen sanitiser tablets are effective over a set pH range which do not lose their biocidal activity even in the presence of the water conditioner. In addition, the product produced results relative to the use of chlorine at the recommended concentrations for hot tub sanitation (Karagianni, 2022). Following these results, the company wanted

to assess how quickly the Active Oxygen sanitiser tablets kill bacteria and for how long they remain active in the water. In regards to the water conditioner, attempts were made to isolate the protein present but protein quantification procedures did not show the presence of any protein.

Therefore, this current project aimed to answer the following questions using Eco3spa's products:

- What is the time dependency of the Active Oxygen sanitiser tablets?
- How long do the Active Oxygen sanitiser tablets remain active in the water after differing periods of time?
- What Active Oxygen species are present in the Active Oxygen sanitiser tablets?
- What chlorine species are present in the chlorine granules?
- What effect does pH have on the sanitising efficacy of the Active Oxygen tablets and how does this differ from the use of chlorine?
- Does the water conditioner contain active enzymes contributing to water sanitation?

1.15 Impact on research

Due to ion chromatography experiments being conducted for the first time and only towards the later stages of the project, experiments were performed under N=1 conditions. Also, further delays were experienced for lab reoccupation following fire and water damage to the building and chemical engineering labs. Therefore, IEC training could only be taken once labs were fully reinstated with equipment fully tested and validated prior to other users being given access. In addition, since this was a one-year project, biofilm removal experiments could only be conducted on both strains at 37^{o}C to best represent the usage of the products at operating temperatures of the hot tub.

Chapter 2: Materials and Methods

2.1 Media composition

Table 2.1. Media used in this study

Medium		g/L
Luria-Bertani (LB)	Casein Digest Peptone	10
	Yeast extract	5
	NaCl	5
	Agar	15 (only for solid media)
Minimal media (M9)	Na_2PO_4	33
	KH_2PO_4	15
	NH_4Cl	5
	NaCl	2.5
	$MgSO_4$	2
	Glucose	20
	$CaCl_2$	0.1

2.1.1 Media preparation

LB broth and agar

To make LB broth, 20g of LB Broth powder (Melford) was added to 1 litre of distilled water in a 1L sterile glass bottle. The bottles were then autoclaved at 121°C for 15 minutes. To make LB agar, 10g of Lennox L Broth powder was added 500ml of distilled water in a 1L sterile glass bottle. This was followed by adding 7.5g of agar (Sigma-Aldrich) and autoclaving the solution at 121°C for 15 minutes. The media was then poured into a series of 90mm sterile petri dishes and allowed to solidify in a preparation flow hood at room temperature for 20 minutes. Once solidified, the plates were placed in autoclavable plastic bags and kept in a cold room set at 4°C. Plates were used within a week of preparation.

M9 Minimal media

56.4g of M9 Sigma-Aldrich UK minimal salts (5X) was added to 1 litre of distilled water and dissolved. Following sterilisation, 400µl of 1M $MgSO_4$ was added to 40ml of M9 minimal salts and 156ml distilled water and autoclaved at 121°C for 15 minutes. Then, 4ml of glucose 20% and 20µl of $CaCl_2$ was added aseptically to create total volume of 200ml.

2.2 Buffers and dyes

Live-Dead staining

For live-dead staining procedures, SYTO 9 (Invitrogen, S34854, 5 mM) and Propidium iodide (Invitrogen, L7012, 20 mM) were used. For 200µl of samples from biofilm prevention assays, 0.6µl of

SYTO 9 and propidium iodide were added to microtiter wells and thoroughly mixed. Then, the microtiter plate was covered in foil and incubated in the dark for 15 minutes. Then, 10µl samples were pipetted onto a microscope slide and viewed using a Zeiss fluorescent microscope (schematic shown in Fig. 2.1). Alexa Fluor 488 and Rhodamine Red-X were the fluorescent filters used which are described in Table 2.2. Zen 3.1 software was used for data analysis and images were captured using an Axiocam MR R3 camera for fluorescent images and an Axiocam 503 camera for light microscopy images.

Table 2.2. Excitation and emission wavelengths of fluorescent filters

Filter	Colour	Excitation/Emission wavelength (nm)
Alexa Fluor 488 (AF488)	Green	494/517
Rhodamine Red-X (RhReX)	Red	573/591

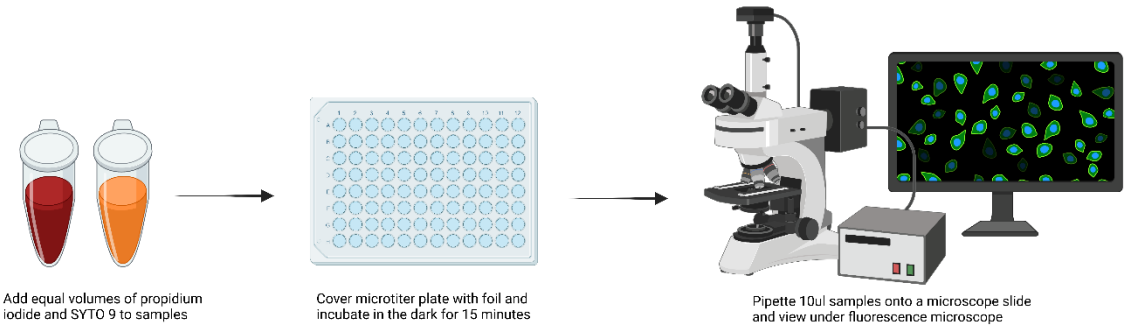

Figure 2.1. Schematic of the fluorescent staining process using SYTO 9 and propidium iodide. Created with BioRender.com.

Phosphate buffered saline (PBS)

PBS is a liquid based salt solution consisting of sodium phosphate and sodium chloride with a pH of 7.25. The composition of PBS (Melford) was Potassium phosphate (monobasic) 0.14g, Sodium chloride 9g and Trisodium phosphate 0.795g. To make a 1x PBS solution, one tablet weighing 1.033g was dissolved in 100ml distilled water followed by autoclaving at 121°C for 15 minutes.

Crystal violet solution (0.1% w/v)

0.1g of crystal violet powder (Sigma-Aldrich UK) was dissolved in 100ml of distilled water in a glass bottle. The solution was then shaken to ensure thorough mixing, wrapped in tin foil and stored away from light to prevent the risk of photodegradation.

MOPS-SDS Running Buffer

To prepare 500ml of 20x MOPS SDS Running Buffer (50 mM MOPS, 50 mM Tris Base, 0.1% SDS, 1 mM EDTA, pH 7.7), 104.6g of MOPS, 60.6g of Tris Base, 10g of SDS and 3g of EDTA was dissolved in 400ml of distilled water. The volume was adjusted with distilled water to reach a final volume of 500ml. Before electrophoresis, the buffer was diluted to 1x with water.

Coomassie stain

For staining of protein gels, 0.5g of Coomassie Brilliant Blue R-250 was dissolved in 400ml distilled water followed by 500ml methanol and 100ml glacial acetic acid.

Coomassie gel destaining solution

To prepare the destaining solution, 400ml of distilled water was added to a 500ml glass bottle followed by 50ml of glacial acetic acid (Fisher) and 50ml of methanol (Fisher). This gave a solution with concentration 10% acetic acid : 10% methanol v/v.

2.3 Protein assays

2.3.1 Enzymes

The water conditioner product (Product 2) is stated to contain protease, amylase and lipase enzymes. Therefore, the following enzymes were purchased from Sigma (Table 2.3).

Table 2.3. Enzymes used including origin and protein activity

Enzyme	Origin	Protein activity
Protease	Bacillus amyloliquefaciens	≥ 0.8 U/g
Lipase	Aspergillus oryzae	≥ 20,000 U/g
α-Amylase	Aspergillus oryzae	≥ 800 FAU/g

2.3.2 Bicinchoninic Acid (BCA) and Bradford assays

In order to quantify the concentration of protein within commercial enzyme solutions e.g. water conditioner, two colorimetric protein assays were performed. The Pierce Bicinchoninic Acid (BCA) protein assay kit (ThermoFisher, 23225) and Bradford Assay (Biorad, 5000202) were used for protein quantification. In each protein assay, bovine serum albumin standards were prepared from a stock at concentration 2000 µg/ml in accordance with manufacturer instructions to generate a standard curve.

2.3.3 Protein precipitation

2.3.3.1 Acetone precipitation

For acetone precipitation procedures, 50µl of water conditioner was added to a microcentrifuge tube followed by 200µl of cold acetone. The tubes were vortexed and incubated at -20^{o}C for 30 minutes. The tubes were then centrifuged at 17,000 x g for 10 minutes and the supernatant was removed. In order to allow any remaining acetone to evaporate, the tubes were left at room temperature with the lid open for 30 minutes. Then, 50µl of ultrapure water was added to each tube and vortexed to dissolve any protein pellets.

2.3.3.2 Trichloroacetic acid (TCA) precipitation

For TCA precipitation, 50µl of water conditioner was added in a microcentrifuge tube followed by 450µl ultrapure water, 100µl sodium deoxycholate (Sigma) and 100µl of trichloroacetic acid 72% v/v (Fisher). Tubes were incubated at room temperature for 10 minutes before centrifugation at 17,000 x g for 10 minutes. A protein pellet was formed and the supernatant removed. The protein pellet was resuspended in 200µl of 5% Sodium dodecyl sulphate (SDS) in 0.1M Sodium hydroxide (NaOH) and vortexed thoroughly to dissolve the protein pellet.

2.3.4 Ultrasonic bath

In order to thoroughly mix the contents of the water conditioner, the Fisherbrand™ 11203 Series Advanced Ultrasonic Cleaner was used. Samples of water conditioner were transferred to a 25ml plastic container. The container was placed in a 100ml beaker filled with distilled water. The ultrasonic bath was filled with distilled water and the water conditioner was incubated at a temperature of 30^{o}C for 90 minutes using the pulse setting.

2.3.5 Freeze-drying

In order to further precipitate proteins from the water conditioner, freeze drying procedures were carried out using a Modulyo freeze dryer. Samples of water conditioner were placed into 50ml Falcon tubes and stored in a -80^{o}C fridge until frozen. The following day, tubes were wrapped in foil and placed in a pipette box for transportation. Samples were placed under a bell jar in a plastic beaker with the vacuum pump was turned on and air valve tightened. Samples were left to freeze dry for 2 days (Fig. 2.2).

A 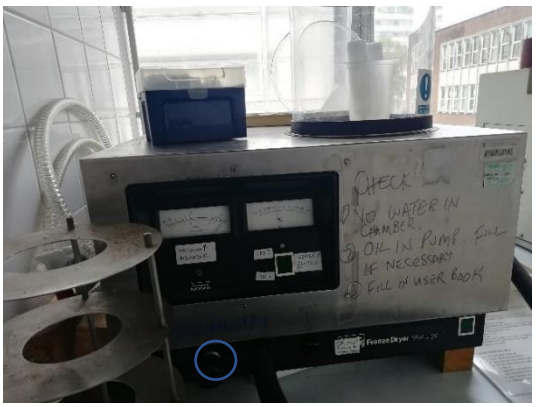

B 
C 

Figure 2.2. Components of the Modulyo freeze dryer. The air valve (circled) was tightened (A) and samples were placed under a bell jar (B) before turning on the vacuum pump (C) to initiate the freeze-drying process (Chau, 2022).

2.3.6 Protein gel electrophoresis

Novex Nupage 10% Bis-Tris Gels from ThermoFisher were used along with the MOPS-SDS running buffer with a final pH of 7.7. The protein ladder used to quantify the amount of protein was the PageRuler Prestained Protein Ladder 10 to 180kDa (Thermo Scientific, 26617). The XCell SureLock™ Mini-Cell apparatus was used for gel electrophoresis in accordance with manufacturer instructions. For analysis of the water conditioner, 150mg of freeze-dried product was added to 1ml dH_2O and vortexed thoroughly. A small volume of each sample (Table 2.4) was added to a microcentrifuge tube followed by 4.2µl loading dye, 2µl 1M DTT and dH_2O to make a total volume of 25µl. Tubes were then punctured with a needle and heated at 95°C for 5 minutes.

Table 2.4. Enzymes used in study including volume of sample added

Sample	Volume of sample added
Protease (1:10 diluted)	1.5µl
Amylase (1:100 diluted)	1.9µl
Lipase (1:10 diluted)	4.5µl
Water conditioner	3.2µl

10µl of each sample (containing 10µg of protein) and 5µl of protein standards were loaded into the wells and electrophoresis was run at 200V at room temperature for 55 minutes. The gel was then removed and left to stain with Coomassie blue stain on a See-Saw Rocker (Cole-Parmer) for 30 minutes. The gel was then destained with 10% acetic acid:10% methanol until clear bands appeared and imaged using the Bio-Rad ChemiDoc™ Imaging System. Image analysis was performed using the Bio-Rad Image Lab Software ver 6.1.

2.3.7 Lugol iodine amylase assay

Lugol iodine solution was used (Sigma, 32922). 5g of soluble starch was added to 500ml of water and boiled until transparent. In an Eppendorf, 300µl of starch and 300µl of sample was added, vortexed to ensure thorough mixing and 100µl samples were withdrawn at different time points, mixed with 100µl of Lugol solution in a microtiter plate and the colour change was observed and compared to the positive control, which was the commercial amylase solution.

2.4 Bacterial strains

In this thesis, two strains were used: *Escherichia coli* K12 and *Pseudomonas aeruginosa* PA01 (Delaney, 2018; Karagianni, 2022).

2.5 Storage and treatment

Each strain was grown overnight in LB media and 1ml of the overnight culture was added to 1ml of 40% glycerol to create glycerol stocks. The glycerol stocks were stored in a -80^{o}C fridge for long term storage.

2.6 Components of Eco3spa

Table 2.5. Overview of biofilm prevention and removal products

Name	Appearance	Functional role	Manufacturer instructions	Product number
Eco3spa Hot tub cleaner	Blue liquid	Removes biofilms from hot tubs, pipes and scale from surfaces	Empty all contents into hot tub (1200L)	1
Eco3spa Water Conditioner	Opaque liquid	Stabilises water pH and alkalinity	Add 300ml into hot tub (1200L)	2
Eco3spa Active Oxygen tablets	White tablets with blue specks	Growth prevention	Use two tablets upon first use (FA) and one tablet for subsequent use (SA) in hot tub (1200L)	3

2.6.1 Product 1 (Hot tub cleaner) dilutions

The product instructions state that 500ml should be added to hot tub water (1200L).

Therefore, 500ml is needed per 1,200,000ml water

If total volume of 480ml water is required,

1,200,000/480 = 2500x less of product needed

500/2500 = 0.2ml Hot tub cleaner required

To make a stock solution of hot tub cleaner (2x concentrated), 400µl of hot tub cleaner was added to 480ml water.

2.6.2 Product 2 (Water conditioner) dilutions

The product instructions state that 300ml should be added to hot tub water (1200L).

Therefore, 300ml is needed per 1,200,000ml water

If total volume of 500ml is required,

1,200,000/500 = 2400x less of product needed

300/2400 = 0.125ml Water Conditioner required

To make a stock solution of water conditioner (2x concentrated), 250µl of water conditioner was added to 500ml water.

2.6.3 Product 3 (Active Oxygen tablet) dilutions

The product instructions state that two tablets should be added to hot tub water (1200L) for the first use (FA). Two of the Active Oxygen sanitiser tablets weigh approximately 40g.

Therefore, 40g needed per 1,200,000ml water

If total volume of 300ml water is required,

1,200,000/300 = 4000x less of product needed

40/4000 = 0.01g Active Oxygen powder required

To make a stock solution of Active Oxygen (20x concentrated), 0.2g of Active Oxygen powder was added to 300ml water heated to 37°C and mixed until thoroughly dissolved (Fig. 2.3).

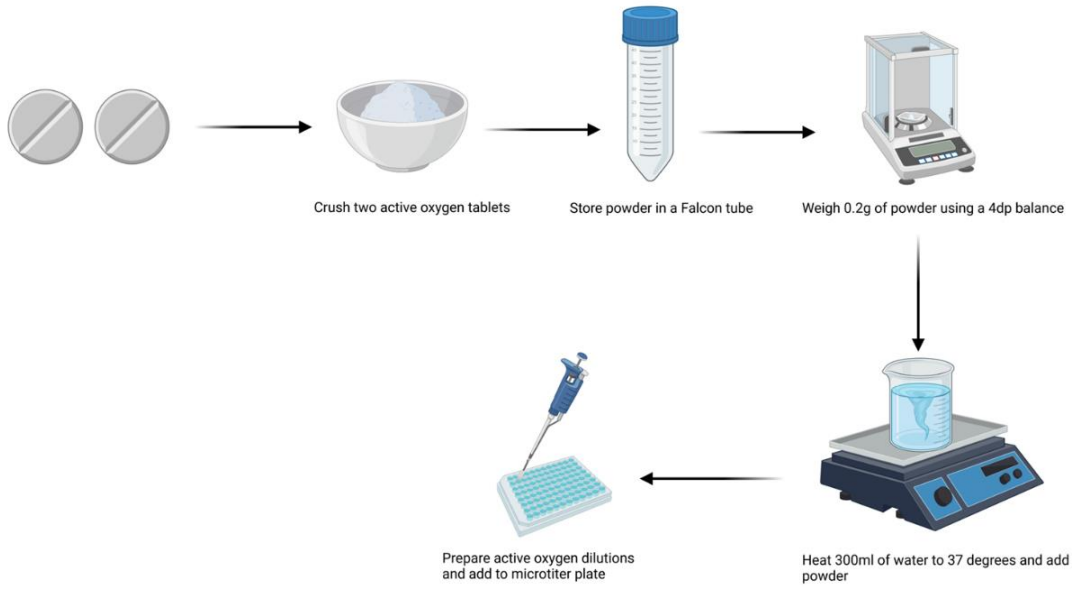

Figure 2.3. Preparation of Active Oxygen. Created with BioRender.com.

Figure 2.4 describes the series dilutions required to dilute a stock solution of Active Oxygen (20x concentrated) to achieve standard operating procedure (SOP) concentrations at the first application (SOP^{FA}) and follow on applications (SOP^{SA}).

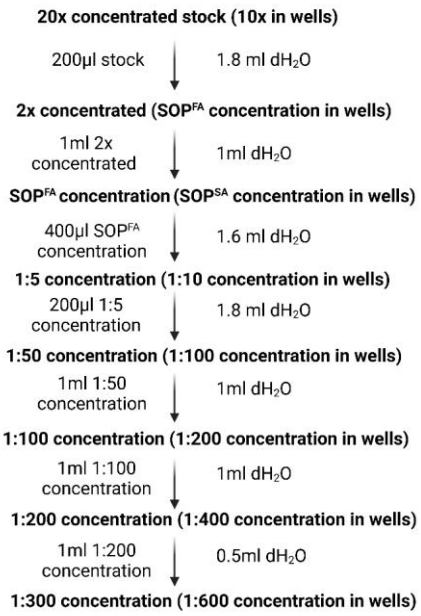

Figure 2.4. Dilution series of Active Oxygen from 20x concentrated stock solution. Created with BioRender.com.

2.7 96 well plates for static biofilm assays

For planktonic and crystal violet measurements, 96 well plates purchased from Thermo Fisher Scientific were used (table 2.6).

Table 2.6. Properties of 96 well plates used in this study

Name	Costar 3598	Nunclon Delta Surface
Material	Polystyrene	Polystyrene
Surface treatment	Tissue culture treated	Nunclon Delta-Treated
Well volume	360µl	400µl
Well working volume	75-200µl	200µl
Plate geometry	Flat bottom	Flat bottom

2.7.1 Static growth and biofilm prevention assays

Using sterile tweezers, a colony of *E. coli* or *P. aeruginosa* was obtained from a streaked LB agar plate using a sterile toothpick and placed into 5ml of M9 minimal media in a 30ml universal tube. The universal was placed in a shaking incubator set at 37°C with a speed of 200 rpm for 18 hours. The overnight culture was diluted 1:100 by pipetting 60µl of overnight culture into 5940µl of double strength media. Samples were vortexed thoroughly and 100µl was aliquoted into the wells of a 96-well plate. Wells containing 200µl of media were used as negative controls and positive control wells contained 100µl of bacteria in double strength media and 100µl dH_2O. The bacteria were diluted in double strength media to achieve single strength as the final concentration. Separate plates were used for each bacterial strain. Then, 100µl of the Active Oxygen and water conditioner dilutions were added to the wells. The plates were covered with the lids and placed in two incubators set at 37°C and 25°C for 24h.

After 24 hours, 50µl samples were pipetted into a new microtiter plate and the optical density was measured at 595nm (OD_{595}) to determine planktonic growth in a Multiskan Skyhigh plate reader with the pathlength correction setting applied. Four biological repeats were used. For *E. coli*, wells were washed once with 200µl of PBS and three washes were carried out for plates containing *P. aeruginosa*. This was followed by tapping gently into a hazardous waste bag to discard the PBS. Plates were then left to dry inverted in the flow hood for 2 hours. Cells in the biofilm were then stained with 200µl of 0.1% crystal violet solution and incubated at room temperature for 15 minutes. The crystal violet was emptied into a biohazard bag by tapping gently and rinsed by submerging in tap water three times before allowing plates to dry overnight. The crystal violet was then re-solubilised with 30% acetic acid solution in order to dissociate the crystal violet stain from materials in the biofilm before transferring to a new microtiter

plate to measure absolute biofilm formation at OD_{595} in a Multiskan Skyhigh plate reader. Absolute biofilm readings were divided by planktonic growth readings to obtain values for specific biofilm formation.

The following terms in relation to growth and biofilm are explained below:

- Planktonic growth is measured by the OD_{595} of the liquid culture in the microtiter plate
- Absolute biofilm formation is measured by the OD_{595} after staining adherent cells with crystal violet
- Specific biofilm formation is calculated by dividing the absolute biofilm reading at OD_{595} by the planktonic growth reading at OD_{595}

2.7.2 Dynamic biofilm removal assays

Biofilm removal assays were performed according to Abidi et al (2014) and Lim et al (2019) with several adaptations. Using sterile tweezers, a colony of *E. coli* or *P. aeruginosa* was obtained from a streaked LB agar plate using a sterile toothpick and placed into 5ml of M9 minimal media in a 30ml universal tube. The universal was placed in a shaking incubator set at 37°C with a speed of 200 rpm for 18 hours. The overnight culture was diluted 1:100 by pipetting 60µl of overnight culture into 5940µl of double strength media. Samples were vortexed thoroughly and 100µl was aliquoted into the wells of a 96-well plate. The plates were covered with their lids and placed in a static incubator set at 37°C for 24h. After 24 hours, samples were emptied into a biohazard waste bag and washed once with PBS (three PBS washes were required for *P. aeruginosa*). Then, 200µl of the Active Oxygen dilutions or biofilm remover were added to the wells. For product combinations, 100µl of Active Oxygen dilutions was added to 100µl of biofilm remover to reach SOP concentrations of Active Oxygen and the biofilm remover. Three replicate wells were used as a negative control containing 100µl of media and 100µl of dH_2O was added as a positive control. Then, plates were placed in a Multiskan Skyhigh plate reader set at 37°C and shaken using the medium speed option for 1h. Following incubation for 1h with shaking, the contents of each well were emptied by tapping into a biohazard waste bag. Then, each well was washed once with PBS to remove any residual product in the wells. Cells in the biofilm were then stained with 200µl of 0.1% crystal violet solution and incubated at room temperature for 15 minutes. The crystal violet was emptied into a biohazard bag by tapping gently and rinsed by submerging in tap water once before allowing plates to dry overnight. The crystal violet was then re-solubilised with 30% acetic acid solution in order to dissociate the crystal violet stain from materials in the biofilm before transferring to a new microtiter plate to measure the absolute biofilm formation at OD_{595} in a Multiskan Skyhigh plate reader. Three biological repeats were used.

2.7.3 Benchmarking of plate readers

Using sterile tweezers, a colony of *P. aeruginosa* was obtained from a streaked LB agar plate using a sterile toothpick and placed into 5ml of LB media in a 30ml universal tube. The universal was placed in a shaking incubator set at 37°C with a speed of 200 rpm for 18 hours. After growth of the overnight culture, the culture was diluted by a factor of 10 and OD measured in a spectrophotometer at OD_{595}. Dilutions were prepared in microcentrifuge tubes corresponding to the following OD_{595} values: 0.01, 0.05, 0.1, 0.2, 0.4, 0.6, 0.8 and 1. These samples were measured in Kartell semi-micro 1.5 cuvettes (Fisher Scientific) of 1.5ml capacity and 1cm path length in a DU 730 UV/Vis spectrophotomer (Beckman Coulter) to ensure the correct OD_{595} readings had been achieved by diluting the overnight culture. Then, 50µl samples of each OD preparation were pipetted into the wells of a Costar 96-well plate and the absorbance measured at OD_{595} with pathlength correction setting activated. Three biological repeats were used for each OD preparation. Wells containing only LB media were used as controls to allow pathlength correction to be applied to measurements.

2.7.4 Microplate readers

The microplate readers used in this project were FLUOstar and POLARstar Omega Microplate readers (BMG Labtech) and a Multiskan Skyhigh microplate reader (Fisher Scientific).

Omega Software v5.70 and MARS software was used for data visualization. SkanIt Software ver. 6.1.1.7 was used for data outputs and analysis from the Multiskan Skyhigh plate reader. The pathlength correction setting was applied throughout all measurements.

2.8 Generation of OD_{595} vs Total cell count vs CFU calibration curve

Using sterile tweezers, a colony of *E. coli* or *P. aeruginosa* was obtained from a streaked LB agar plate using a sterile toothpick and placed into 5ml of M9 minimal media in a 30ml universal tube. The universal was placed in a shaking incubator set at 37°C with a speed of 200 rpm for 18 hours. After growth of the overnight culture, the culture was diluted by a factor of 10 and its OD measured in a spectrophotometer at OD_{595}. Dilutions were prepared in microcentrifuge tubes (N=3) corresponding to the following OD values: 0.01, 0.05, 0.1, 0.2, 0.4, 0.6, 0.8 and 1. These samples were measured in Kartell semi-micro 1.5 cuvettes (Fisher Scientific) in a spectrophotomer to ensure the correct OD readings had been achieved by diluting the overnight culture. A series of dilutions were prepared from each OD sample by diluting the sample 1:5, 1:10 and 1:50. 75µl samples of the diluted sample were pipetted onto a Helber Thoma Chamber (Hawksley), the cover slip was placed on top and cleaned with a Kim wipe to remove any excess liquid. Cells were counted in 16 squares under a light microscope using the 40x objective lens. If cell counts fell below 35, the lower dilutions of each OD were used

instead. The number of cells per ml of sample was calculated by dividing the number of cells per square by the volume of the square per ml. This was followed by multiplication by the dilution at which cells were counted to achieve the number of cells per ml of sample.

In order to determine colony forming units (CFU) at each OD, 200µl of each sample was pipetted into a vertical row of wells in a sterile microtiter plate and serially diluted by pipetting 20µl of the first column into 180µl of water. A multichannel pipette was used to carry out each dilution and the mixing function was applied before moving onto the next serial dilution. Then, 10µl samples of each serial dilution were pipetted onto LB agar plates (N=3) and left to dry in a flow hood for 30 minutes before incubating at 16h at 37°C. Viable cell counts were determined at dilutions where an observable number of colonies could be counted using a manual cell counter. This gave the number of CFU per 10µl of sample. Therefore, to obtain the number of CFU per ml, the value was multiplied by 100. The final number of CFU/ml was calculated by multiplying by the dilution at which CFU were counted. These results allowed the generation of a calibration curve plotting the association between OD_{595}, CFU and cell count for *E. coli* and *P. aeruginosa* (Fig. 2.5). Three biological repeats were used for each data point.

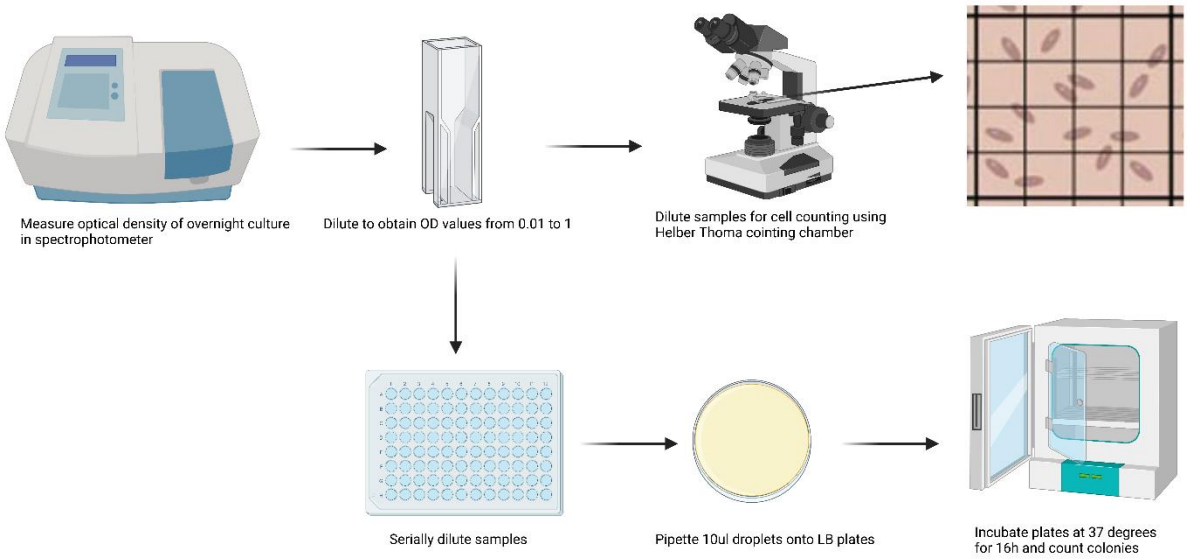

Figure 2.5. Schematic of steps required to generate OD vs Total cell count vs CFU calibration curve. Created with BioRender.com.

2.9 pH microelectrode measurements

A glass pH microelectrode (Fisher, 11716908) with BNC connector was used in combination with a Jenway 570 pH meter to measure the pH of media in microtiter plates. Initially, 100µl of media was added followed by 100µl of prepared Active Oxygen dilutions. The pH microelectrode was conditioned

prior to use by soaking in 0.1M NaOH for 5 seconds followed by rinsing with distilled water and placing in water acidified with hydrochloric acid to a pH of 4.21 for storage. The instrument was calibrated using buffer solutions at pH 7 and 10 prior to measurements. For each measurement, three biological repeats were used. The pH microelectrode was washed with distilled water between measurements to prevent the risk of contamination.

2.10 Time-kill assay

Using sterile tweezers, a colony of *E. coli* was obtained from a streaked LB agar plate using a sterile toothpick and placed into 5ml of M9 minimal media at pH 7.4 in a 30ml universal tube. The universal was placed in a shaking incubator set at 37°C with a speed of 200 rpm for 18 hours. The OD_{595} of the overnight culture was measured in a spectrophotometer before being diluted with media to OD_{595} = 0.5. Then, 100µl of the diluted overnight culture was aliquoted into the wells of the microtiter plate. Different concentrations of Active Oxygen were added, the plate covered with the lid and placed in a static incubator set at 37°C for differing time periods. Chlorine was used as a positive control in experiments.

At set time points, samples were withdrawn and serially diluted by pipetting 20µl of sample into 180µl of diluent. Following serial dilution which took place within minutes of plating, the concentration of chlorine dropped significantly. Therefore, the shortest time following exposure to chlorine was used following incubation at 37°C. As a result, sodium thiosulphate was not used as a quenching agent to neutralise biocide activity. 10µl samples were pipetted onto LB agar plates and left to dry in a flow hood for 30 minutes. For each dilution, three biological repeats were used. Plates were then incubated at 30°C for 24h and colony forming units were determined by counting the number of colonies.

2.11 Decay of Active Oxygen

Using sterile tweezers, a colony of *E. coli* was obtained from a streaked LB agar plate using a sterile toothpick and placed into 5ml of M9 minimal media at pH 7.4 in a 30ml universal tube. The universal was placed in a shaking incubator set at 37°C with a speed of 200 rpm for 18 hours.

The OD of the overnight culture was measured in a spectrophotometer before being diluted with media to OD_{595} = 0.5. Different concentrations of Active Oxygen were prepared in Eppendorf tubes, placed in a rack and incubated at 37°C for 1,3, 5 and 7 days before being added to 100µl of bacteria in 96 well plates. Each sample was serially diluted by pipetting 20µl of sample into 180µl of diluent. Then, 10µl samples were pipetted onto LB agar plates. For each dilution, three biological repeats were used. Plates were incubated at 30°C for 24h and colony forming units were determined by counting the number of colonies.

2.12 Ion chromatography (IC)

IC analysis was performed using the Dionex™ Integrion™ HPIC™ System fitted with the Dionex IonPac AS14A-5µm analytical column (3 x 150 mm), IonPac AG14-5µm guard column (3 x 30 mm) and an electrolytic suppressor (AERS500, 2mm) as shown in Fig. 2.6. A mixture of 8.0 mM sodium carbonate and 1.0 mM sodium bicarbonate prepared in MilliQ Type 1 ultrapure water with a resistance of 18.2 MΩ-cm was used as the mobile phase with a flow rate of 0.5 mL/min. The loop volume was 5µl for sample injection and Chromeleon 7.2 was used for data acquisition and analysis.

Various standards of known concentrations ranging from 25mg/L to 200mg/L were prepared by dissolving 0.0330g of sodium chloride (Sigma Aldrich) and 0.0296g of sodium sulphate (Fisher) in MilliQ Type 1 ultrapure water which was also used to dilute samples. Chlorite (Thermo Scientific, 303167) and chlorate (Thermo Scientific, 303170) standards with a concentration of 1000mg/L in deionised water were purchased from Thermo Scientific. Calibration graphs were generated for each analyte of interest in order to quantify the concentration of anions in the chlorine granules and Active Oxygen tablets.

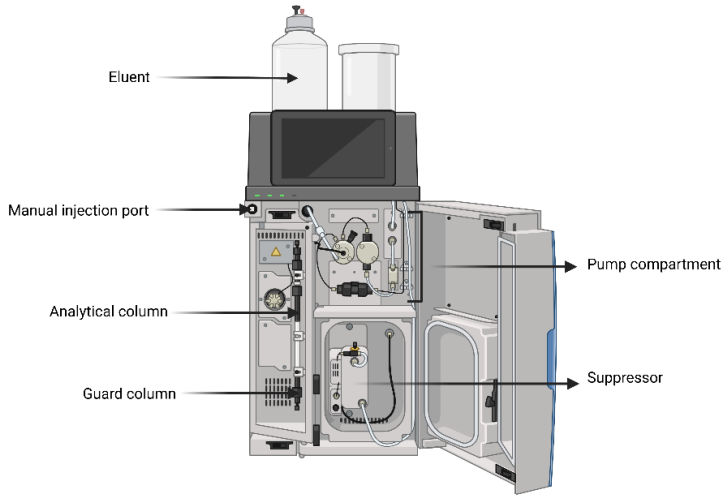

Figure 2.6. Overview of the Dionex™ Integrion™ HPIC™ System. Created with BioRender.com.

2.13 Statistical analyses

The graphing software used throughout the project was GraphPad Prism 9.3.0 and SigmaPlot 10.0. Statistical analysis was performed using GraphPad Prism 9.3.0 and IBM SPSS Statistics 28. Tests of normality such as Shapiro-Wilk were used to determine whether the data was normally or non-normally distributed. This resulted in parametric tests such as unpaired and paired t-tests, ANOVAs with Dunnett's or Tukey's multiple comparisons tests and non-parametric tests such as Mann Whitney U and Schreier-Ray-Hare tests being conducted. Significant p values in this thesis are shown by an asterisk in the following manner: * $p<0.05$, ** $p<0.01$ and *** $p<0.001$.

Chapter 3: Optimisation, calibration and benchmarking

3.1 Introduction

This chapter describes the experimental conditions that allow optimal results to be obtained in biofilm formation assays using *E. coli* K12 and *P. aeruginosa* PA01 strains which are common biofilm-forming microorganisms in hot tubs. Experimental parameters discussed along with their justification are media selection, incubation temperature, incubation time, washing/staining of biofilms and quantification of biofilms. In addition, the generation of a calibration curve in order to calculate log reductions, comparison of OD readings between plate readers and benchmarking of Active Oxygen against chlorine in preventing planktonic growth and biofilm formation is discussed here.

3.1.1 Media selection

LB media

LB media is used in the cultivation of microbial cultures due to the nutrient rich environment it provides. This results in high yields and fast growth of many bacterial species. Therefore, *E. coli* and *P. aeruginosa* are commonly grown in LB media (Christofi et al., 2019; Sezonov et al., 2007). In addition, the nutrient-rich environment provided by LB media reflects the nutrient-rich environment of the hot tub piping.

M9 minimal media

M9 minimal media is a defined microbial culture medium which provides a source of nitrogen and salts which are often supplemented with a carbon source and amino acids. Only the metabolites needed for microbial growth are provided which makes M9 minimal media an appropriate choice of media for growing *E. coli* and *P. aeruginosa* (Carfrae et al., 2020; Paliy and Gunasekera, 2007). Also, the minimal nutrient conditions provided by M9 media simulate the hot tub water environment.

3.1.2 Incubation temperature

Incubation temperatures used this project were selected in order to replicate operating conditions found in hot tubs. At hot tub maintenance temperatures, water is kept at 25^{o}C whereas a normal operating temperature of a hot tub is 37^{o}C. *E. coli* K12 can form biofilms following incubation for 24 hours at 37^{o}C (Mathlouthi, Pennacchietti and Biase, 2018) while *P. aeruginosa* has the ability to form biofilms with rigid structure at 37^{o}C and even temperatures as low as 20^{o}C (Kannan and Gautam, 2015; Kim et al., 2020).

3.1.3 Incubation time

The amount of time required to grow an overnight culture of *E. coli* K12 and *P. aeruginosa* PA01 under shaking conditions was chosen as 18 hours based on literature which shows that this is required for growth at 37^{o}C (Rasamiravaka et al., 2015). The incubation time of diluted overnight cultures in 96-

well plates at 25°C and 37°C was selected in order to allow sufficient biofilms to grow. Previous studies demonstrate that 24-hour incubation time periods are needed for *E. coli* and *P. aeruginosa* to form biofilms (Cochran et al., 2000; Skandamis et al., 2009). Therefore, samples were incubated for 24 hours to allow sufficient biofilm formation.

1.3.4 Phosphate Buffered Saline (PBS) washes

PBS is a sterile salt solution often used in washing steps, transport media for cells or tissue and dilution steps. In this project, PBS was used to wash away any non-adherent planktonic cells prior to crystal violet staining so that quantification of biofilm formation and specific biofilm could be carried out. Successful removal of planktonic cells as well as excess dye is noted in literature (Hung et al., 2013). Furthermore, previous experiments show that three PBS washes are required to remove adherent planktonic cells of *P. aeruginosa* in 96 well plates (Anversa et al., 2019; Delaney, 2018; Kaya et al., 2020). However, for *E. coli*, only one PBS wash is needed to remove *E. coli* planktonic cells since further washes lead to subsequent degradation of biofilms, under-quantification and large variance (Delaney, 2018).

1.3.5 Crystal violet solution

Crystal violet is a vital part of the biofilm formation assay which stains adherent cells in biofilms by binding to negatively charged surfaces present in cell membrane surfaces or polysaccharides in biofilm matrices (Li, Yan and Xu, 2003). Several studies show that 0.1% solutions of crystal violet are appropriate for biofilm formation assays. After wells are washed with PBS, crystal violet is added and incubated at room temperature for 15 minutes which is consistent with published protocols for crystal violet staining for *E. coli* and *P. aeruginosa* by O'Toole (2011).

1.3.6 Acetic acid solubilization

Acetic acid is used to resolubilize cells stained by crystal violet. Appropriate concentrations of acetic acid are prepared as a 30% v/v solution which is commonly used in measuring biofilm formation levels of *E. coli* and *P. aeruginosa* (Buck et al., 2021; Hwang et al., 2021). Samples re-solubilized with 30% acetic acid is in accordance with published protocols (Merritt, Kadouri and O'Toole, 2005).

1.3.7 Edge effect in microtiter plates

A drawback of the biofilm formation assay conducted in 96 well plates is the edge effect which shows that corner and edge wells suffer from evaporation in comparison to inner wells of the plate. Addition of bacterial cells to outer wells can cause a 35% reduction in metabolic activity compared to central wells (Mansoury et al., 2021). Furthermore, planktonic cell growth and biofilm formation levels of *E. coli* K12 and *P. aeruginosa* PA01 in outer wells of microtiter plates have been found to exhibit higher optical densities compared to inner wells (Karagianni, 2022). Therefore, studies aim to mitigate the

edge effect by storing plates with adhesive seals to prevent evaporation or adding buffer or water in wells to reduce levels of evaporation (Shukla and Rao, 2017). Due to issues caused by the edge effect, experiments conducted in this project only utilised the inner wells of the 96 well plate.

3.2 Results

3.2.1 OD_{595} vs Total cell count vs CFU calibration curve

Optical density measurements can vary between cell numbers, size and morphology (Stevenson et al., 2016). Therefore, a calibration curve was required in order to relate total cell counts and colony forming units to OD measurements. In addition, assays conducted based on OD measurements required fewer resources and were much quicker as this was only a one-year project. Calibration curves were also needed in order to calculate log reduction data following exposure to Active Oxygen.

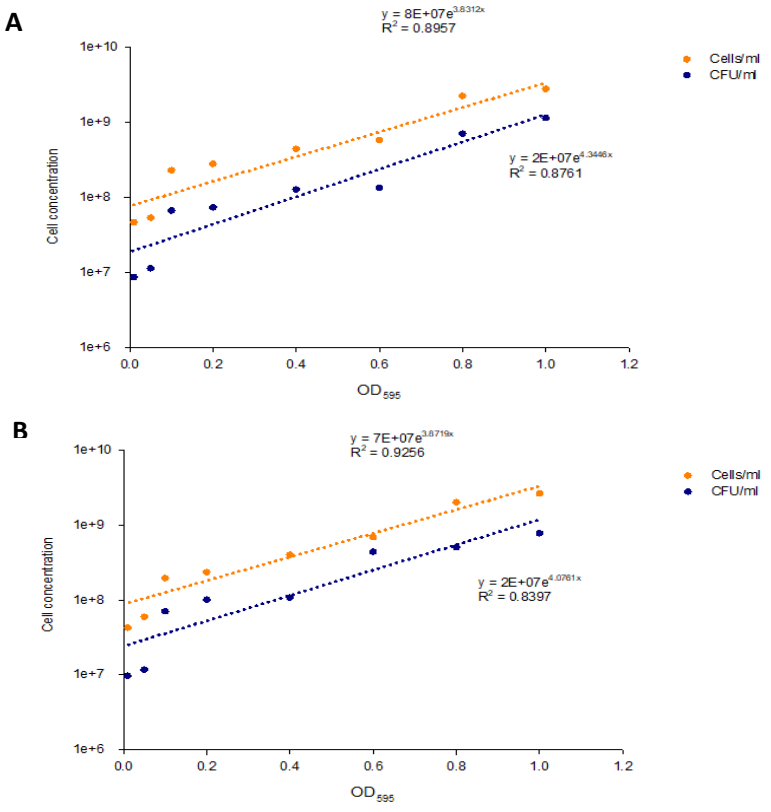

Figure 3.1. Relationship between optical density at 595nm (OD_{595}), total cell count (cells/ml) and colony forming units (CFU/ml) of *E. coli* K12 (A) and *P. aeruginosa* PA01 (B). Each bacterial strain was grown in LB media and diluted to optical densities ranging from 0.01 to 1. Trendline equations are shown for each set of data. N=3 for each data point with error bars illustrating standard error of the mean (SEM).

Each calibration graph spans a range of 4 logs incorporating optical densities (OD_{595}) between 0.01 and 1 (Fig. 3.1). Trendline equations obtained for total cell counts per ml for both bacterial strains exceed

trendlines observed for CFU counts per ml. This is expected since total cell counts involve the counting of live and dead cells which would contribute to higher trendline values. In addition, the relationship between OD and CFU counts per ml for both bacterial species are denoted by trendline equations being $y = 2E+07e^{4.3446x}$ and $y = 2E+07e^{4.0761x}$ respectively.

3.2.2 Benchmarking of plate readers

Plate readers are useful instruments for measuring bacterial growth and biofilm formation levels based on OD readings. However, differences in readings between plate readers can arise based on background absorbance given off in neighboring wells and surface treatment (Pape-Bub, 2020). In addition, there is a lack of studies which compare OD measurements between different plate readers. Therefore, it was decided to assess the accuracy of different plate readers by comparing OD measurements taken from a spectrophotomer and several plate readers with pathlength correction applied.

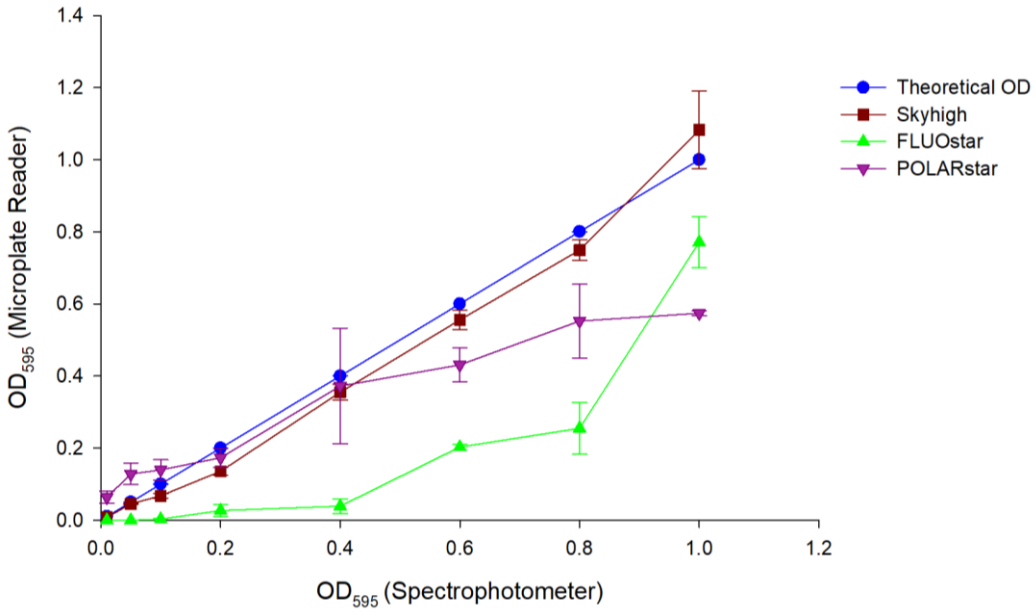

Figure 3.2. Comparison between optical density measurements of *P. aeruginosa* grown in LB media at 595nm (OD_{595}) in a spectrophotometer and in Skyhigh, FLUOstar and POLARstar plate readers. Pathlength correction was applied to each set of data. N=3 for each data point with error bars illustrating standard error of the mean (SEM).

The optical densities measured in different plate readers and the spectrophotometer are shown in Fig. 3.2. The Skyhigh plate reader gave the most accurate values which are in accordance with the theoretical optical densities expected. However, POLARstar optical density measurements deviated where values expected at OD= 1 were 40% lower. Extremely low OD values were obtained with the FLUOstar plate reader which did not match the theoretical OD values expected. However, it is important to note that previous damage to the FLUOstar plate reader may have affected these

readings. Based on these results, it was decided going forward that the Skyhigh plate reader was the best option for OD measurements in experiments. This provides insights into the comparisons of results in this study to those generated previously (Delaney, 2018; Karagianni, 2022).

3.2.3 Benchmarking of Active Oxygen against chlorine

In order to demonstrate the efficacy of Active Oxygen in comparison to common products used for water sanitation, recommended concentrations of chlorine in hot tubs (3ppm and 5ppm) were tested for their ability to prevent planktonic growth and biofilm formation. The pH values used in these experiments range from 7 to 8 based on literature by Deborde and Gunten (2008) which shows that chlorine displays optimal activity at around pH 7.4. The data was analysed statistically as referred to in Chapter 2 (see section 2.13). This led to unpaired t-tests and Mann Whitney U-tests being conducted. These tests were used to determine any significant differences in efficacy between chlorine and Active Oxygen in preventing planktonic growth and biofilm formation of *E. coli* and *P. aeruginosa*.

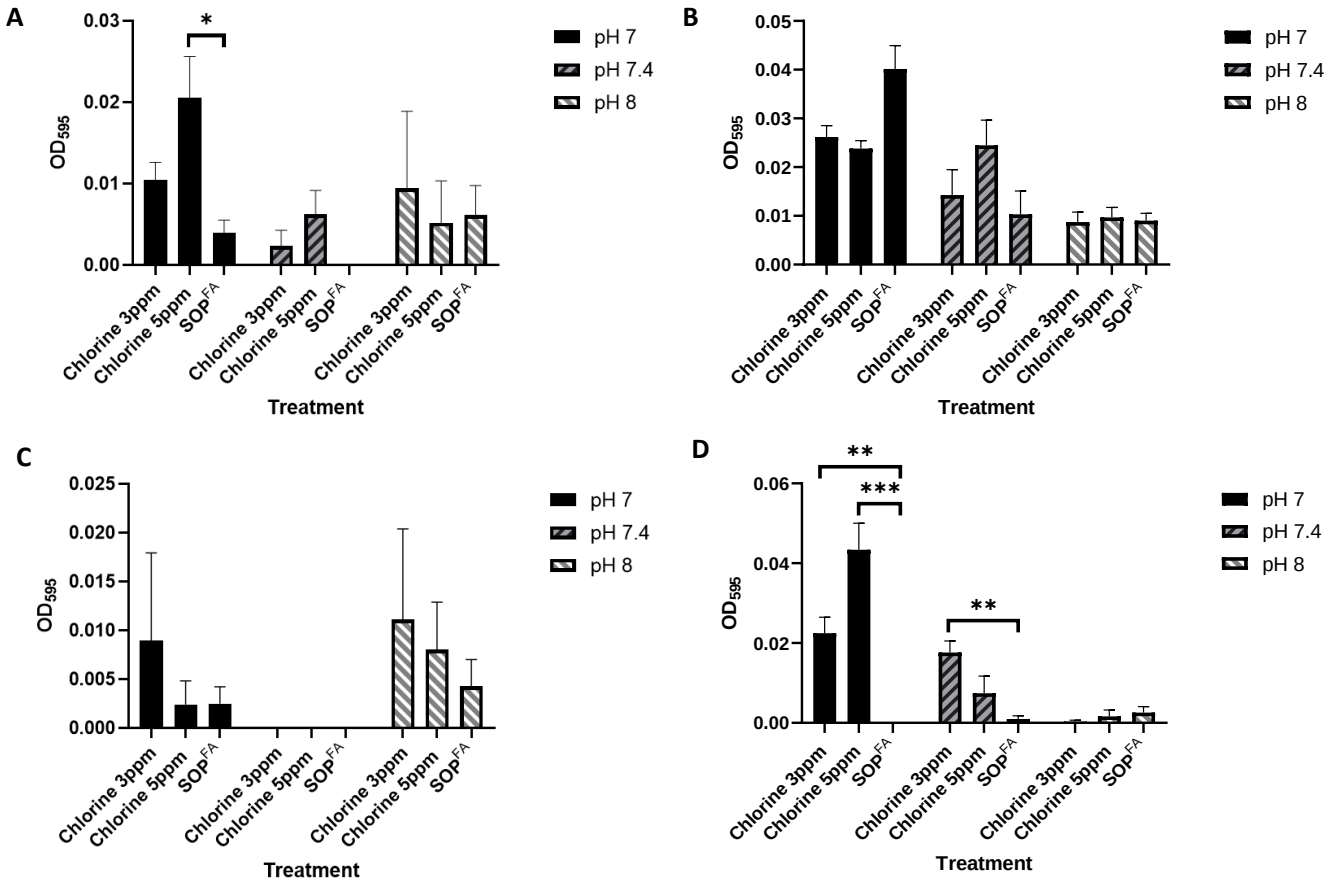

Figure 3.3. Impact of pH on chlorine and Active Oxygen to prevent planktonic growth (A and C) and biofilm formation (B and D) of *E. coli* K12 grown in M9 minimal media (indicated as OD_{595}) at 25°C (top) and 37°C (bottom). Initial dosage is the addition of two Active Oxygen tablets to hot tub water (labelled as SOP^{FA}) and recommended concentrations of chlorine are 3ppm and 5ppm. N=4 for each data point and error bars represent standard error of the mean (SEM).

Figures 3.3 and 3.4 show the effect of pH on the efficacy of Active Oxygen and chlorine to prevent planktonic growth and biofilm formation at recommended concentrations used in hot tubs. Across all pH values tested, the use of Active Oxygen at the initial dosage in hot tubs resulted in very low levels of planktonic growth of *E. coli* at 25°C. In addition, higher levels of planktonic growth were observed at pH 7 and 8 using chlorine at recommended concentrations in hot tubs. A statistically significant difference was found between chlorine at 5ppm and SOP^{FA} at pH 7 ($p = 0.0209$, unpaired t-test). Slightly higher levels of biofilm formation were observed for SOP^{FA} at pH 7 in comparison to chlorine at 3ppm and 5ppm. However, the error bar shown for this data point is larger which would cause a higher value to be shown. At pH 7.4 and 8, adding Active Oxygen resulted in values below 0.02 whereas at pH 7.4, addition of chlorine appeared to increase biofilm formation. At 37°C, Active Oxygen was effective at preventing planktonic growth of *E. coli* without losing efficacy over all pH values tested. In particular,

at pH 7.4 all treatments were effective at preventing planktonic growth whereas higher planktonic growth was seen at pH 7 and 8 using chlorine at 3ppm and 5ppm. In regards to biofilm formation, little to no biofilm formation was seen across all pHs tested using Active Oxygen. Statistical analyses at pH 7 and 7.4 showed statistically significant differences illustrating that Active Oxygen performs better than chlorine at preventing biofilm formation at 37°C ($p = 0.0014$, $p = 0.0006$ and $p = 0.0015$, unpaired t-test). It is also evident that at pH 7, higher levels of biofilm formation are observed using chlorine at 3ppm with higher concentrations causing greater levels of biofilm to be formed.

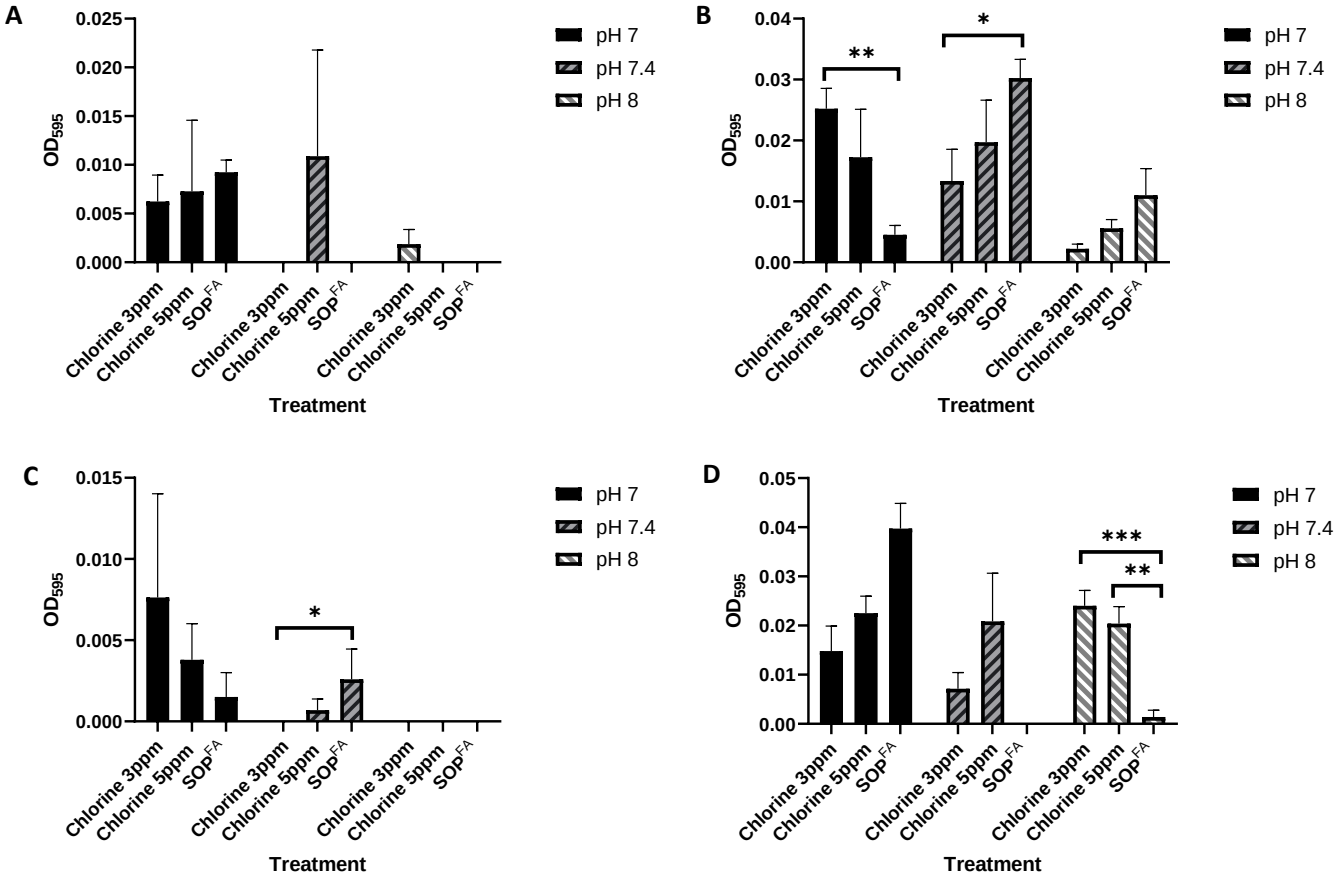

Figure 3.4. Impact of pH on chlorine and Active Oxygen to prevent planktonic growth (A and C) and biofilm formation (B and D) of *P. aeruginosa* PA01 grown in M9 minimal media (indicated as OD_{595}) at 25°C (top) and 37°C (bottom). Initial dosage is the addition of two Active Oxygen tablets to hot tub water (labelled as SOP^{FA}) and recommended concentrations of chlorine are 3ppm and 5ppm. N=4 for each data point and error bars represent standard error of the mean (SEM).

Following exposure to Active Oxygen at 25°C, Active Oxygen is able to completely inhibit planktonic growth of *P. aeruginosa* at pH 7.4 and 8. The highest levels of planktonic growth were observed at pH 7 where Active Oxygen performed similarly to chlorine in preventing planktonic growth. Furthermore, Active Oxygen performed as well as chlorine in preventing biofilm formation across all pHs tested

whereas the efficacy of chlorine was affected at pH 7. Comparisons between chlorine at 3ppm and Active Oxygen returned significance at both pH 7 and 7.4 ($p = 0.0014$ and $p = 0.0309$, unpaired t-test). At 37°C, little to no planktonic growth was observed across all pH following treatment with Active Oxygen. Active Oxygen did not lose efficacy over the pH values tested whereas higher planktonic growth was observed when *P. aeruginosa* was treated with chlorine at pH 7.4 ($p = 0.0286$, Mann Whitney U-test). All treatments were able to completely prevent planktonic growth at pH 8 in comparison to other pHs. Active Oxygen performed optimally in preventing biofilm formation at pH 7.4 and 8 in comparison to chlorine with OD_{595} values being below 0.01 which showed statistical significance ($p = 0.0005$ and $p = 0.0022$, unpaired t-test). In addition, chlorine was less effective at preventing biofilm formation at pH values outside its stated pH for optimal activity.

3.3 Discussion

3.3.1 OD_{595} vs Total cell count vs CFU calibration curve

Cell counting using counting chambers and CFU enumeration are valuable tools for estimating the cell density of *E. coli* and *P. aeruginosa* in LB media (Bapat et al., 2006; Hazan et al., 2012; Nguyen et al., 2018). *E. coli* cell counts obtained at OD of 0.4 are approximately 4×10^8 cells/ml. This is in accordance with cell counts observed by Stevenson et al (2016) at the same OD. In addition, *E. coli* cell counts at OD of 0.8 are approximately 2×10^9 cells/ml. This is in agreement with figures seen by Sohbatzadeh, et al (2010). With regards to *P. aeruginosa*, viable cell counts at ODs below 0.1 correspond with figures reported by Hsieh et al (2014) measured at OD_{595}. Also, *P. aeruginosa* viable cell counts measured at OD of 1 are approximately 8×10^8 cells/ml which is consistent with *P. aeruginosa* PA01 cell counts stated in literature (Badar et al., 2010). Furthermore, linear relationships between OD and viable cell counts (CFU/ml) denoted by trendline equations for both species are $y = 2E+07e^{4.3446x}$ and $y = 2E+07e^{4.0761x}$ which are closely related with trendline equations derived from calibration curves in previous studies (Kim et al., 2012).

3.3.2 Benchmarking of plate readers

There is a lack of information which discusses differences in OD measurements between microplate readers. Previous data has found that OD measurements between different spectrophotometers can vary significantly in liquid cultures of *E. coli* (Stevenson et al., 2016). Microplate measurements in this study used pathlength correction which normalises OD readings to give values that correspond with absorbance found in a standard cuvette with 1cm path length. Optical density measurements taken from a spectrophotometer, Skyhigh, FLUOstar and POLARstar plate reader with pathlength correction demonstrated that the Skyhigh plate reader gave the most accurate readings in comparison to theoretical ODs measured in cuvettes in a spectrophotometer whereas the FLUOstar plate reader

deviated at each OD. However, previous damage to the FLUOstar plate reader at the time of measurement is a major factor to be considered. Optical density measurements in the spectrophotometer and Skyhigh plate reader is replicated in studies by Abkar et al (2022) and Warren (2008) which both show similar OD readings in spectrophotomers and pathlength corrected readings from plate readers.

3.3.3 Benchmarking of Active Oxygen against chlorine

In planktonic prevention assays, Active Oxygen was found to perform better than chlorine at preventing planktonic growth of *E. coli* at pH 7 and 8 which was confirmed as significant by statistical testing between chlorine and Active Oxygen. This is in agreement with the distribution of chlorine species at 25°C described by Deborde and Gunten (2008) which indicates that chlorine loses efficacy at pH values outside of its optimum at around pH 7.4. Interestingly, at pH 7.4, the optimum pH for chlorine efficacy against planktonic cells, treatment appeared to cause increased levels of biofilm formation. Comparison between chlorine-based disinfectants against *E. coli* in biofilms after 2 hours of exposure a high number of bacteria are still able to survive (Farkas et al., 2014). This suggests that higher levels of biofilm formation could be linked with repeated exposure to chlorine. In addition, chlorine displayed optimal activity in preventing planktonic growth and biofilm formation of *E. coli* at pH 7.4 whereas activity was affected by changes in pH. Active Oxygen did not lose efficacy in preventing planktonic growth and biofilm formation across all pH values tested at 37°C. Significantly different levels of biofilm formation were found between chlorine and Active Oxygen treatments. This indicates that Active Oxygen exhibits higher efficacy than chlorine in preventing biofilm formation across all pHs tested.

Furthermore, Active Oxygen completely prevented planktonic growth of *P. aeruginosa* at 25°C at pH 7.4 and 8 whereas growth was still seen with cells treated with chlorine. Active Oxygen performed as well as chlorine in preventing biofilm formation across all pHs tested with statistical significance being found between chlorine and Active Oxygen treatments at pH 7. Strong efficacy against planktonic growth was observed at 37°C across all pH values for Active Oxygen except at pH 7.4 where higher levels of planktonic growth were observed which a Mann Whitney U-test found to be statistically significant. Loss of efficacy was observed for chlorine at pH values outside its optimum whereas the efficacy of Active Oxygen was generally maintained across all pH values. This was confirmed as statistically significant between chlorine and Active Oxygen treatments at pH 7.4 and 8.

These results show that the efficacy of Active Oxygen to prevent planktonic growth and biofilm formation is maintained across a defined pH range from 7 to 8 at normal operating temperatures and maintenance temperatures in hot tubs. An explanation for the higher efficacy of Active Oxygen

compared to chlorine could be due to the effect of acetic acid used in the resolubilization of crystal violet. Acetic acid tested at concentrations of 0.31% v/v and lower has been shown to be effective in preventing biofilm formation of *E. coli* and *P. aeruginosa* in crystal violet assays. Further experiments show that acetic acid at concentrations from 0.16% to 5% v/v exhibit a dose dependent manner in preventing biofilm formation of *P. aeruginosa* (Halstead et al., 2015). This suggests that acetic acid could have a direct impact in preventing biofilm formation. Previously, acetic acid has been shown to have antibacterial activity against *E. coli* and *P. aeruginosa* both in the planktonic and biofilm states (Bjarnsholt et al., 2015). However, only the mechanisms involved in the killing of planktonic bacteria have been addressed with limited studies investigating the mechanisms on bacteria present in biofilm matrices. Kundukad et al (2017) utilised a microfluidic system to assess the effect of acetic acid on biofilms formed by *P. aeruginosa*. Live-dead staining procedures revealed that the absence of live cells stained with green fluorescent protein was due to the killing action of acetic acid. This conveyed that acetic acid penetrates the biofilm matrix and diffuses through the cell wall of *P. aeruginosa* causing acidification of cytoplasmic contents, protein denaturation and DNA damage resulting in cell death.

In addition, loss of activity of chlorine at pH values outside its optimum is consistent with previous project results (Karagianni, 2022) which coupled with degradation by sunlight highlights the need for an alternative sustainable option which can overcome these problems. Therefore, Active Oxygen is an attractive option for preventing planktonic growth and biofilm formation of *E. coli* and *P. aeruginosa* in hot tubs.

Chapter 4: Efficacy of Active Oxygen, water conditioner and product combinations on growth and biofilm prevention under static conditions including effects on cell viability and cell morphology

4.1 Introduction

In this chapter, the efficacy of Eco3spa's products were investigated for their ability to prevent planktonic growth and biofilm formation under static conditions. The Eco3spa Water conditioner (Product 2) is added every month which softens water and hydrates skin since it is comprised of coconut and plant extracts. The Water conditioner is intended for use in addition with Eco3spa Water Sanitiser tablets (Product 3) which form Active Oxygen species that exhibit antibacterial properties. Initially, two Active Oxygen tablets are added to the hot tub and follow on applications before using the hot tub requires one additional tablet. These are represented in experiments as SOP^{FA} and SOP^{SA}. As the company's main focus was on Active Oxygen, various concentrations were tested for their efficacy in preventing planktonic growth and biofilm formation to generate a dose response curve. An important aim of the project was to assess the efficacy of Active Oxygen over a wider pH range. Therefore, biofilm prevention assays utilising Active Oxygen were conducted over a pH range from 5.2 to 8. Log reduction experiments following exposure to Active Oxygen at different concentrations are also shown here which were derived from calibration curves shown in Chapter 3. The Water conditioner and Active Oxygen products were added alone or in combination with each other and their effect on planktonic growth and biofilm formation of *E. coli* K12 and *P. aeruginosa* PA01 is described here. The project also aimed to determine how long Active Oxygen takes to kill bacteria and the stability of Active Oxygen at first and follow on applications after being added to water. As a result, cell viability assays were conducted using *E. coli* K12 grown in minimal media M9 at pH 7.4 to investigate the time dependency and stability of Active Oxygen. Furthermore, previous project results indicated that Active Oxygen in combination with Product 2 could possibly lead to the cells adopting a viable but non culturable (VBNC) state. Therefore, it was decided to repeat light and fluorescent microscopy experiments under statistically robust conditions to confirm if the same observations were seen.

4.2 Results

4.2.1 Appearance of overnight cultures in M9 minimal media

As additional pH values were investigated to provide more insights into the effect of pH on the efficacy of Active Oxygen, cultures of *E. coli* K12 grown in M9 minimal media were also observed for their appearance following overnight incubation (Fig. 4.1).

A

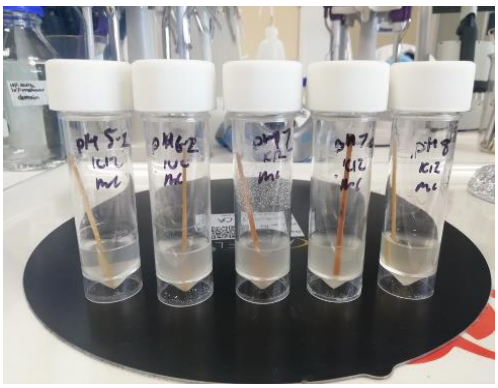

B

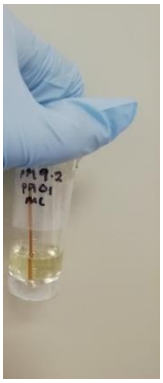

Figure 4.1. Appearance of overnight cultures of *E. coli* (A - from left to right: pH 5.2, 6.2, 7, 7.4, 8) and *P. aeruginosa* (B - pH 9.2) grown in M9 minimal media (Chau, 2022).

The colour of overnight cultures of *E. coli* grown in M9 minimal media under shaking conditions changed from clear to a pale white colour following incubation at 37°C for 18 hours. However, *E. coli* overnight cultures grown in M9 minimal media at pH 5.2 showed a very pale white colour with low turbidity in comparison to all other pHs (Fig. 4.1A). Overnight cultures of *P. aeruginosa* also showed low levels of growth at pH 5.2 where the optical density measured at 595nm in a spectrophotometer was found to be 0.360. In addition, overnight cultures of *P. aeruginosa* were also grown in M9 minimal media at pH 9.2 to investigate the effect of extreme pH values. The colour of the media turned from clear to light yellow with no growth being observed which was confirmed by OD measurements in a spectrophotomer which was found to be zero (Fig. 4.1B). Therefore, it was decided to use overnight cultures grown in M9 minimal media at pH 5.2 as opposed to pH 9.2 for further experiments.

4.2.2 pH microelectrode results

To evaluate the effect of Active Oxygen on the pH of M9 minimal media, a glass pH microelectrode was used to measure the pH of media in microtiter plates following the addition of different concentrations of Active Oxygen (Fig. 4.2).

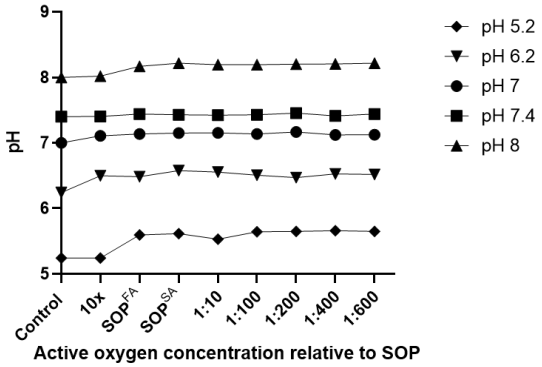

Figure 4.2. Effect of Active Oxygen concentration on pH of M9 minimal media. N=3 for each data point.

Across all Active Oxygen concentrations, there were small changes in pH when added to media. The pH of media at pH 7, 7.4 and 8 remained relatively consistent upon addition of Active Oxygen at all concentrations. The most notable increases in pH were observed when Active Oxygen was added to the media at pH 5.2 and 6.2. The pH of media at 5.2 increased by 0.42 pH units at the Active Oxygen 1:400 concentration whereas media at pH 6.2 rose by 0.34 pH units at the SOP^{SA} concentration.

4.2.3 Prevention of planktonic growth following treatment with Active Oxygen

Various concentrations of Active Oxygen were tested for their efficacy in preventing planktonic growth of *E. coli* K12 (Fig. 4.3) and *P. aeruginosa* (Fig. 4.4) in M9 minimal media following static incubation at 25°C or 37°C for 24h. Since there is a lack of information regarding the effect of pH on the activity of Active Oxygen and the previous project only tested pHs from 7 to 8, the following results show the activity of Active Oxygen over a pH range from 5.2 to 8. The initial dosage of Active Oxygen is two tablets added to hot tub water (SOP^{FA}) and follow on applications prior to each hot tub use require one additional tablet (SOP^{SA}).

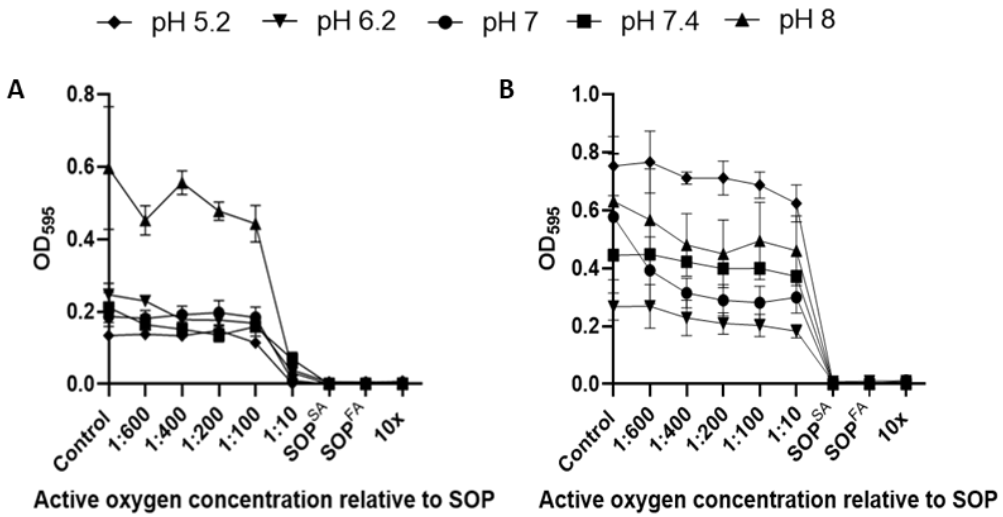

Figure 4.3. Impact of pH on efficacy of Active Oxygen to prevent planktonic growth of *E. coli* K12 in M9 minimal media (indicated as OD_{595}) at 25°C (A) and 37°C (B). Initial dosage is the addition of two Active Oxygen tablets to hot tub water (labelled as SOP^{FA}) and follow on applications require the use of one additional tablet (SOP^{SA}). N=4 for each data point and error bars represent standard error of the mean (SEM).

At 25°C, addition of Active Oxygen at 10x, SOP^{FA} and SOP^{SA} concentrations successfully prevented planktonic growth of *E. coli* across all pHs tested (Fig. 4.3A). One-way ANOVAs with Dunnett's multiple comparisons tests at the same concentrations confirmed that these were statistically significant reductions in planktonic growth compared to untreated controls across all pHs tested (all $p<0.001$).

Low levels of planktonic growth were also observed at the 1:10 Active Oxygen concentration whereas at sublethal concentrations (1:100,1:200,1:400 and 1:600), sharp increases in planktonic growth were observed. One-way ANOVAs found that Active Oxygen at 1:10,1:100, 1:200 and 1:400 concentrations were able to significantly reduce planktonic growth at pH 6.2 (all $p<0.05$). Additional statistical analyses between datasets in all other pHs did not return statistical significance. Optical density measurements across all treatments from pH 5.2 to 7 were similar with the highest OD_{595} values only exceeding 0.2. However, concentrations lower than 1:10 Active Oxygen at pH 8 caused sharp increases in planktonic growth which were more elevated in comparison to values obtained at the other pH values.

Active Oxygen concentrations ranging from 10x concentrated to SOP^{SA} also prevented planktonic growth of *E. coli* at 37°C across all pHs tested (Fig. 4.3B). This was confirmed by one-way ANOVAs with Dunnett's multiple comparisons tests conducted across all pHs which were significantly different to control wells (all $p<0.01$). In addition, Active Oxygen concentrations 1:10 and lower led to higher levels of planktonic growth which was evident across all pHs tested. Despite there being a small difference in OD measurements between *E. coli* treated with Active Oxygen at 1:10 concentration and untreated control wells, one-way ANOVAs returned statistical significance was found at pH 7.4 ($p=0.0071$). The highest planktonic growth was found at pH 5.2 followed by pH 8, pH 7, pH 7.4 and pH 6.2.

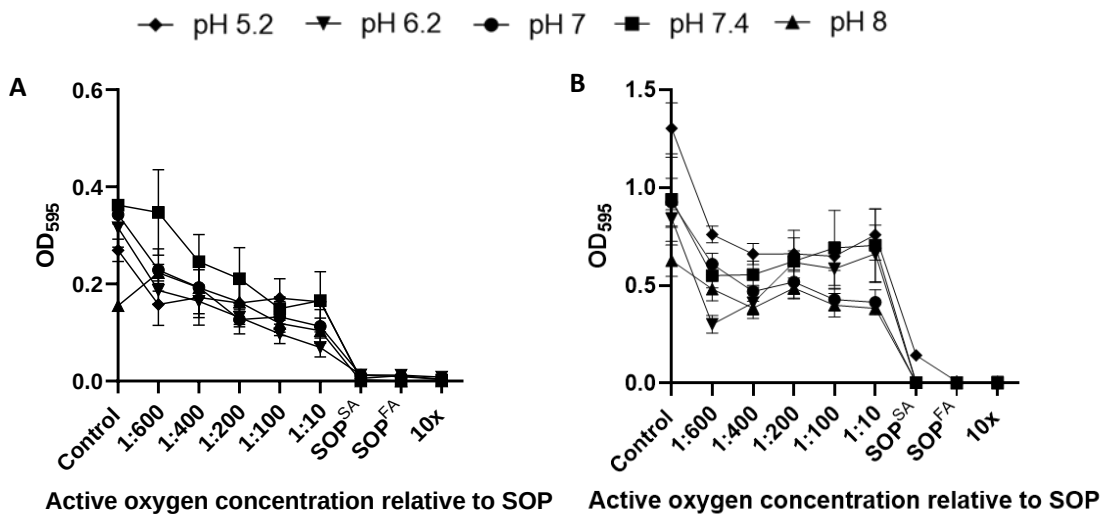

Figure 4.4. Impact of pH on efficacy of Active Oxygen to prevent planktonic growth of *P. aeruginosa PA01* in M9 minimal media (indicated as OD_{595}) at 25°C (A) and 37°C (B). Initial dosage is the addition of two Active Oxygen tablets to hot tub water (labelled as SOP^{FA}) and follow on applications require the use of one additional tablet (SOP^{SA}). N=4 for each data point and error bars represent standard error of the mean (SEM).

Furthermore, Active Oxygen at concentrations from 10x concentrated to SOP^{SA} were effective at reducing planktonic growth of *P. aeruginosa* at 25°C (Fig. 4.4A). However, very low levels of planktonic growth could be seen at pH 5.2, 6.2 and 7. This was not observed at pH 7.4 and 8 where the same concentrations of Active Oxygen successfully prevented planktonic growth of *P. aeruginosa*. One-way ANOVAs showed statistical significance across all pHs tested for Active Oxygen concentrations ranging from 10x concentrated to SOP^{SA} (all $p<0.001$). Active Oxygen concentrations at 1:10 resulted in higher levels of planktonic growth which was consistent across all pHs tested. Interestingly, sublethal concentrations of Active Oxygen were also found to cause significant reductions in planktonic growth at pH 7 (1:10, 1:100, 1:200 and 1:400) and pH 7.4 (1:10 and 1:100) where one-way ANOVAs returned statistical significance (all $p<0.05$). Interestingly, all concentrations of Active Oxygen returned significant outcomes in reducing planktonic growth of *P. aeruginosa* at pH 6.2 (all $p<0.01$).

At 37°C, Active Oxygen at concentrations from 10x concentrated to SOP^{SA} successfully prevented planktonic growth of *P. aeruginosa* across all pHs except 5.2 where growth was observed at the follow-on application (SOP^{SA}) as shown in Fig. 4.4B. One-way ANOVAs with Dunnett's multiple comparisons tests showed statistical differences between Active Oxygen concentrations from 10x concentrated to SOP^{SA} across all pHs tested (all $p<0.001$). All concentrations of Active Oxygen significantly decreased planktonic growth of *P. aeruginosa* at pH 5.2 and 7 ($p<0.01$). Active Oxygen at concentrations 1:400 and 1:600 appeared to have higher efficacy in reducing planktonic growth of *P. aeruginosa* compared to other sublethal concentrations (1:10 to 1:200) at pH 6.2 and 7.4. This was confirmed by one-way ANOVAs which returned statistical significance at pH 6.2 at 1:400 and 1:600 concentrations ($p<0.05$). At pH 8, the only sublethal concentrations of Active Oxygen which caused significant reductions in planktonic growth were 1:10, 1:100 and 1:400 respectively (all $p<0.01$). In addition, the highest levels of planktonic growth were observed at the pH 5.2. whereas low levels of planktonic growth were observed at pH 8.

4.2.4 Prevention of biofilm formation following treatment with Active Oxygen

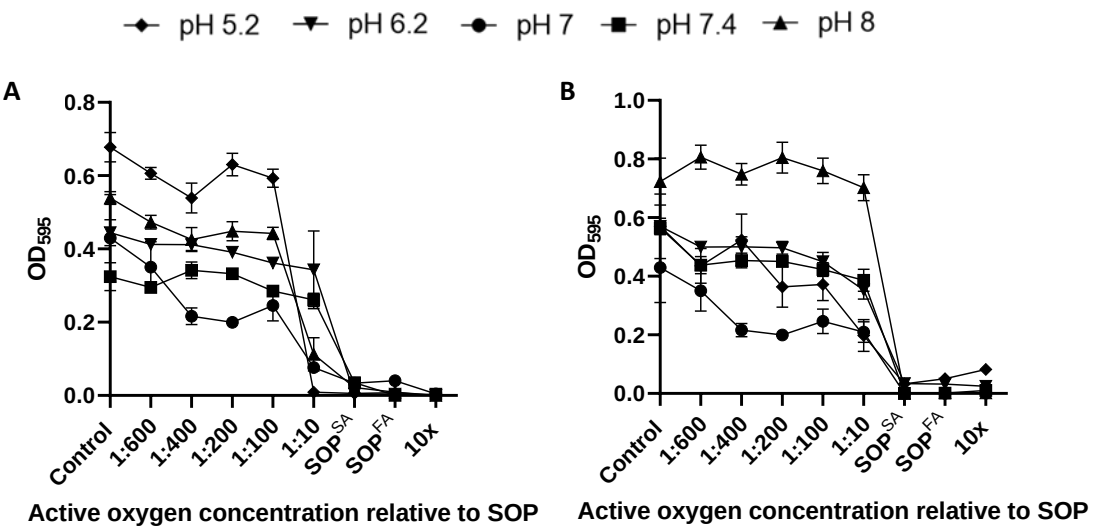

Figure 4.5. Impact of pH on efficacy of Active Oxygen to prevent biofilm formation of *E. coli* K12 in M9 minimal media (indicated as OD_{595}) at 25°C (A) and 37°C (B). Initial dosage is the addition of two Active Oxygen tablets to hot tub water (labelled as SOP^{FA}) and follow on applications require the use of one additional tablet (SOP^{SA}). N=4 for each data point and error bars represent standard error of the mean (SEM).

At the lowest pH tested, Active Oxygen concentrations from 10x concentrated ranging from 10x concentrated to 1:10 caused low levels of *E. coli* biofilm formation at 25°C (Fig. 4.5A) which one-way ANOVAs found statistically lower compared to control wells (all $p<0.001$). This was accompanied by a sharp rise in biofilm formation levels at Active Oxygen 1:100 concentration which was 66 times higher than that at the 1:10 concentration. The efficacy of Active Oxygen at the 1:400 concentration was higher than other sublethal concentrations at both pH 5.2 and 8 which also returned significant outcomes in one-way ANOVAs ($p=0.0024$ and $p=0.0116$). At pH 7, only 10x concentrated Active Oxygen was able to successfully prevent biofilm formation of *E. coli* which was followed by very low levels of biofilm formation detected at first and follow on applications. Active Oxygen at 1:200 and 1:400 concentrations also displayed higher efficacy in comparison to the remaining sublethal concentrations at pH 7. One-way ANOVAs indicated that these Active Oxygen concentrations resulted in significantly lower biofilm formation levels (all $p<0.05$). Extremely low levels of biofilm formation were found at Active Oxygen concentrations from 10x concentrated to SOP^{SA} across all pHs which one-way ANOVAs found statistically significant compared to control wells (all $p<0.001$) with the largest increases in biofilm formation levels observed at pH 7.4 and 8 as Active Oxygen concentration decreased. Sharp

rises in biofilm formation levels between SOP^{SA} and 1:10 are seen at pH 6.2 and 7.4 whereas there was less variation between OD measurements at pH 7 and 8.

At 37°C, low levels of biofilm formation were also observed at 10x concentrated, SOP^{FA} and SOP^{SA} concentrations of Active Oxygen across all pHs tested (Fig. 4.5B) which conducted one-way ANOVAs found statistically significant (all $p<0.001$). However, when *E. coli* was grown in M9 minimal media at pH 5.2, the 10x concentrated Active Oxygen appeared to be less effective than first and follow on applications at preventing biofilm formation. Differences in OD measurements were found between Active Oxygen at the SOP^{SA} and 1:10 concentrations which were consistent across all pHs tested. Although the levels of biofilm formation were elevated, conducted one-way ANOVAs still found these to be statistically significant from control wells at pH from 5.2 to 7.4. This trend was more pronounced at pH 8 where the OD increased rapidly from 0 to 0.702. One-way ANOVAs with Dunnett's multiple comparisons tests conducted between Active Oxygen at the 1:10 concentration and control wells did not return significant outcomes ($p>0.05$).

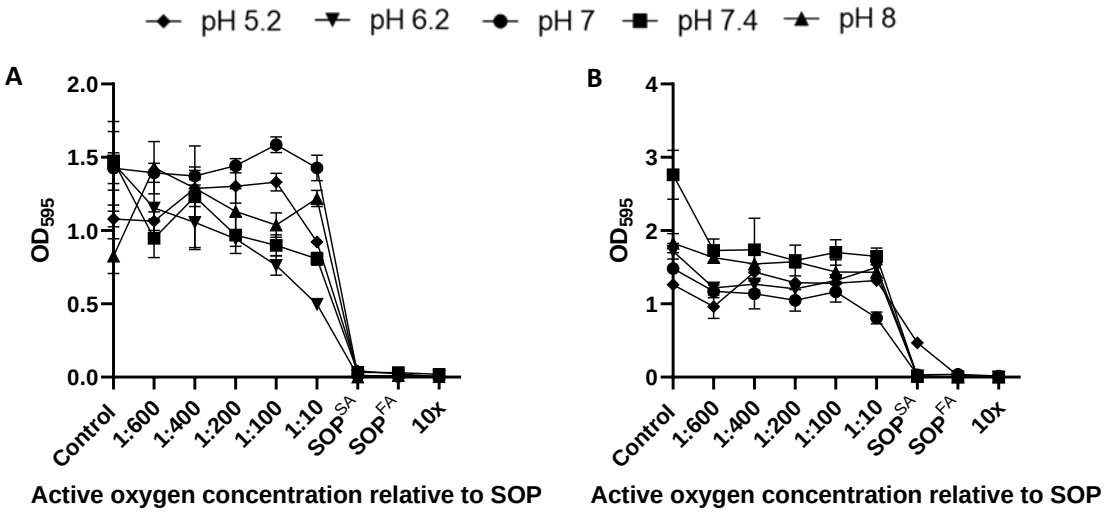

Figure 4.6. Impact of pH on efficacy of Active Oxygen to prevent biofilm formation of *P. aeruginosa* PA01 in M9 minimal media (indicated as OD_{595}) at 25°C (A) and 37°C (B). Initial dosage is the addition of two Active Oxygen tablets to hot tub water (labelled as SOP^{FA}) and follow on applications require the use of one additional tablet (SOP^{SA}). N=4 for each data point and error bars represent standard error of the mean (SEM).

P. aeruginosa exhibited low levels of biofilm formation at 25°C across all pHs tested using Active Oxygen concentrations ranging from 10x concentrated to SOP^{SA} (Fig. 4.6A). One-way ANOVAs with Dunnett's multiple comparison tests demonstrated that these Active Oxygen concentrations significantly reduced biofilm formation across all pHs tested (all $p<0.001$). In addition, when *P. aeruginosa* was grown in M9 minimal media at pH 7, 7.4 and 8, biofilm formation levels were elevated

at sublethal concentrations (1:100 at pH 7, 1:400 at pH 7.4, 1:10 and 1:600 at pH 8). One-way ANOVAs conducted found statistical significance between 1:10 ($p=0.0447$) and 1:600 ($p=0.0010$) when compared against biofilm formation levels in control wells at pH 8.

Stronger concentrations of Active Oxygen (10x concentrated to SOP^{SA}) were also effective at preventing biofilm formation levels at 37°C across all pHs tested as shown in Fig. 4.6B which was statistically significant in one-way ANOVAs (all $p<0.001$). However, there was a detectable increase in absorbance from 0 to 0.468 at the SOP^{SA} concentration at pH 5.2 which was followed by lower efficacy at Active Oxygen concentrations from 1:10 to 1:400 which exceeded biofilm formation levels observed in control wells. One-way ANOVAs illustrated that the levels of biofilm formation at these Active Oxygen concentrations were not significantly different to levels observed in control wells (all $p>0.05$). At pH 6.2, Active Oxygen at the 1:10 concentration resulted in higher levels of biofilm formation of *P. aeruginosa* whilst lower concentrations demonstrated higher efficacy in preventing biofilm formation. This was confirmed by one-way ANOVAs where all Active Oxygen concentrations lower than 1:10 were found to be statistically significant (all $p<0.001$).

4.2.5 Impact of pH and temperature on efficacy of Active Oxygen to prevent planktonic growth

The results obtained in planktonic growth prevention assays were also used to provide insights into the effect of pH and temperature on the efficacy of Active Oxygen to prevent planktonic growth at specific pH values (Fig. 4.7).

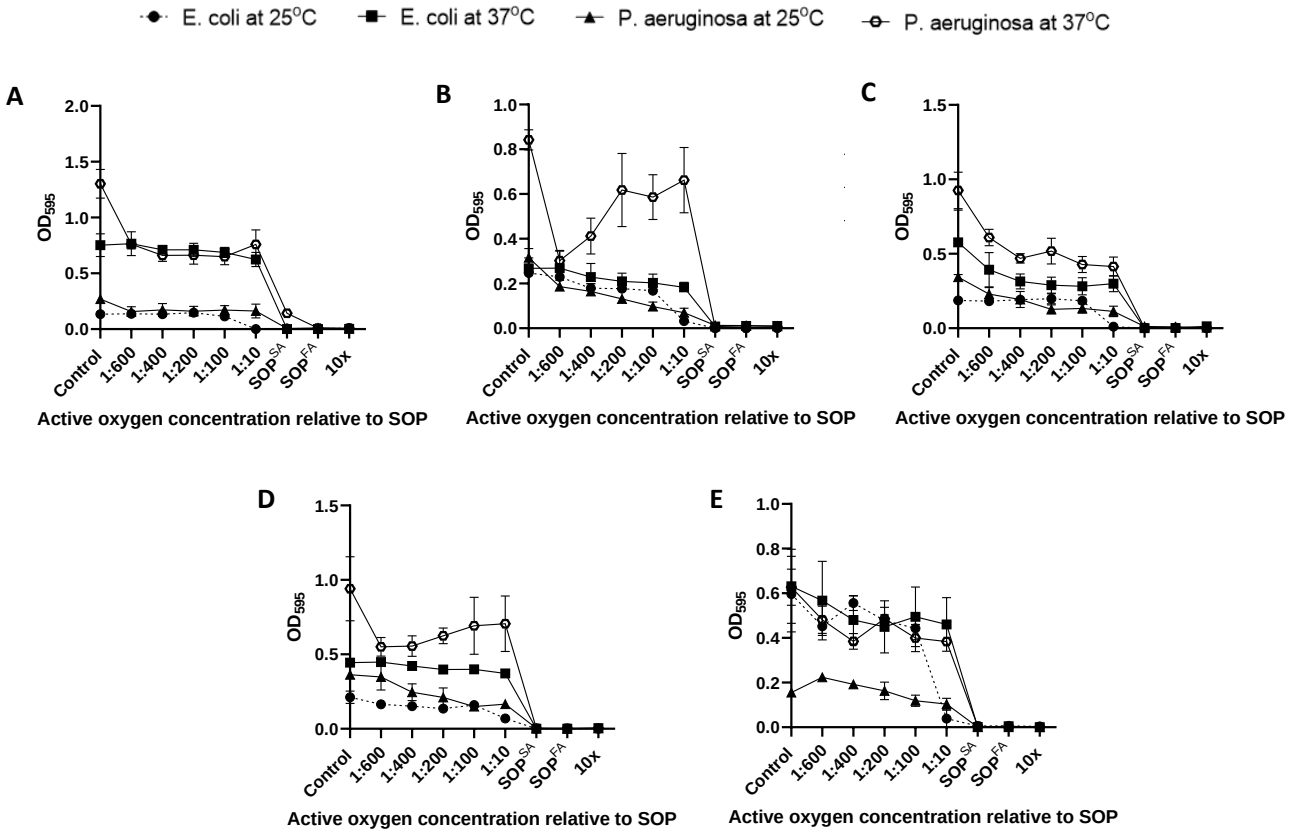

Figure 4.7. *E. coli* K12 and *P. aeruginosa* PA01 planktonic growth (indicated as OD_{595}) in M9 minimal media at pH 5.2 (A), 6.2 (B), 7 (C), 7.4 (D) and 8 (E) grown at 25°C and 37°C in the presence or absence of Active Oxygen. Initial dosage is the addition of two Active Oxygen tablets to hot tub water (labelled as SOP^{FA}) and follow on applications require the use of one additional tablet (SOP^{SA}). N=4 for each data point and error bars represent standard error of the mean (SEM).

At pH 5.2, the highest levels of planktonic growth were shown by *P. aeruginosa* at 37°C in control wells which were 79% higher than levels seen in control wells at 25°C (Fig. 4.7A). In addition, levels of planktonic growth displayed by *P. aeruginosa* were also 79% higher at 37°C compared to 25°C at the 1:10 concentration of Active Oxygen. Levels of *E. coli* planktonic growth were found to be 82% higher at 37°C compared to 25°C in control wells. Interestingly, similar levels of planktonic growth were noted when *E. coli* and *P. aeruginosa* were grown at 25°C in the presence of Active Oxygen concentrations

ranging from 1:100 to 1:600. This trend was also observed when both strains were grown at 37°C at the same Active Oxygen concentrations. One-way ANOVAs conducted with Tukey's multiple comparisons tests indicated that planktonic levels were significantly different at Active Oxygen concentrations ranging from 1:10 to 1:600 between *E. coli* grown at 25°C compared against *E. coli* and *P. aeruginosa* grown at 37°C (all $p<0.001$). Statistically significant results were also observed between *E. coli* grown at 37°C and *P. aeruginosa* grown at 25°C as well as comparisons between *P. aeruginosa* grown at 25°C and 37°C (all $p<0.001$). Comparisons between planktonic levels of *P. aeruginosa* grown at 37°C at the SOP^{SA} Active Oxygen concentration were found to be significantly higher than levels observed across all other temperature and strain conditions (all $p<0.001$).

The highest levels of planktonic growth were also seen in control wells containing *P. aeruginosa* grown at 37°C in M9 minimal media at pH 6.2 (Fig. 4.7B). Active Oxygen at concentrations ranging from 1:100 to 1:600 showed similar efficacy in preventing planktonic growth of *E. coli* and *P. aeruginosa* at 25°C. This was followed by slightly higher levels of planktonic growth in control wells containing *P. aeruginosa* compared to wells containing *E. coli*. Furthermore, the lowest concentration of Active Oxygen used in experiments (1:600) showed higher efficacy than levels of planktonic growth observed at 1:10, 1:200 and 1:400 concentrations when *P. aeruginosa* was grown at 37°C. One-way ANOVAs conducted with Tukey's multiple comparisons tests revealed that planktonic levels were significantly different at 1:400 concentration between growth of *E. coli* grown at 25°C and *P. aeruginosa* grown at 37°C and *P. aeruginosa* grown at 25°C and 37°C ($p<0.05$). Statistical significance was found between levels of planktonic growth at Active Oxygen concentrations from 1:10 to 1:400 between *E. coli* at 25°C and 37°C compared with *P. aeruginosa* at 37°C as well as *P. aeruginosa* grown at 25°C and 37°C (all $p<0.05$).

The highest levels of planktonic growth were shown by *P. aeruginosa* at 37°C followed by *E. coli* at 37°C (Fig. 4.7C). Levels of planktonic growth in control wells were 63% and 68% higher at 37°C compared to 25°C for both strains. Planktonic growth of *E. coli* at 37°C as well as *P. aeruginosa* at 25°C and 37°C was consistent across Active Oxygen concentrations ranging from 1:10 to 1:400. However, at the lowest Active Oxygen concentration tested, lower efficacy was observed. This differed when *E. coli* were grown at 25°C at sublethal concentrations were levels of planktonic growth were comparable to those observed in control wells. One-way ANOVAs conducted with Tukey's multiple comparisons tests demonstrated that planktonic levels between *E. coli* 25°C compared with *P. aeruginosa* at 37°C and *P. aeruginosa* at 25°C and 37°C were significantly different at sublethal concentrations (all $p<0.05$). In addition, planktonic growth of *E. coli* was significantly higher at 37°C compared to 25°C at the 1:10 concentration ($p=0.0036$).

At pH 7.4, the highest levels of planktonic growth were found at 37°C which were 52% and 62% higher than 25°C for *E. coli* and *P. aeruginosa* respectively (Fig. 4.7D). Planktonic growth of *E. coli* was consistent across Active Oxygen concentrations ranging from 1:10 to 1:600 at 25°C and 37°C. However, sublethal concentrations resulted in higher planktonic growth of *P. aeruginosa* at 25°C whereas at 37°C, higher efficacy was displayed at sublethal concentrations. One-way ANOVAs conducted with Tukey's multiple comparisons tests revealed that planktonic levels were significantly different between *E. coli* at 25°C and 37°C and *P. aeruginosa* at 37°C at 1:400 and 1:600 concentrations (all $p<0.05$). Statistical significance was also found between levels of planktonic growth of *P. aeruginosa* at 25°C and 37°C at 1:400 ($p=0.0022$). Further statistical analyses demonstrated that levels differed at 1:10 and 1:100 concentrations between *E. coli* at 25°C and *P. aeruginosa* at 37°C and *P. aeruginosa* at 25°C and 37°C (all $p<0.05$). Levels of planktonic levels were significantly different between all datasets at 1:200 except comparisons between *E. coli* and *P. aeruginosa* grown at 25°C (all $p<0.05$).

Interestingly, similar levels of planktonic growth were observed in control wells containing *P. aeruginosa* at 37°C and *E. coli* at 25°C and 37°C (Fig. 4.7E). This was also evident at the 1:200 concentration where OD measurements were close to each other. A small peak in planktonic growth was noted at the 1:400 Active Oxygen concentration when *E. coli* were grown at 25°C and 37°C as well as *P. aeruginosa* grown at 25°C. However, at the same Active Oxygen concentration *P. aeruginosa* grown at 37°C demonstrated similar efficacy in preventing planktonic growth which was comparable with that seen at 1:10 and 1:100 concentrations. One-way ANOVAs conducted with Tukey's multiple comparisons tests showed that planktonic levels were significantly different between *E. coli* and *P. aeruginosa* grown at 25°C at 1:400 and 1:600 concentrations of Active Oxygen ($p<0.05$). This was also found between planktonic growth of *P. aeruginosa* at 25°C and *E. coli* at 37°C at 1:100 ($p=0.0244$). Several other comparisons showed statistical significance between levels of planktonic growth exhibited by *E. coli* at 25°C and 37°C and *P. aeruginosa* at 37°C including *E. coli* and *P. aeruginosa* at 25°C and *P. aeruginosa* at 37°C (all $p<0.05$).

4.2.6 Impact of pH and temperature on efficacy of Active Oxygen to prevent biofilm formation

The results obtained in biofilm prevention assays were also used to provide insights into the effect of pH and temperature on the efficacy of Active Oxygen to prevent biofilm formation at specific pH values (Fig. 4.8).

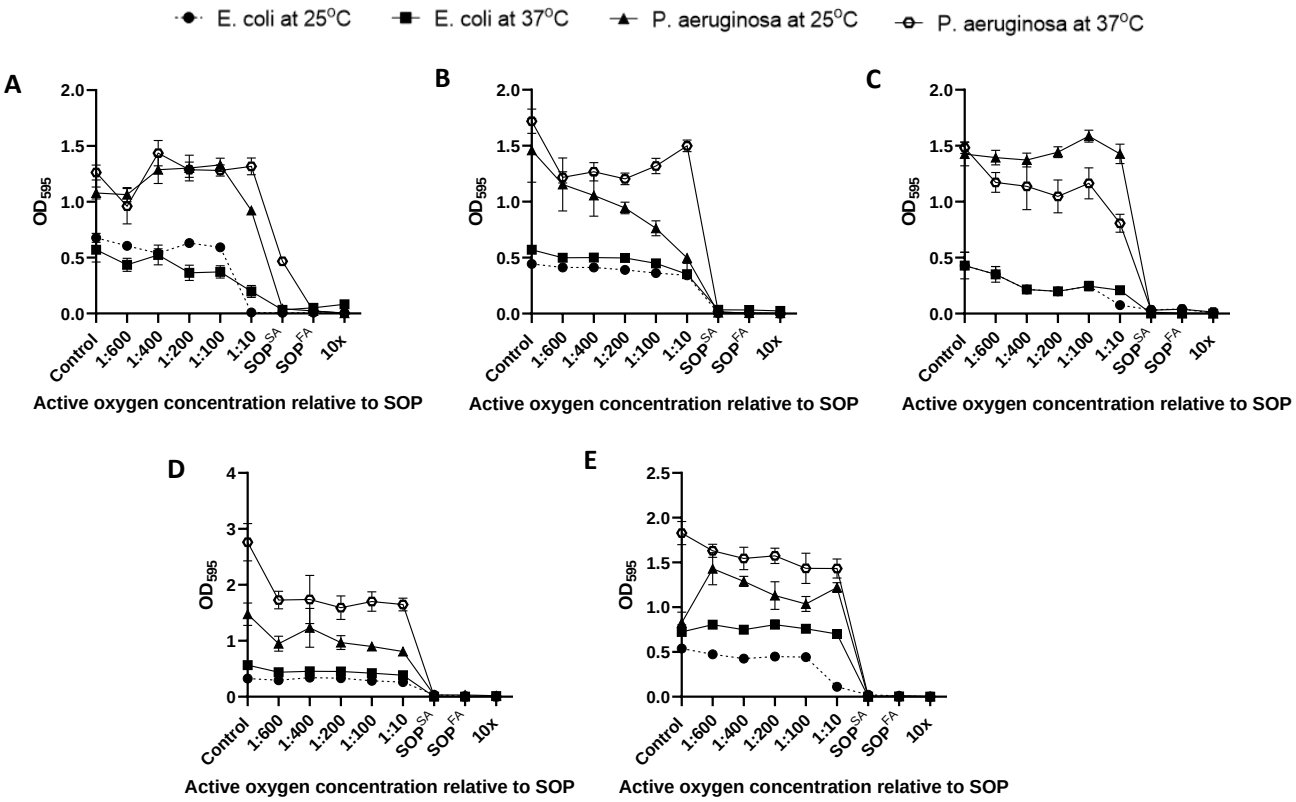

Figure 4.8. Quantitation of *E. coli* K12 and *P. aeruginosa* PA01 biofilm formation (indicated as OD_{595}) in M9 minimal media at pH 5.2 (A), 6.2 (B), 7 (C), 7.4 (D) and 8 (E) grown at 25°C and 37°C in the presence or absence of Active Oxygen. Initial dosage is the addition of two Active Oxygen tablets to hot tub water (labelled as SOP^{FA}) and follow on applications require the use of one additional tablet (SOP^{SA}). N=4 for each data point and error bars represent standard error of the mean (SEM).

Active Oxygen concentrations ranging from 10x concentrated SOP^{SA} displayed low levels of *E. coli* biofilm formation across both temperatures. However, there was peak in OD at pH 5.2 to 0.4678 when *P. aeruginosa* were grown at 37°C in the presence of the SOP^{SA} concentration which was not observed at 25°C (Fig. 4.8A). At the 1:10 concentration, sharp rises in biofilm formation were shown by *P. aeruginosa* at 25°C and 37°C whereas much lower levels of biofilm formation were exhibited by *E. coli* at both temperatures with higher efficacy found at 25°C compared to 37°C. Furthermore, *E. coli* biofilm formation appeared to be higher at 25°C compared to 37°C at 1:100, 1:200 and 1:600 Active Oxygen concentrations. The levels of biofilm formed by *E. coli* were almost identical at the 1:400 concentration

whereas this was found at the 1:100 and 1:200 concentrations with *P. aeruginosa* at both temperatures. One-way ANOVAs conducted with Tukey's multiple comparisons test revealed that there were significantly different levels of biofilm formation of *E. coli* at 25°C and *P. aeruginosa* at 25°C as well as between *E. coli* at 37°C and *P. aeruginosa* at both temperatures (all $p<0.05$) at concentrations from 1:10 to 1:600.

High efficacy was shown across both temperatures at pH 6.2 using both strains at Active Oxygen concentrations ranging from 10x concentrated to SOP^{SA} (Fig. 4.8B). Levels of biofilm formation rose sharply at the 1:10 concentration where the OD reached a value of approximately 1.5 when *P. aeruginosa* was grown at 37°C which exceeded levels observed in the remaining sublethal concentrations. This was confirmed by one-way ANOVAs which showed that biofilm formation was significantly different to levels observed with *E. coli* at both temperatures including *P. aeruginosa* at 25°C at the same concentration of Active Oxygen (all $p<0.001$). Varying patterns in biofilm were seen between *E. coli* and *P. aeruginosa* at sublethal concentrations. At 25°C, *P. aeruginosa* showed lower efficacy at lower concentrations of Active Oxygen whereas at 37°C, higher efficacy was found as Active Oxygen concentration fell. This trend was not observed for *E. coli* as sublethal concentrations of Active Oxygen resulted in relatively consistent levels of biofilm formation across both temperatures. Furthermore, similar levels of biofilm formation were shown by *E. coli* at 1:10 concentration for both temperatures whereas this was evident at the lowest Active Oxygen concentration with *P. aeruginosa*.

High efficacy was shown across both temperatures at pH 7 using both strains at Active Oxygen concentrations ranging from 10x concentrated to SOP^{SA} (Fig. 4.8C). There was a small difference in biofilm formation exhibited by *E. coli* at both temperatures at the 1:10 concentration whereas *P. aeruginosa* showed levels that were 43% higher at 25°C compared to 37°C. One-way ANOVAs confirmed that these levels were significantly different to *P. aeruginosa* grown at 37°C and *E. coli* at both temperatures at the same concentration (all $p<0.001$). Interestingly, the results showed that biofilm formation levels of *P. aeruginosa* were higher at 25°C compared to 37°C at sublethal concentrations of Active Oxygen which one-way ANOVAs found significantly different (all $p<0.01$).

High efficacy was shown across both temperatures at pH 7.4 using both strains at Active Oxygen concentrations ranging from 10x concentrated to SOP^{SA} (Fig. 4.8D). All Active Oxygen concentrations were effective in preventing biofilm formation of *E. coli* at both temperatures which is denoted by the low OD measurements. One-way ANOVAs conducted with Tukey's multiple comparisons tests demonstrated that the levels of biofilm formation at all Active Oxygen concentrations except SOP^{SA} were not significantly different between *E. coli* at 25°C and 37°C as OD measurements were similar

across all Active Oxygen concentrations (all p>0.05). In contrast, this did not occur with *P. aeruginosa* where the efficacy of Active Oxygen was lower at sublethal concentrations.

High efficacy was shown across both temperatures at pH 8 using both strains at Active Oxygen concentrations ranging from 10x concentrated to SOP^{SA} (Fig. 4.8E). At the 1:10 concentration, levels of biofilm formation shown by *E. coli* were 84% higher at 37°C compared to 25°C whereas there was only a 15% difference in biofilm formation levels of *P. aeruginosa* at the same concentration. One-way ANOVAs conducted with Tukey's multiple comparison tests revealed levels of biofilm formed by *P. aeruginosa* at 37°C were significantly higher than levels observed with *E. coli* at both temperatures (all p<0.001). Furthermore, at Active Oxygen concentrations below SOP^{SA}, levels of biofilm formation increased rapidly when *P. aeruginosa* was grown at 25°C and 37°C which was also observed with *E. coli* grown at 37°C.

4.2.7 Prevention of biofilm formation following exposure to Active Oxygen (Specific biofilm formation)

This section includes the specific biofilm formation of *E. coli* K12 and *P. aeruginosa* PA01 calculated by dividing the biofilm formation optical density by the planktonic cell optical density reading. These values represent the biofilm forming capacity of an organism per amount of biomass present.

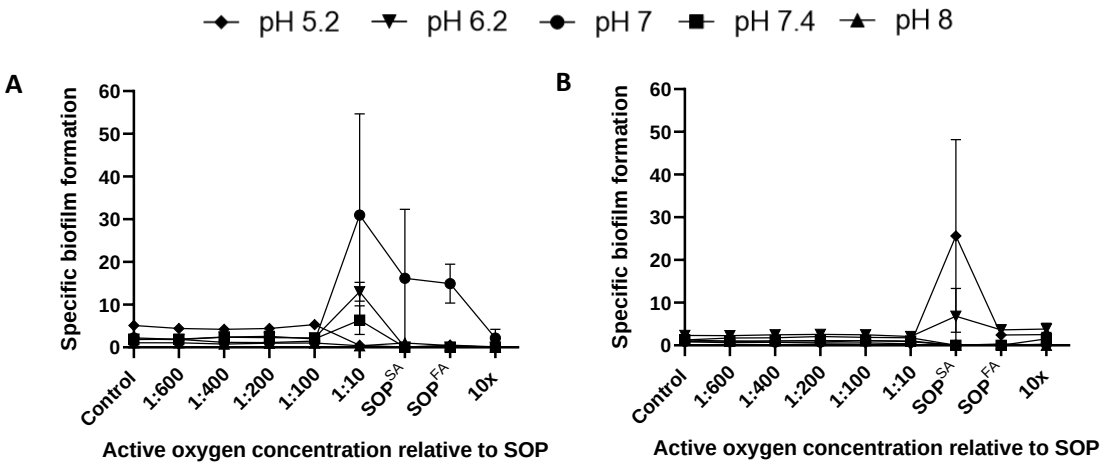

Figure 4.9. Levels of specific biofilm formation exhibited by *E. coli* K12 at 25°C (A) and 37°C (B) in M9 minimal media at five different pHs in the presence or absence of Active Oxygen. Initial dosage is the addition of two Active Oxygen tablets to hot tub water (labelled as SOP^{FA}) and follow on applications require the use of one additional tablet (SOP^{SA}). N=4 for each data point and error bars represent standard error of the mean (SEM).

Across both temperatures, the levels of biofilm formation exhibited by *E. coli* were low (Fig. 4.8). Therefore, the calculated values for specific biofilm formation were also low (Fig. 4.9). In addition, the

difference in OD measurements between planktonic and biofilm formation resulted in large spikes which are seen notably at SOP^{FA}, SOP^{SA} and 1:10 concentrations at 25°C as well as SOP^{SA} concentration at 37°C.

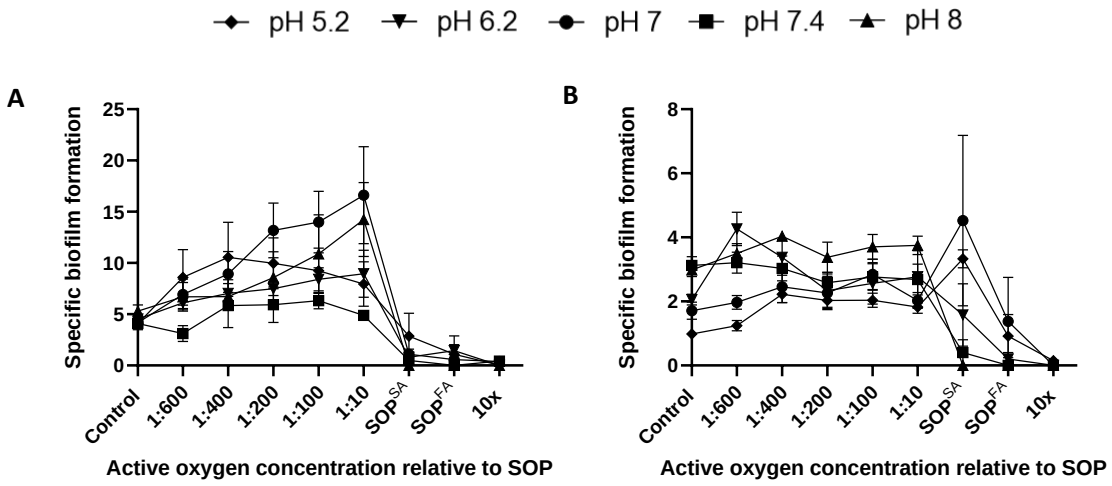

Figure 4.10. Levels of specific biofilm formation exhibited by *P. aeruginosa* PA01 at 25°C (A) and 37°C (B) in M9 minimal media at five different pHs in the presence or absence of Active Oxygen. Initial dosage is the addition of two Active Oxygen tablets to hot tub water (labelled as SOP^{FA}) and follow on applications require the use of one additional tablet (SOP^{SA}). N=4 for each data point and error bars represent standard error of the mean (SEM).

At 25°C, stronger concentrations of Active Oxygen (10x, SOP^{FA} and SOP^{SA}) showed high efficacy which is denoted by the low levels of specific biofilm formation shown by *P. aeruginosa* across all pHs tested (Fig. 4.10A). Peaks in specific biofilm formation were most prominent at the 1:10 concentration across all pHs tested. The highest specific biofilm formation was observed at pH 6.2, 7 and 8 respectively. At concentrations lower than 1:10, there was a gradual decrease in specific biofilm formation which was seen across all pHs tested. Across all concentrations and pHs tested, Active Oxygen was more effective at 37°C compared to 25°C based on the lower scale plotted on the Y axis (Fig. 4.10B). There was no specific biofilm formation in the presence of Active Oxygen at the 10x concentration. This was followed closely by specific biofilm formation at the SOP^{FA} and SOP^{SA} concentrations of Active Oxygen where spikes in specific biofilm formation were noted at pH 5.2, 6.2 and 7. In contrast, at the SOP^{SA} concentration, low levels of specific biofilm formation were maintained at the remaining pHs tested (pH 7.4 and 8).

4.2.8 Effect of Active Oxygen on cell viability

4.2.8.1 Log reduction data (OD_{595}-CFU derived)

Due to time constraints and since this was only a one-year project, the results shown in this section reflect log reductions in cell viability of *E. coli* K12 and *P. aeruginosa* PA01. As previous results showed the generation of a calibration curve for *E. coli* and *P. aeruginosa* (Chapter 3), the OD of planktonic cell cultures was used to calculate log reductions in cell viability.

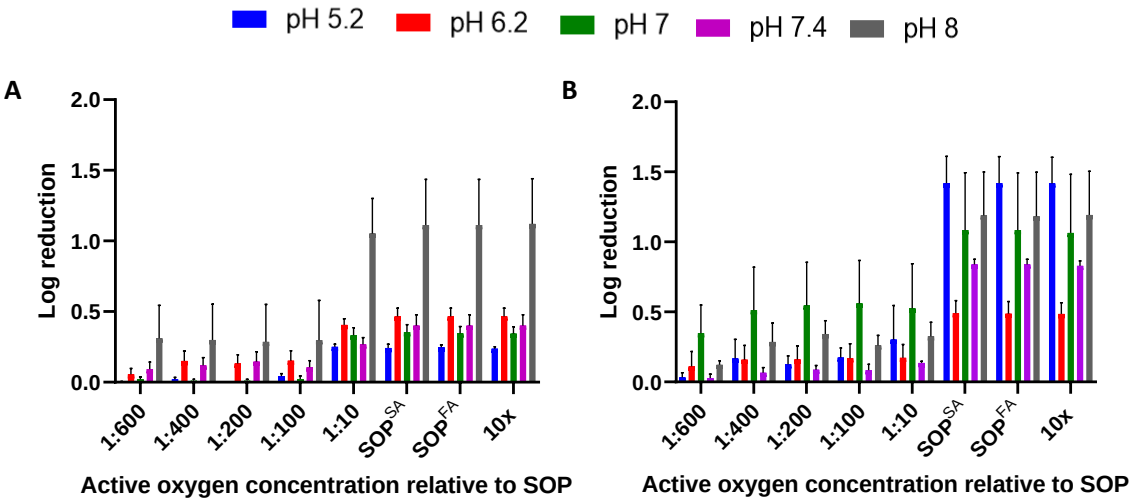

Figure 4.11. Log reductions in cell viability of *E. coli* K12 grown in M9 minimal media (calculated from OD_{595}-CFU calibration curves) following treatment with Active Oxygen at five different pHs at 25°C (A) and 37°C (B). Initial dosage is the addition of two Active Oxygen tablets to hot tub water (labelled as SOP^{FA}) and follow on applications require the use of one additional tablet (SOP^{SA}). N=4 for each data point with error bars illustrating standard error of the mean (SEM).

The highest log reductions in *E. coli* at 25°C were observed at pH 8 where Active Oxygen concentrations ranging from 10x concentrated to SOP^{SA} achieved log reductions higher than 1. In contrast, log reductions noted at other pHs fellow 0.5 across all Active Oxygen concentrations (Fig. 4.11A). Furthermore, Active Oxygen was most effective at reducing cell viability of *E. coli* at 37°C in M9 minimal media at pH 5.2 (Fig. 4.11B). Active Oxygen concentrations ranging from 10x concentrated to SOP^{SA} resulted in an average log reduction of 1.42. This was followed closely by decreases in cell viability noted at pH 7 and 8 with log reductions higher 1. The lowest log reductions were seen at pH 6.2 which only resulted in log reductions of 0.5 at first and follow on applications of Active Oxygen (SOP^{FA} and SOP^{SA}) including at the 10x concentration.

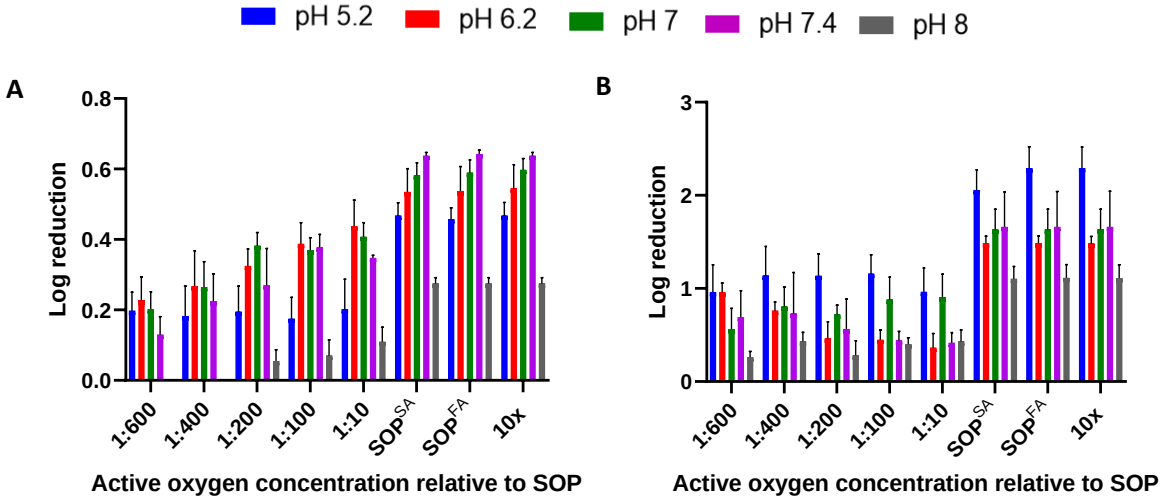

Figure 4.12. Log reductions in cell viability of *P. aeruginosa* PA01 grown in M9 minimal media (calculated from OD_{595}-CFU calibration curves) following treatment with Active Oxygen at five different pHs at 25°C (A) and 37°C (B). Initial dosage is the addition of two Active Oxygen tablets to hot tub water (labelled as SOP^{FA}) and follow on applications require the use of one additional tablet (SOP^{SA}). N=4 for each data point with error bars illustrating standard error of the mean (SEM).

At 25°C, the highest log reductions were noted at pH 7.4 followed by 7, 6.2, 5.2 and 8 where higher concentrations of Active Oxygen only resulted in average log reductions of 0.3 (Fig. 4.12A). Active Oxygen showed higher efficacy in reducing cell viability of *P. aeruginosa* at sublethal concentrations in M9 minimal media at pH 5.2, 6.2, 7 and 7.4 compared to 8. At pH 8, *P. aeruginosa* treated with the lowest concentrations of Active Oxygen (1:400 and 1:600) did not result in log reductions in cell viability. In addition, Active Oxygen concentrations higher than 1:10 at 37°C resulted in log reductions of *P. aeruginosa* higher than 2 at pH 5.2 (Fig. 4.12B). This was followed closely with log reductions of higher than 1.5 at pH 7 and 7.4, 1.5 at pH 6.2 and 1.1 at pH 8. At sublethal concentrations of Active Oxygen, there was still a 1 log reduction in *P. aeruginosa* at pH 5.2 whereas at other pHs, log reductions fell below 1.

4.2.8.2 Time-kill assays

To determine how quickly the Active Oxygen tablets kill bacteria, overnight cultures of *E. coli* grown at in M9 minimal media at pH 7.4 were diluted to OD_{595} = 0.5 before addition of Active Oxygen at the initial dosage and follow on application (SOP^{FA} and SOP^{SA}). Samples were incubated at 37°C under static conditions for 0, 5, 10, 30 and 60 min as similar studies have observed decreased viability within 30 min of treatment with KMPS (Oliveira et al., 2022). Ampicillin was chosen as a bactericidal antibiotic

and erythromycin as a bacteriostatic antibiotic to provide insights into the mechanism of action exhibited by Active Oxygen. Chlorine at 5ppm was also used as a positive control.

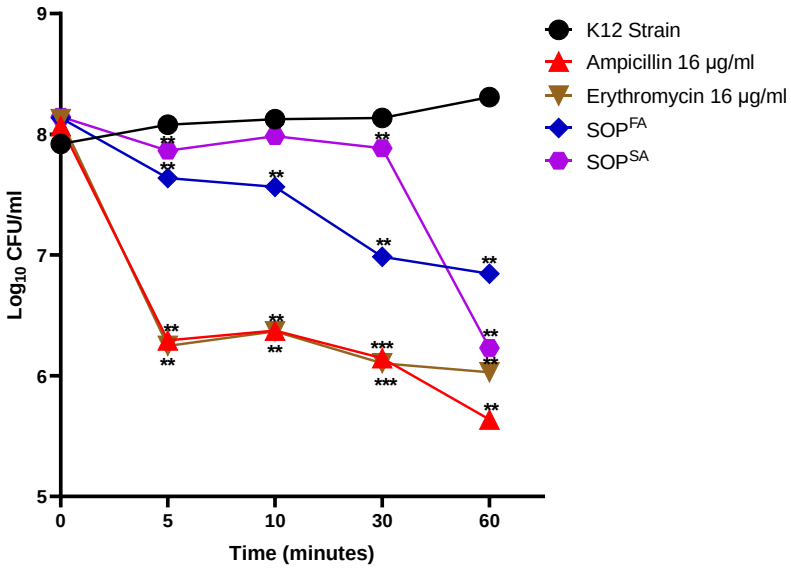

Figure 4.13. Time-kill of *E. coli* K12 in M9 minimal media at pH 7.4 following treatment with Active Oxygen at first and follow on applications (SOP^{FA} and SOP^{SA}). Viable cell counts are expressed as Log_{10} CFU/ml. *E. coli* K12 was used as a negative control. N=3 for each data point and error bars represent standard error of the mean (SEM). Paired t-test was conducted between treated and control samples at each time point and is indicated by **p<0.01;***p<0.001.

Figure 4.13 shows the results from time-kill assays after counting the number of colonies on LB plates indicated as Log_{10} CFU/ml. After 5 minutes of exposure with Active Oxygen at both concentrations, there was an observable decrease in cell viability which a paired t-test found significantly lower (both p<0.01). Viable cell counts increased slightly at 10 and 30 minutes at the SOP^{SA} concentration whereas there was a more observable decrease in cell viability at the SOP^{FA} concentration which was denoted by statistical significance (both p<0.01). The most notable reductions in cell viability with SOP^{FA} and SOP^{SA} were observed after 60 minutes which declined by 18% and 25% respectively which were also statistically significant. Interestingly, viable cell counts at the SOP^{FA} concentration were higher compared to those observed at the SOP^{SA} concentration where there was a more rapid decrease in viability between 30 and 60 min. Ampicillin showed bactericidal activity with subsequent reductions in cell viability after 60 minutes. In contrast, after 60 minutes of exposure to erythromycin the number of viable bacteria started to plateau. *E. coli* cells treated with chlorine at the recommended concentration of chlorine (5ppm) did not lead to any CFU formation after incubation (data not shown).

4.2.8.3 Decay of Active Oxygen

In order to provide insights into the stability of Active Oxygen species, experiments were conducted to investigate the effect of different time periods of incubation on antibacterial activity against *E. coli* grown at 37°C in M9 minimal media at pH 7.4. Active Oxygen at the initial dosage (SOP^{FA}) and follow on application (SOP^{SA}) was incubated at 37°C under static conditions for 0, 1, 3, 5 and 7 days before being added to diluted overnight cultures of *E. coli*. It was decided to test the stability of Active Oxygen at 1, 3 and 5 days as product instructions indicate to add one tablet every day if hot tub water becomes "dull or foamy." The stability of Active Oxygen was also tested after 7 days since product instructions state that prior to each hot tub use customers should add "at least two tablets each week to keep the water sanitised."

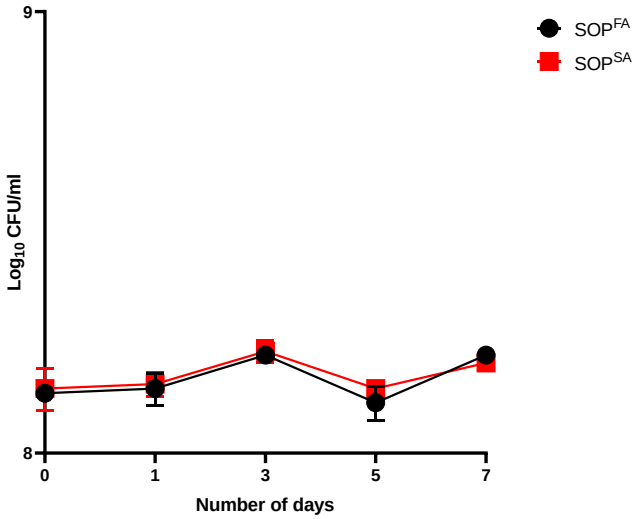

Figure 4.14. Stability of Active Oxygen at first and follow on applications (SOP^{FA} and SOP^{SA}) after incubation at 37°C for 1, 3, 5 and 7 days. Viable cell counts of *E. coli* K12 are expressed as Log_{10} CFU/ml. N=3 for each data point and error bars represent standard error of the mean (SEM).

Figure 4.14 demonstrates the stability of Active Oxygen after incubation at 37°C for various time periods and counting the number of colonies on LB plates indicated as Log_{10} CFU/ml. After 7 days, viable cell counts remained relatively consistent with small fluctuations observed at day 3 and 7. Cell viability was almost identical at 1 and 5 days in comparison to 0 days where Active Oxygen was added directly to *E. coli*. In addition, at day 5, Active Oxygen at SOP^{FA} concentration showed antibacterial activity against *E. coli* as cell viability dropped slightly.

4.2.9 Prevention of planktonic growth following treatment with Active Oxygen and Water conditioner (Product 2)

This section shows the efficacy of Active Oxygen at various concentrations in combination with Water conditioner (Product 2) in preventing planktonic growth of *E. coli* and *P. aeruginosa* in M9 minimal media grown at 25°C or 37°C. The initial dosage of Active Oxygen is two tablets added to hot tub water (SOP^{FA}) and follow on applications prior to each hot tub use require one additional tablet (SOP^{SA}). Since the main focus of the project was on Active Oxygen, the pH range used in these experiments ranges from 7 to 8 to simulate the conditions in a hot tub. In addition, Product 2 was only tested at the SOP concentration.

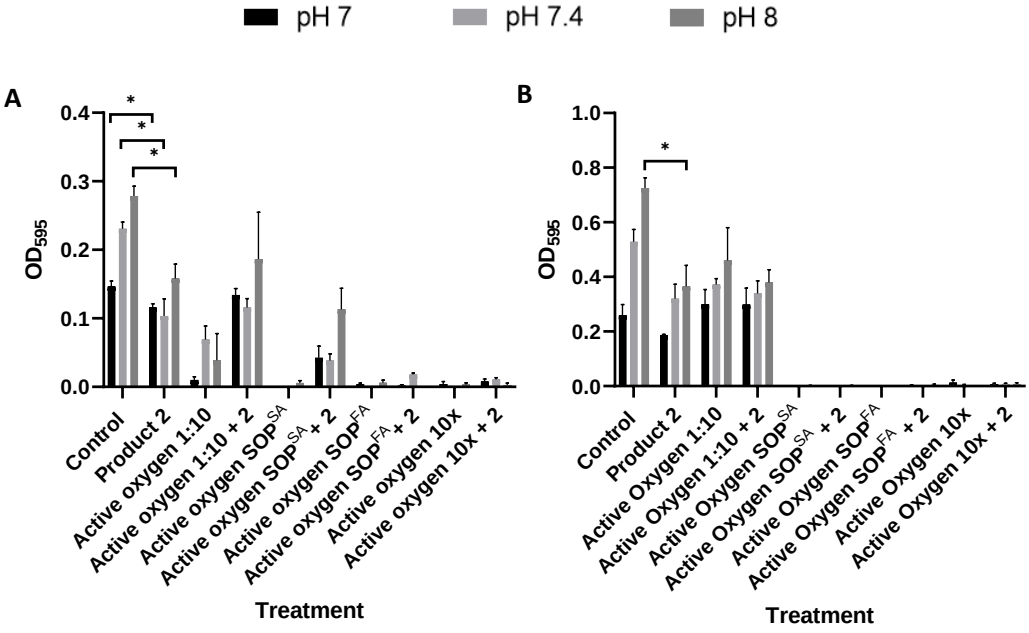

Figure 4.15. Planktonic growth of *E. coli* K12 in M9 minimal media at pH 7, 7.4 and 8 (indicated as OD_{595}) in the presence of Active Oxygen or in combination with Product 2 at 25°C (A) and 37°C (B). SOP^{FA} and SOP^{SA} indicate the initial dosage and follow on applications of Active Oxygen. N=4 for each data point and error bars represent standard error of the mean (SEM). Paired t-test was conducted between treated and control samples and is indicated by *p<0.05.

Across all Active Oxygen concentrations tested, low levels of planktonic growth exhibited by *E. coli* were observed across all pHs tested at 25°C (Fig. 4.15A). Active Oxygen in combination with Product 2 led to higher levels of planktonic growth at all pHs tested compared with Active Oxygen alone. The highest levels of planktonic growth were observed at Active Oxygen 1:10 in combination with Product 2 with an OD of 0.186 at pH 8. Product 2 showed a statistically significant effect in reducing planktonic growth of *E. coli* across all pHs tested (p=0.0118, p= 0.0344 and p=0.0283, paired t-test). Scheirer-Ray-

Hare tests and two-way ANOVAs revealed that Active Oxygen, Product 2 and in combination with Product 2 had a significant effect in reducing planktonic growth across all pHs tested (all $p<0.05$).

At 37°C, Active Oxygen concentrations ranging from 10x concentrated to SOP^{SA} alone and in combination with Product 2 were effective at preventing planktonic growth of *E. coli* across all pHs tested (Fig. 4.15B). However, this was not evident at the 1:10 concentration alone and in combination with Product 2 where levels of planktonic growth increased rapidly. Addition of Product 2 by reduced planktonic growth of *E. coli* by 28%, 39% and 50% at all pHs tested. Paired t-test conducted between control and treated samples showed that Product 2 had a statistically significant effect in reducing planktonic growth of *E. coli* at pH 8 ($p=0.0369$). Two-way ANOVAs indicated that Active oxygen at concentrations 10x, SOP^{FA} and SOP^{SA} were effective at reducing planktonic growth across pHs tested (all $p<0.001$). However, the same Active Oxygen concentrations only showed a significant interaction in combination with Product 2 at pH 7.4 and 8 where Product 2 by itself also achieved statistical significance (all $p<0.05$).

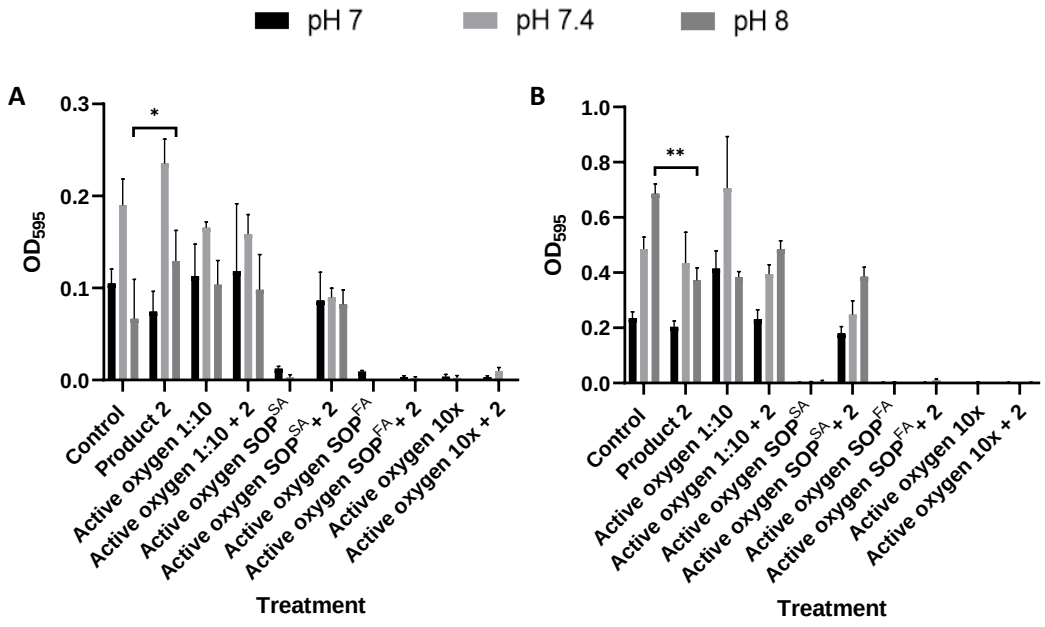

Figure 4.16. Planktonic growth of *P. aeruginosa* PA01 in M9 minimal media at pH 7, 7.4 and 8 (indicated as OD_{595}) in the presence of Active Oxygen or in combination with Product 2 at 25°C (A) and 37°C (B). SOP^{FA} and SOP^{SA} indicate the initial dosage and follow on applications of Active Oxygen. N=4 for each data point and error bars represent standard error of the mean (SEM). Paired t-test was conducted between treated and control samples and is indicated by *$p<0.05$;**$p<0.01$.

Active Oxygen showed high efficacy in preventing planktonic growth of *P. aeruginosa* at 25°C at 10x, SOP^{FA} and SOP^{SA} concentrations across all pHs tested (Fig. 4.16A). However, at the SOP^{SA} in combination with Product 2 there was sharp rise in planktonic growth which gave similar OD measurements with

an average reading of 0.086 across all pHs. This was also seen at the Active Oxygen 1:10 alone and in combination with Product 2 which exceeded planktonic growth observed in control wells at pH 7 and 8. Product 2 was only able to reduce planktonic growth at pH 7 whereas it promoted planktonic growth at pH 7.4 and 8 which achieved statistical significance ($p=0.0261$, paired t-test). Scheirer-Ray-Hare tests and two-way ANOVAs demonstrated that Active Oxygen at SOP^{FA} and 10x concentrations significantly reduced planktonic growth of *P. aeruginosa* across all pHs tested (all $p<0.01$). Further statistical analyses showed that only Active Oxygen at the SOP^{SA} concentration in combination with Product 2 showed a significant interaction in reducing planktonic growth at pH 7 ($p=0.0082$) whereas Product 2 was found to significantly lower planktonic growth at pH 7.4 and 8 (both $p<0.05$).

Active Oxygen was also effective at concentrations ranging from 10x to SOP^{SA} at 37°C in reducing planktonic growth of *P. aeruginosa* across all pHs tested (Fig. 4.16B). Similar to the observations found at 25°C, at the SOP^{SA} concentration in combination with Product 2, there were higher levels of planktonic growth which rose as pH increased. Active Oxygen 1:10 showed higher efficacy with Product 2 at pH 7 and 7.4 with levels of planktonic growth being 44% lower than that seen at the 1:10 concentration alone at both pHs whereas planktonic growth was increased at pH 8. Product 2 decreased planktonic growth of *P. aeruginosa* by 13% at pH 7 and 10% at pH 7.4 but caused the highest reduction at pH 8 by 46% which achieved statistical significance ($p=0.0092$, paired-test). Scheirer-Ray-Hare tests and two-way ANOVAs illustrated that Active Oxygen was effective in reducing planktonic growth of *P. aeruginosa* across all pHs tested (all $p<0.05$) but no significant effect was seen at 1:10 concentration at pH 7.4 and 8. Active Oxygen at the SOP^{SA} concentration in combination with Product 2 showed a significant effect in decreasing planktonic growth at pH 7 and 7.4 (both $p<0.05$) whereas all product combinations including Product 2 alone significantly lowered planktonic growth at pH 8 (all $p<0.01$).

4.2.10 Prevention of biofilm formation following treatment with Active Oxygen and Water conditioner (Product 2)

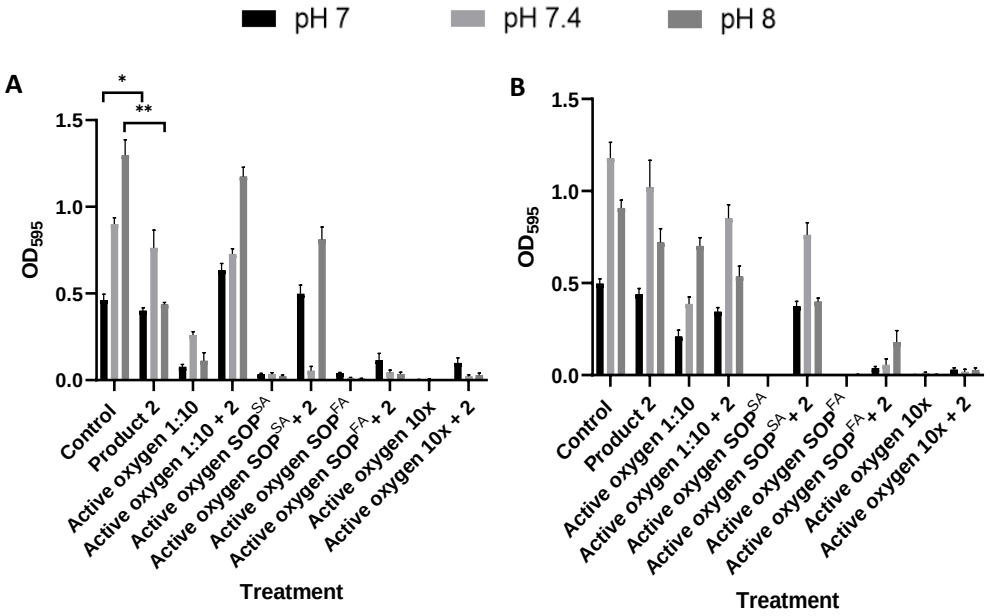

Figure 4.17. Quantification of *E. coli* K12 biofilm formation in M9 minimal media at pH 7, 7.4 and 8 (indicated as OD_{595}) in the presence of Active Oxygen or in combination with Product 2 at 25°C (A) and 37°C (B). SOP^{FA} and SOP^{SA} indicate the initial dosage and follow on applications of Active Oxygen. N=4 for each data point and error bars represent standard error of the mean (SEM). Paired t-test was conducted between treated and control samples and is indicated by *p<0.05;**p<0.01.

Active Oxygen at all concentrations successfully prevented biofilm formation of *E. coli* at 25°C which is denoted by the low levels of biofilm formation observed across all pHs tested (Fig. 4.17A). At the SOP^{SA} concentration in combination with Product 2, high efficacy was shown in preventing biofilm formation at pH 7.4 whereas there was a rapid increase in levels of biofilm formation observed at pH 7 and 8. Across all pHs tested, Active Oxygen 1:10 in combination with Product 2 resulted in high levels of biofilm formation. The addition of Product 2 caused small reductions in biofilm formation at pH 7 and 7.4 whereas levels of biofilm formation decreased by 66% at pH 8. Statistical analyses found that Product 2 significantly lowered levels of biofilm formation at pH 7 and 8 (p=0.0381 and p=0.0028, paired t-test). Scheirer-Ray-Hare tests and two-way ANOVAs showed that Active Oxygen significantly reduced biofilm formation of *E. coli* at pH 7.4 and 8 (all p<0.01) which did not achieve statistical significance at the 1:10 concentration at pH 7 . All product combinations including Product 2 by itself caused a significant effect at pH 7 and 8 (all p<0.05) whereas this was only observed at the 1:10 concentration in combination with Product 2 at pH 7.4 (p=0.0064).

At 37°C, low levels of biofilm formation were observed following treatment with Active Oxygen which increased at the 1:10 concentration as pH increased (Fig. 4.17B). All Active Oxygen concentrations in combination with Product 2 resulted in increases in biofilm formation with the most pronounced effect being observed at pH 7.4. In the presence of Product 2, there were low reductions in biofilm formation which ranged from 12% to 21% which statistical analyses did not find statistically significant ($p>0.05$). Scheirer-Ray-Hare tests and two-way ANOVAs confirmed that Active Oxygen at all concentrations significantly reduced biofilm formation across all pHs tested (all $p<0.01$). Active Oxygen at SOP^{SA} and 1:10 concentration in combination with Product 2 reduced biofilm formation at pH 7 and 7.4 whereas only Active Oxygen concentrations higher than 1:10 significantly reduced biofilm formation at pH 8 (all $p<0.05$). Product 2 had a significant effect on biofilm formation at pH 7 and 7.4 at the SOP^{SA} concentration as well as at pH 8 at the 1:10 concentration (both $p<0.01$).

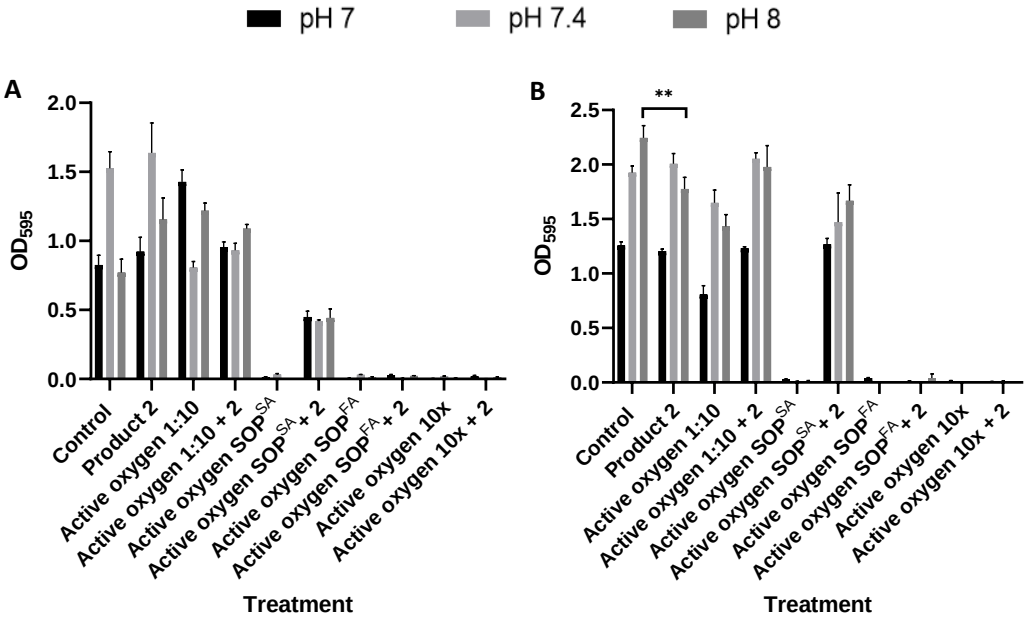

Figure 4.18. Quantification of *P. aeruginosa* PA01 biofilm formation in M9 minimal media at pH 7, 7.4 and 8 (indicated as OD_{595}) in the presence of Active Oxygen or in combination with Product 2 at 25°C (A) and 37°C (B). SOP^{FA} and SOP^{SA} indicate the initial dosage and follow on applications of Active Oxygen. N=4 for each data point and error bars represent standard error of the mean (SEM). Paired t-test was conducted between treated and control samples and is indicated by * *$p<0.01$.

Active Oxygen demonstrated high efficacy in preventing biofilm formation of *P. aeruginosa* at 25°C across all pHs tested (Fig. 4.18A). However, at SOP^{SA} and 1:10 concentrations of Active Oxygen in combination with Product 2, elevated levels of biofilm formation were observed. Levels of biofilm formation at the 1:10 concentration in the presence of Product 2 were 33% and 11% lower at pH 7 and 8 compared with 1:10 concentration alone whereas enhanced biofilm formation was seen at pH 7.4.

In all cases, the addition of Product 2 led to increased biofilm formation of *P. aeruginosa* across all pHs tested. Scheirer-Ray-Hare tests and two-way ANOVAs conveyed that Active Oxygen at all concentrations significantly reduced biofilm formation across all pHs tested (all $p<0.05$). Further analyses revealed that Active Oxygen at the 1:10 concentration in combination with Product 2 significantly reduced biofilm formation whereas at the SOP^{SA} concentration, Product 2 appeared to significantly reduced biofilm formation at pH 7 and 8 (all $p<0.05$).

At 37°C, Active Oxygen concentrations except 1:10 prevented biofilm formation of *P. aeruginosa* across all pHs tested (Fig. 4.18B). Active Oxygen at the SOP^{SA} concentration in combination with Product 2 resulted in sharp rises in levels of biofilm formation. This was also observed at the 1:10 concentration where biofilm formation was higher by 53%, 25% and 11% compared with the 1:10 concentration alone. In the presence of Product 2, *P. aeruginosa* exhibited similar levels of biofilm formation to control wells at pH 7 and 7.4 whereas it was reduced at pH 8 which a paired t-test found statistically significant ($p=0.0011$). Scheirer-Ray-Hare tests and two-way ANOVAs indicated that all concentrations of Active Oxygen except the 1:10 concentration and Product 2 by itself significantly reduced biofilm formation (all $p<0.05$). Active Oxygen at SOP^{SA} concentration in combination with Product 2 showed a significant interaction at pH 7 and 7.4 whereas all product combinations significantly lowered biofilm formation at pH 8.

4.2.11 Effect of Active Oxygen in combination with Water conditioner (Product 2) on cell morphology

In order to validate the conclusions based on single observations (N=1) in the previous project, light microscopy and live-dead staining procedures were performed on planktonic cell cultures used in growth and biofilm prevention assays following incubation under static conditions at 37°C. The fluorescent dyes used to assess cell viability were SYTO 9 and Propidium iodide. SYTO 9 is a green fluorescent stain which exhibits high affinity for DNA and penetrates bacterial cell membranes by staining nucleic acids. In contrast, propidium iodide is a red fluorescent stain which binds to DNA or RNA through the action of intercalating between bases. As propidium iodide is impermeable to live cells and can only enter cells that have impaired membrane structures, it is widely used as a viability tool for viewing dead cells in a population. Therefore, SYTO 9 and propidium iodide is commonly used to assess the viability of *E. coli* and *P. aeruginosa* (Puthia et al., 2022). Due to time constraints, the results shown here were only carried out using *E. coli* grown in M9 minimal media at pH 7.4.

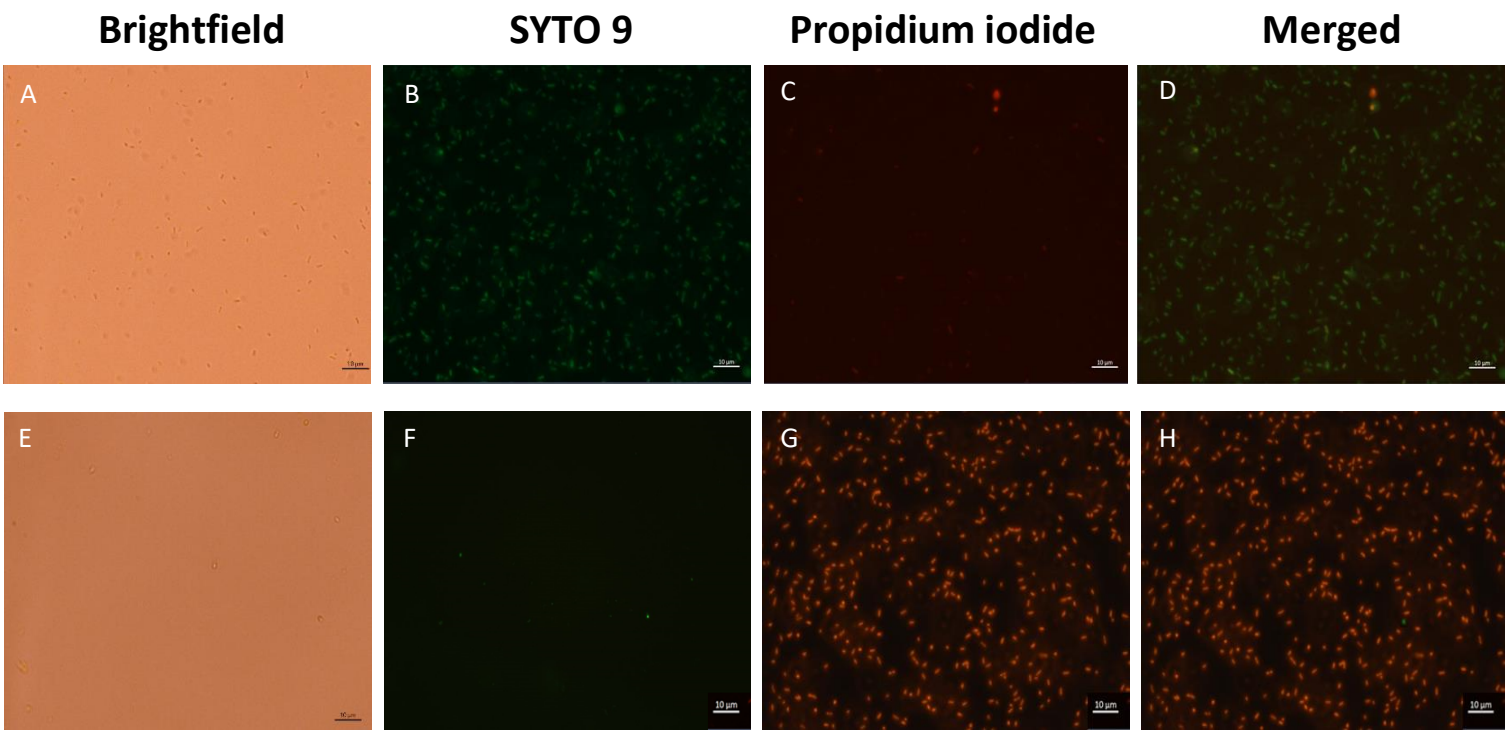

Figure 4.19. Light and fluorescence microscopy images of *E. coli* K12 planktonic cell cultures grown in M9 minimal media at pH 7.4 for 24h at 37°C in untreated wells (A-D) and in the presence of chlorine at 5ppm (E-H). Brightfield and fluorescent images were captured using a Zeiss fluorescent microscope using a 63x objective lens. Live bacteria were stained with SYTO 9 (green) and dead bacteria were stained with propidium iodide (red). Scale bar represents 10 µm.

Figure 4.19 shows the cell morphology of *E. coli* grown at 37°C for 24h in M9 minimal media at pH 7.4 without treatment and in the presence of chlorine at 5ppm, the recommended concentration used in hot tubs. Untreated *E. coli* retained cell viability with a large proportion of cells staining green with and minimal numbers of cells fluorescing red. In contrast, wells treated with chlorine at 5ppm led to high numbers of dead cells being viewed under the fluorescent microscope with little to no live cells fluorescing green.

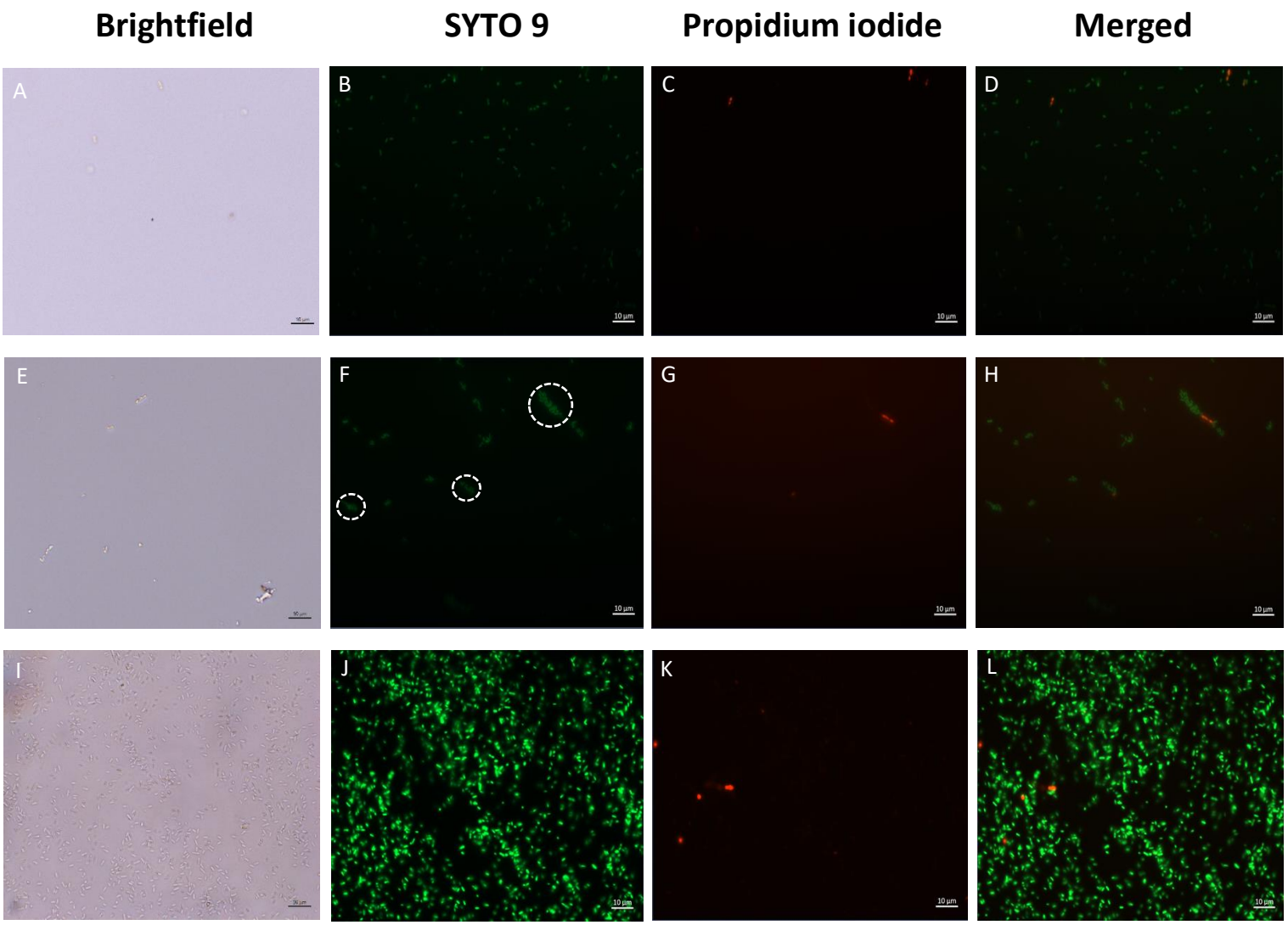

Figure 4.20. Light and fluorescence microscopy images of *E. coli* K12 planktonic cell cultures grown in M9 minimal media at pH 7.4 for 24h at 37°C in the presence of Active Oxygen at the initial dosage SOP^{FA} (A-D), SOP^{FA} concentration in combination with Product 2 (E-H) or Product 2 alone (I-L). Brightfield and fluorescent images were captured using a Zeiss fluorescent microscope with a 63x objective lens. Live bacteria were stained with SYTO 9 (green) and dead bacteria were stained with propidium iodide (red). Scale bar represents 10 µm.

As shown in figure 4.20*, E. coli* treated with Active Oxygen at the initial dosage (SOP^{FA}) showed the presence of live cells and a small proportion of dead cells. This was also observed at the SOP^{FA} concentration in combination with Product 2 which resulted in cells adopting a structure where they bunched together (circled in Fig. 4.20F). Comparing the fluorescent images taken between the SOP^{FA} concentration of Active Oxygen and in combination with Product 2, similar numbers of red fluorescing dead cells were observed. Furthermore, the addition of Product 2 caused high levels of live cells to be observed with high fluorescent intensity in comparison to all other treatments. To some degree, red fluorescing dead cells were seen but a large proportion of cells remained in their viable state. Cell viability assays showed that addition of Product 2 led to no CFU formation.

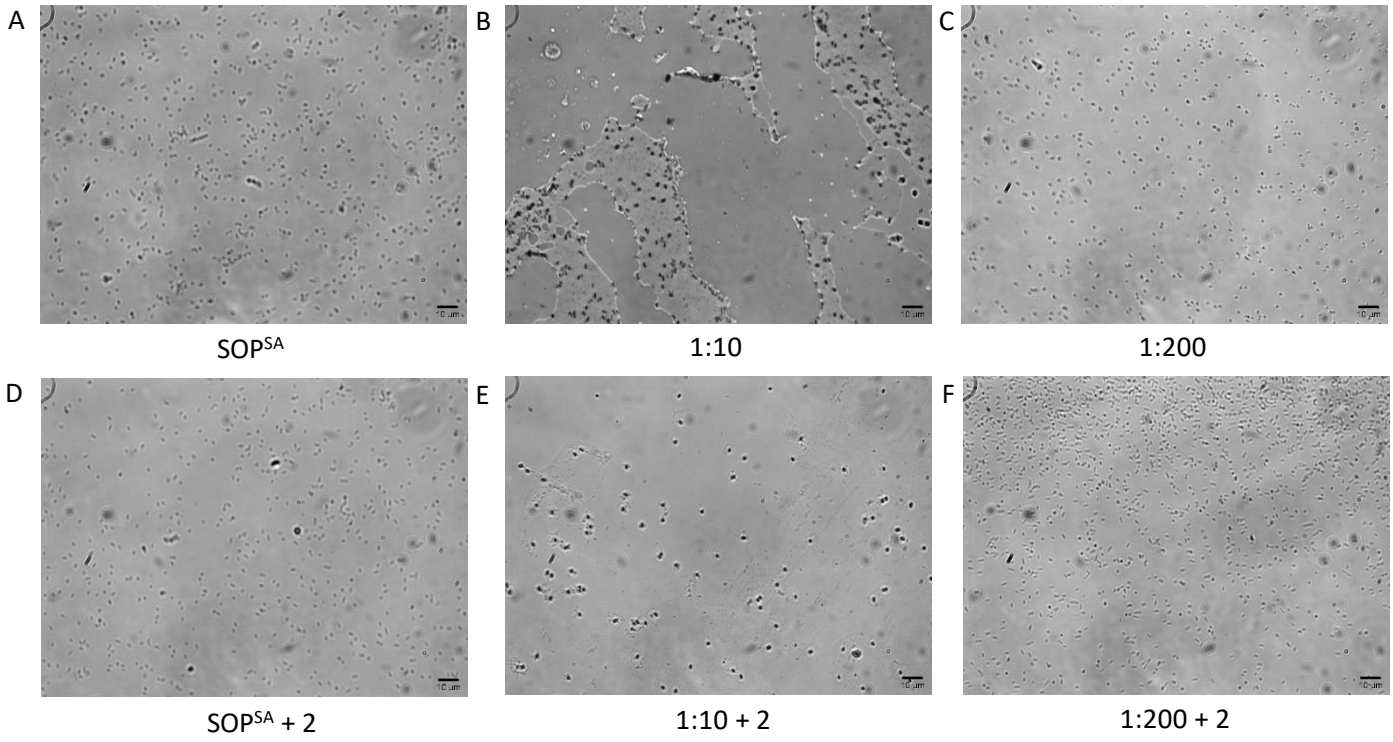

Figure 4.21. Brightfield microscopy images of *E. coli* K12 in M9 minimal media at pH 7.4 grown at 37°C for 1h in the presence of Active Oxygen at SOP^{SA} (A), 1:10 (B) and 1:200 (C) or in combination with Product 2 (D-F) using a 60x objective lens. Scale bar represents 10 µm.

Further light microscopy was also undertaken in order to investigate the effect of different Active Oxygen concentrations alone and in combination with Product 2 on the cell morphology of *E. coli*. Due to the lack of accessibility to microscopes in the final stages of the project, the following images shown in Fig. 4.21 were captured using an EXi Aqua camera attached to a Nikon Eclipse E600 microscope as a result. In addition, since time kill assays demonstrated that Active Oxygen was able to kill *E. coli* cells within 1h, samples were only incubated for 1h before being pipetted onto a microscope slide. At follow on applications of Active Oxygen alone and in combination with Product 2, there was no observable change in the cell morphology of *E. coli* as the number and shape of cells seen under the microscope was similar (Fig. 4.21A and D). However, at the 1:10 concentration of Active Oxygen, cells appeared to aggregate in large clusters which were encased in a layer (Fig. 4.21B). This was not seen in combination with Product 2 where cell morphology was more dot-like (Fig. 4.21E). At sublethal concentrations of Active Oxygen (1:200) there was a marked increase in the number of cells viewed under the light microscope with the addition of Product 2 promoting the growth of *E. coli* as denoted by the higher number of cells (Fig. 4.21C and F).

4.3 Discussion

4.3.1 Growth of overnight cultures

Following overnight incubation for 18h at 37°C under shaking conditions, *E. coli* overnight cultures grown in M9 minimal media at pH 5.2 showed weak levels of growth with low turbidity. This agrees with results obtained by Tawfik et al (2019) which illustrated that *E. coli* K12 strains grown in M9 minimal media under acidic conditions at pH 4.5 exhibit poor levels of growth. Recently, the optical density of *E. coli* K12 overnight cultures measured over a 4h period has been found to be extremely low with growth rates of less than 0.01 h^{-1} (Yang et al., 2022). Furthermore, overnight cultures of *P. aeruginosa* grown in M9 minimal media at extreme pH values (pH 9.2) showed no growth after overnight incubation. The slight change in colour from clear to clear yellow is most likely attributed to the production of the siderophore pyoverdine which gives *P. aeruginosa* its characteristic yellow-green colour. Siderophores such as pyoverdine are iron-chelating compounds which possess high affinity for the binding of iron. The method of iron uptake into *P. aeruginosa* cells is through the action of outer-membrane receptors, ATP-binding cassette transporters, haem scavengers or protein channels through which ferrous ion (Fe^{2+}) can diffuse directly from the outer membrane into the cytoplasm (Cartron et al., 2006; Dumas et al., 2013; Ochsner et al., 2000; Wandersman and Delepelaire, 2012). The presence of *Pseudomonas* strains in environments with high pH have been linked with a higher probability of *pvdL* being present but no pyoverdine production occurring (Butaitė et al., 2018). This suggests that high pH values restrict the ability of *P. aeruginosa* to produce pyoverdine by interfering with gene expression.

4.3.2 pH microelectrode results

From pH microelectrode measurements, the addition of Active Oxygen did not affect the pH of M9 minimal media at pH 7, 7.4 or 8. Small deviations in pH were found when Active Oxygen at the 1:400 concentration and SOP^{SA} concentration were added to M9 minimal media at pH 5.2 and 6.2 respectively. Despite this, the pH change was small and indicates that the addition of Active Oxygen does not influence the pH of the media.

4.3.3 Planktonic growth – Effect of pH

Active oxygen concentrations ranging from 10x concentrated to SOP^{SA} prevented planktonic growth of *E. coli* and *P. aeruginosa* at both temperatures and all pHs tested with the exception of observable growth of *P. aeruginosa* at 37°C at the SOP^{SA} concentration. One-way ANOVAs with Dunnett's post-hoc tests confirmed that these concentrations resulted in significantly lower planktonic growth across all pHs tested whereas all Active Oxygen concentrations had a significant effect in reducing planktonic growth of *P. aeruginosa* at pH 6.2 (25°C), 5.2 and 7 (37°C). Active Oxygen at the 1:10 concentration

showed higher efficacy at 25°C compared to 37°C across all pHs tested. In addition, Active Oxygen concentrations below 1:10 resulted in greater levels of planktonic growth which was found across both temperatures and pHs tested. These findings are consistent with results obtained in the previous project (Karagianni, 2022). However, the levels of planktonic growth exhibited by *E. coli* at 25°C were considerably higher at pH 8 in comparison to other pH values which showed similar growth. This is in agreement with previous studies have observed optimal growth of *E. coli* at pH 8 after a 24h incubation period (Rahman et al., 2012). The rise in levels of planktonic growth could also be attributed to upregulation of inner membrane proteins such as YqjA which transports sodium or potassium ions in order to maintain a cytoplasmic pH of approximately 7.6 which has been found to be essential for *E. coli* survival at alkaline pHs (Kumar, Tiwari and Doerrler, 2017). *E. coli* strains deficient in *yqiA* cannot grow under alkaline pH environments as the proton motive force required to facilitate transport of cations is unstable. Growth of *E. coli* can only be restored through overexpression of *yqjA* and under conditions where sodium and potassium concentrations in growth media exceed 100mM (Kumar and Doerrler, 2015). M9 minimal media is comprised of M9 salts containing disodium phosphate, potassium dihydrogen phosphate and sodium chloride with a concentration of 22mM in single strength media which could influence osmotic pressure encouraging the transport of cations sufficient to allow for further growth of *E. coli* under alkaline conditions.

Interestingly, *E. coli* and *P. aeruginosa* grown at 37°C displayed highest levels of planktonic growth in M9 minimal media at pH 5.2. This was unexpected as overnight cultures of *E. coli* and *P. aeruginosa* did not grow to a large extent. This could give insights into the acid-tolerance response (ATR) systems that *E. coli* and *P. aeruginosa* possess which allow them to support further growth under acidic conditions. In response to acidic environments, there is increased expression of genes which are vital for the synthesis of unsaturated fatty acids such as *fabA* and *fabB* resulting in elevated protein and mRNA levels. The *fabB* gene appears to promote survival at higher temperatures and the ATR system has also been found to be conserved in *P. aeruginosa* PA01 strains where higher levels of protein and mRNA have also been detected (Xu et al., 2020). Therefore, the change in lipid composition influences membrane structure and activity of proton pumps as a mechanism to achieve a stable intracellular pH following exposure to acidic conditions. Recently, *E. coli* K12 has been investigated in the presence of organic acids at pH 4.8. Results showed that there were significantly higher growth rates in response to acid stress and genetic constructs containing a vector for insertion of the *RffG* gene was associated with survival rates higher than 4500-fold (Yang et al., 2022). The effect of eDNA on growth of *P. aeruginosa* planktonic cultures in LB media indicates that acidic environments with pH 5.5 result in the activation of *cyoABCDE* genes which code for a cytochrome that can only be produced under oxygen-rich environments. In addition, the same study identified several antibiotic resistance genes which are

induced by eDNA which could suggest a shift towards an antibiotic resistant phenotype following treatment with Active Oxygen at pH 5.2 which is denoted by the higher levels of planktonic growth (Lewenza et al., 2020).

4.3.4 Biofilm formation – Effect of pH

Stronger concentrations of Active Oxygen (10x concentrated, SOP^{FA} and SOP^{SA}) showed high efficacy in preventing biofilm formation of *E. coli* and *P. aeruginosa* at both temperatures and all pHs tested. This was confirmed by one-way ANOVAs with Dunnett's post-hoc tests which indicated that these concentrations significantly reduced planktonic growth across all pHs with the 1:10 concentrations also having a significant effect against *E. coli* at pH 5.2 (25°C) and pH values from 5.2-7.4 (37°C). At pH 5.2, Active Oxygen at the 10x concentration was less effective at preventing biofilm formation of *E. coli* in comparison to the first and follow on applications (SOP^{FA} and SOP^{SA}) whereas there was a slight elevation in biofilm formed by *P. aeruginosa* at the SOP^{SA} concentration at 37°C. *E. coli* K12 has been shown to exhibit higher levels of biofilm formation in crystal violet assays at 37°C compared to 25°C at pH 5.5 which indicates that acidic pH environments can promote biofilm formation (Mathlouthi, Pennacchietti and Biase, 2018). In addition, peracetic acid is a disinfectant with low pH which, when employed at concentrations of up to 1500ppm has been shown to result in high viability of cells in *P. aeruginosa* biofilms. (Akinbobola et al., 2017). This suggests that high concentrations may lead to reduced susceptibility to disinfectants in low pH environments.

Furthermore, the 1:10 concentration resulted in low levels of biofilm formation shown by *E. coli* grown at 25°C at pH 7 and 8 with little to no biofilm being detected at pH 5.2. Sublethal concentrations of Active Oxygen showed high efficacy at pH 5.2 and 8 (1:400) including at pH 7 (1:200 and 1:400) against *E. coli* grown at 25°C. This was not observed for *P. aeruginosa* grown at 25°C following treatment with sublethal concentrations of Active Oxygen since elevated levels of biofilm formation were detected at pH 7 (1:100), 7.4 and 8 (1:10 and 1:600). All sublethal concentrations at pH 6.2 were more effective compared to the 1:10 concentration in preventing biofilm formation of *P. aeruginosa* grown at 37°C. This differed at pH 5.2 where lower efficacy was demonstrated across Active Oxygen concentration from 1:10 to 1:400 resulting in biofilm formation levels which exceeded those seen in control wells.

4.3.5 Planktonic growth – Effect of temperature

The highest levels of planktonic growth were observed at pH values ranging from 5.2 to 7.4 in control wells containing *P. aeruginosa* grown at 37°C. This was confirmed by one-way ANOVAs and Tukey's post-hoc tests which demonstrated that planktonic growth of *P. aeruginosa* at 37°C was significantly higher compared to 25°C and *E. coli* grown at both temperatures. At pH 8, it appeared that planktonic growth was similar in control wells between *P. aeruginosa* grown at 37°C and *E. coli* grown at both

temperatures. The lowest concentrations of Active Oxygen (1:400 and 1:600) resulted in greater planktonic growth of *E. coli* compared with *P. aeruginosa* at 25°C which was confirmed by statistical significance in a one-way ANOVA. These findings were also seen in the previous project where the media was half the strength with less nutrients available (Karagianni, 2022). There is evidence to suggest that activation of cold shock proteins or increased expression of stress response genes such as *RpoS* promotes growth of *E. coli* at lower temperatures. In response to low temperature environments, cold shock proteins function as RNA/DNA binding proteins which are stimulated and unfold the structure of RNA in order to enable translation to continue (Gottesman, 2018). This cold shock response acts as protective mechanism which facilitates bacterial growth. Overexpression of cold shock proteins such as CsdA promotes cell division whereas defective mutants negatively impact purine and ribose metabolic pathways which in turn affects translation rates in *E. coli* (Phadtare, 2012). DNA microarray analyses which assess gene expression levels have identified upregulated expression of genes involved in the cold shock response and stress response suggesting that the systems which regulate these processes may interact with each other. Gene expression levels measured by qRT-PCR also confirmed that the stress response genes *otsA* and *ymgB* are upregulated in *E. coli* at lower temperatures which was evident in both LB and M9 minimal media (White-Ziegler et al., 2008). Various sublethal concentrations led to similar levels of planktonic growth following treatment with Active Oxygen. These were noted at pH 5.2 (1:100 to 1:600) with both strains and temperatures, pH 6.2 (1:100 to 1:600 with *E. coli* and *P. aeruginosa* grown at 25°C, pH 7 (1:10 to 1:400) with *E. coli* grown at 37°C as well as *P. aeruginosa* grown at both temperatures, pH 7.4 (1:10 to 1:600) with *E. coli* at both temperatures and pH 8 (1:10, 1:100 and 1:200) with *P. aeruginosa* grown at 37°C. At 37°C, sublethal concentrations of Active Oxygen demonstrated higher efficacy in preventing planktonic growth of *P. aeruginosa* at pH 6.2 (1:600) and pH 7.4 (1:200, 1:400 and 1:600) whereas at 25°C, planktonic growth increased at lower concentrations.

4.3.6 Biofilm formation – Effect of temperature

Active Oxygen concentrations ranging from 10x concentrated to SOP^{SA} successfully prevented biofilm formation of *E. coli* and *P. aeruginosa* across both temperatures and all pHs tested except pH 5.2 where there was a rise in biofilm formation when *P. aeruginosa* grown at 37°C were treated with the SOP^{SA} concentration. Overall, addition of the 1:10 Active Oxygen concentration caused sharp rises in biofilm formation across all pHs tested of which the effect was most pronounced with *P. aeruginosa* at 37°C. This was confirmed by one-way ANOVAs and Tukey's post-hoc tests which demonstrated that *P. aeruginosa* biofilm formation at 37°C was significantly higher compared to 25°C and *E. coli* grown at both temperatures at pH 5.2, 6.2, 7.4 and 8. Active Oxygen concentrations below SOP^{SA} led to higher levels of biofilm formation at pH 8 against *E. coli* at 37°C and *P. aeruginosa* at both temperatures

whereas at pH 6.2, sublethal concentrations showed similar efficacy in preventing *E. coli* biofilm formation at both temperatures. All Active Oxygen concentrations at pH 7.4 displayed high efficacy in preventing biofilm formation of *E. coli* at both temperatures. In contrast, sublethal concentrations of Active Oxygen were found to have lower efficacy against *E. coli* and *P. aeruginosa* biofilm formation at 25°C compared to 37°C. These results were noted at pH 5.2 (1:100, 1:200 and 1:600) and pH 7 (1:10). Comparisons between *P. aeruginosa* grown at 25°C and 37°C showed that higher temperatures prevented biofilm formation by *P. aeruginosa* to a higher extent following treatment with sublethal concentrations of Active Oxygen at pH 6.2. Interestingly, *P. aeruginosa* exhibited increased biofilm formation at 25°C compared to 37°C and *E. coli* at both temperatures which one-way ANOVAs with Tukey's post-hoc analysis found statistically significant at pH 7. These results are consistent with previous studies which show that at lower temperatures, *P. aeruginosa* can form strong biofilms with higher levels of c-di-GMP levels being observed (Kim et al., 2020; Townsley and Yildiz, 2015). In addition, transcription of the *pel* gene which encodes for proteins which contribute to the exopolysaccharide matrix architecture in *P. aeruginosa* biofilms is dependent on temperature with lower temperatures promoting β-galactosidase activity which contributes heavily to the glucose rich environment of the exopolysaccharide matrix (Sakuragi and Kolter, 2007). Transcriptomic analysis has also identified several phage proteins linked with the EPS matrix which are upregulated at lower temperatures which could explain the elevated levels of biofilm formation at lower temperatures at 25°C (Bisht et al., 2021).

4.3.7 Specific biofilm formation

Active Oxygen resulted in low levels of specific biofilm formation shown by *E. coli* at both temperatures and all pHs tested. This is concurrent with *E. coli* K12 strains which have been shown to exhibit low specific biofilm formation in M9 minimal media supplemented with glucose (Nickerson and McDonald, 2012). There was a more distinctive difference between specific biofilm formation levels of *P. aeruginosa* following treatment with Active Oxygen where higher efficacy was seen at 37°C compared to 25°C. This demonstrates that specific biofilm formation differs between strains. Comparative studies show that staining cells with crystal violet can result in variability in OD measurements between strains after 24h incubation periods (Peeters et al., 2008). Stronger concentrations of Active Oxygen (SOP^{FA}, SOP^{SA} and 1:10) resulted in peaks in *E. coli* specific biofilm formation with large error bars which was also seen with *P. aeruginosa*. This is consistent with observations illustrated by Delaney (2018) and Karagianni (2022). Mathematically, dividing by small numbers leads to large numbers with high variance which is evident in other studies which show the effect of essential oil components on specific biofilm formation of *E. coli* and *P. aeruginosa* (Niu and Gilbert, 2004).

4.3.8 Effect of Active Oxygen on cell viability

4.3.8.1 Log reductions

Active Oxygen was most effective at reducing cell viability of *E. coli* and *P. aeruginosa* at pH 5.2 when grown at 37°C with log reductions derived from planktonic readings taken at OD_{595} exceeding 1.4 and 2 for both strains. Hydroxyl and sulphate radicals generated by potassium peroxymonosulfate are known to exhibit potent antibacterial activity against *E. coli* at 37°C as higher temperatures lead to the formation of larger amounts of Active Oxygen species (Xu et al., 2012). In addition, hydrogen peroxide which forms hydroxyl radicals like the Active Oxygen product, when employed at higher concentrations in low pH environments can enhance antibacterial activity against *E. coli* (Raffellini et al., 2008). In response to increased temperatures, disinfectants have also been shown to have improved efficacy in reducing cell viability of *P. aeruginosa* which has been found to be superior to existing disinfection products (Gedge et al., 2019). However, it should be noted that log reduction data was derived from OD_{595}-CFU calibration curves which may not give an accurate representation as previous project results demonstrated that Active Oxygen can cause log reductions higher than 3.5 for both bacterial strains as determined by direct CFU measurements (Karagianni, 2022).

4.3.8.2 Time-kill assay

Time-kill assays assessed the time-killing effect of Active Oxygen by direct CFU enumeration. Active Oxygen at the first and follow on applications (SOP^{FA} and SOP^{SA}) exhibited antibacterial activity against *E. coli* within 5 minutes of exposure to Active Oxygen. Ampicillin and erythromycin were included as positive controls to determine whether Active Oxygen demonstrates either bactericidal or bacteriostatic activity against *E. coli*. After 60 minutes, there was a marked decrease in cell viability in response to Active Oxygen which followed a trend similar to bactericidal antibiotics such as ampicillin which has been shown previously (Kohanski et al., 2007; Xu et al., 2020). Paired t-tests confirmed that *E. coli* cells treated with Active Oxygen and antibiotics significantly decreased cell viability at all time points except with the SOP^{SA} concentration at 10 min. Viable cell counts of *E. coli* appeared to be higher at the SOP^{FA} concentration compared to SOP^{SA} after 60 minutes of exposure. This was unexpected as it was hypothesised that stronger concentrations of Active Oxygen would lead to decreased cell viability. Chlorine used at recommended concentrations (5ppm) successfully killed *E. coli* within 5 minutes of exposure (data not shown) which is in line with observations seen by Gallandat et al (2017) which revelated that NaDCC solutions prepared from granules as used in this project are effective against *E. coli*. Disk diffusion assays conducted in the previous project demonstrated that Active Oxygen reacts with organic material in the agar and loses efficacy with no halo being observed (Karagianni, 2022). Therefore, it can be deduced that between the time taken for serial dilution and plating on LB agar, the activity of Active Oxygen does not continue.

4.3.8.3 Decay

Currently, there is no published data regarding the stability of KMPS. Cell viability experiments revealed that viable cell counts of *E. coli* were maintained throughout a period of 7 days without losing its antibacterial activity (Fig. 4.14). In similar applications where KMPS is used as a disinfectant, it has been reported that solutions of once prepared remain active for up to 7 days (Griffin, 2012; Sykes and Weese, 2014). According to the European Chemicals Agency, in buffered solutions at pH 7, KMPS has a half-life of 53h at 30°C which would explain the increase in cell viability at day 3 (ECHA, 2022). Higher CFU counts may also be measured due to product instability.

4.3.9 Planktonic growth – product combinations

At 25°C, all Active Oxygen concentrations tested were effective at preventing planktonic growth of *E. coli* whereas at 37°C, there was observable growth at the 1:10 concentration. Active Oxygen concentrations from 10x to SOP^{SA} in combination with Product 2 demonstrated higher efficacy at 37°C where little to no planktonic growth was observed. However, at 25°C, the SOP^{SA} and 1:10 concentration in combination with Product 2 resulted in increased planktonic growth which was highest at pH 8 for both temperatures. Addition of Product 2 led to reductions in planktonic growth of *E. coli* across all pHs and both temperatures which were found to be significantly lower at all pHs at 25°C but only statistical significance could be found at pH 8 at 37°C. This was confirmed by Scheirer-Ray-Hare and two-way ANOVAs which showed that Active Oxygen alone and in combination with Product 2 at all pHs including Product 2 by itself at pH 7.4 and 8 causes a significant reduction in planktonic growth of *E. coli*.

At higher Active Oxygen concentrations (10x, SOP^{FA} and SOP^{SA}), planktonic growth of *P. aeruginosa* was prevented at both temperatures which is denoted by the low OD measurements. The SOP^{SA} concentration in combination with Product 2 enhanced planktonic growth at both temperatures and all pHs tested. Despite this, Schreier-Ray-Hare tests and two-way ANOVAs revealed that Active Oxygen and Product 2 alone including in combination with Product 2 at the SOP^{SA} concentration at pH 7 and 7.4 showed a significant effect in preventing planktonic growth at both temperatures whereas all product combinations were effective at pH 8 when *P. aeruginosa* were grown at 37°C. This was followed by further increases in planktonic growth at the 1:10 concentration with Product 2. The presence of Product 2 at pH 7 was only able to reduce planktonic growth of *P. aeruginosa* grown at 25°C whereas it promoted growth at higher pHs which was significantly higher at pH 8. In contrast, Product 2 lowered planktonic growth across all pHs at 37°C but was most effective against *P. aeruginosa* at pH 8 which was statistically significant.

As the water conditioner contains the surfactant octyldimethylamine oxide it is suggested that it may exhibit antibacterial properties. Several surfactants have been shown to possess antibacterial activity against *E. coli* and *P. aeruginosa* (El-Bana et al., 2022). Previous research also suggests that octyldimethylamine may affect components of the electron transport chain through solubilisation of reaction centres and micelle formation (Gast et al., 1996). However, it is unknown whether the antibacterial activity is attributed to the surfactant or other components present within the water conditioner.

4.3.10 Biofilm formation – product combinations

High efficacy of Active Oxygen across all concentrations was demonstrated at 25°C whereas at the 1:10 concentration, there were higher levels of biofilm formation exhibited by *E. coli* grown at 37°C. In general, Active Oxygen in combination in Product 2 led to elevated levels of biofilm formation at both temperatures with the exception of the SOP^{SA} concentration in combination with Product 2 at 25°C where high efficacy was still observed at pH 7.4 in comparison to pH 7 and 8 which was comparable to SOP^{FA} and 10x concentrations. Scheirer-Ray-Hare tests and two-way ANOVAs indicated that Active Oxygen is effective at reducing biofilm formation across all pHs and both temperatures. All product combinations at pH 7 and 8 were statistically significant at 25°C including at stronger Active Oxygen concentrations in combination with Product 2 at 37°C at pH 8 whereas this was observed at lower concentrations at pH 7 and 7.4. Product 2 showed a significant effect in reducing biofilm formation at all pHs across both temperatures except pH 7.4 at 25°C. Sharp rises in biofilm formation were seen at the 1:10 concentration in combination with Product 2 at both temperatures and pHs tested. Generally, the most substantial increase in biofilm formation was seen at 25°C whereas at 37°C, levels of biofilm formation were lower. Although Product 2 decreased biofilm formation of *E. coli* across both temperatures and all pHs, statistical significance was only achieved at pH 7 and 8 when *E. coli* were grown at 25°C. This suggests that surfactants such as octyldimethylamine oxide present in Product 2 may have a role in preventing biofilm formation of *E. coli*. Surfactants have been known to interfere with curli-integrated film formation in *E. coli*, thus preventing the progression of the biofilm formation process (Wu et al., 2013).

Active Oxygen concentrations ranging from 10x concentrated to SOP^{SA} successfully prevented *P. aeruginosa* biofilm formation whereas the SOP^{SA} and 1:10 concentrations in combination with Product 2 resulted in sharp rises in biofilm formation across both temperatures and pHs tested. This was confirmed by Scheirer-Ray-Hare tests and two-way ANOVAs which demonstrated that Active Oxygen significantly reduced biofilm formation across all pHs including all product combinations at pH 8 whereas this was only evident at 37°C in the presence of the SOP^{SA} concentration at pH 7 and 7.4 as well as the 1:10 concentration at 25°C at pH 7 and 8. Product 2 showed a significant effect in reducing

biofilm formation at all pHs across both temperatures except pH 7.4 at 25°C. Furthermore, at the 1:10 concentration in combination with Product 2, higher efficacy was shown at pH 7 and 8 in preventing biofilm formation compared to pH 7.4 where it enhanced *P. aeruginosa* biofilm formation. In the presence of Product 2, levels of biofilm formation were raised at all pHs at 25°C which surpassed levels observed in control wells. Similar trends were seen at 37°C where the addition of Product 2 showed no effect in preventing biofilm formation of *P. aeruginosa* at pH 7 and 7.4 denoted by levels comparable to that in control wells. However, Product 2 appeared to significantly reduce biofilm formation at pH 8. Surfactant-based dressings are known to be effective at preventing *P. aeruginosa* PA01 biofilm formation as no bacteria present in the biofilm could be detected after 24 hours (Yang et al., 2018). Further studies indicate that exposure to surfactants can prevent *P. aeruginosa* PA01 biofilm formation by significantly reducing the secretion of pyocyanin which is required for robust biofilm architecture (Piecuch et al., 2016).

Therefore, it can be concluded that the addition of Product 2 lowers the efficacy of Active Oxygen in preventing biofilm formation of *E. coli* and *P. aeruginosa* at both temperatures and most pHs tested. It is important to note that Product 2 does not function as a biocide and is only used to improve skin hydration and enhance the skin experience. Product 2 contains sodium cocoate, citric acid, coconut fatty acids and a preservative used to prevent microbial contamination (eco3spa, 2023; Lonza Ltd, 2013). In *P. aeruginosa*, regulatory systems such as TctD-TctE acts on *opdH* which encodes for a porin required for the necessary transport of carboxylic acids such as citric acid (Tamber et al., 2007). It has been shown previously that mutant constructs deficient in TctD-TctE display similar levels of biofilm formation regardless of the concentration of citric acid. This was confirmed by phenotypic microarrays which demonstrated that the same strains of *P. aeruginosa* could not grow in the presence of citric acid (Taylor, Zhang and Mah, 2019). Gas chromatography analysis shows that coconut contains a high proportion of saturated fatty acids such as lauric acid, myristic acid and palmitic acid followed by caprylic acid and capric acid in smaller amounts (Mahayothee et al., 2016). Further studies have used gas chromatography to investigate the fatty acid content of *P. aeruginosa* and *S. typhimurium*. Results revealed that more saturated fatty acids are present in the biofilm state compared to the planktonic state with higher biofilm thickness also being observed (Dubois-Brissonnet, Trotier, and Briandet, 2016). This suggests that the level of saturated fatty acids such as lauric acid, myristic acid and palmitic acid provides nutrients for gram negative bacteria such as *E. coli* and *P. aeruginosa* which contributes to higher levels of biofilm formation. In addition, Product 2 is more effective at preventing biofilm formation of *E. coli* at 25°C whereas this is observed at 37°C for *P. aeruginosa*. This suggests that that the efficacy of Product 2 in preventing biofilm formation may be strain specific.

4.3.11 Light and fluorescence microscopy

Light microscopy revealed a high number of cells in untreated wells which demonstrates that *E. coli* grows well at 37°C in M9 minimal media at pH 7.4 (Fig. 4.19A). This was in line with live-dead staining procedures as denoted by the high numbers of live cells which fluoresced green whereas treatment with chlorine at 5ppm resulted in a large number of dead cells which stained red (Fig. 4.19B and G). *E. coli* cells treated with Active Oxygen for 1h led to decreased cell motility which adopted a structure where cells aggregated into clump-like structures at the 1:10 concentration (Fig. 4.21B). At sublethal concentrations of Active Oxygen (1:200) there was a higher number of cells seen under the light microscope with the addition of Product 2 promoting the growth of *E. coli* (Fig. 4.21C and F). The clump-like structures identified using light microscopy at the 1:10 concentration were also observed in live-dead staining with the SOP^{FA} concentration in combination with the water conditioner where cells present in the clumps were in an apparently viable state. This is in accordance with the observations found in the previous project which suggested that the product combination could lead to a VBNC state (Karagianni, 2022). Cells which adopt the VBNC state are unable to grow on agar and produce colony forming units which presents a challenge as they cannot be detected by common microbiology techniques and increases the risk of false-negative results (Ding et al., 2017). Confocal microscopy and live-dead staining using SYTO 9 and propidium iodide has identified cell clumping in other bacterial species which showed higher bacterial counts compared to CFU enumeration on agar (Auty et al., 2001). This signifies the important of cell viability staining as the VBNC state leads to underestimation of CFU enumeration because bacteria cannot be cultivated on agar. Pyruvate has been shown to play an important role in VBNC *E. coli* cells. Under conditions where nutrients are scarce, pyruvate sensing networks consist of histidine kinase-response regulator systems such as BtsS/BtsR and YpdA/YpdB which have been linked with activation of transporters BtsT and YhjX (Behr, Fried and Jung, 2014;Vilhena et al., 2019). Upon entering the VBNC state, pyruvate uptake is increased in *E. coli* K12 cells through the action of BtsT (Vilhena et al., 2019). This implies that in response to nutrient depletion, pyruvate uptake in *E. coli* cells which are VBNC are the primary carbon source as opposed to glucose because it does not require phosphorylation in order to be activated (Göing and Jung, 2021). The addition of Product 2 resulted in a large proportion of live cells with little to no dead cells being observed.

Treatment with the water conditioner in cell viability assays led to no CFU formation which provides more evidence that it plays an important role in cell clumping and the VBNC state of *E. coli* cells. It is possible that components within the water conditioner may undergo chemical reactions with compounds present in the M9 minimal media which could lead to the VBNC state. An interesting study investigating the effect of surfactants and inorganic salts found a combinatorial effect which can induce

the VBNC state in *E. coli* (Robben et al., 2018). This suggests that the surfactant octyldimethylamine oxide present in the water conditioner could possibly also react with salts in the M9 minimal media and lead to VBNC *E. coli* cells.

Chapter 5: Dynamic biofilm removal using Active Oxygen, biofilm remover and Eco3spa product combinations

5.1 Introduction

In this chapter, the aim was to assess the efficacy of two Eco3spa products for their biofilm removal properties. The first product is eco3spa Step 1 Hot Tub Cleaner (Product 1) which claims to remove biofilms and scale from pipework surfaces. Due to time constraints, the experiments conducted in the previous project (Karagianni, 2022) could not be repeated and the experimental design was adapted to obtain results within a shorter time-frame. The results described in this chapter demonstrate the efficacy of the biofilm remover, Active Oxygen and their product combinations against pre-formed biofilms grown for 24h.

5.2 Results

Due to time constraints as experiments were conducted in the final stages of this one-year project, several adaptations were made to the experimental design in order to obtain results within the remaining time of the project. Firstly, overnight cultures of *E. coli* and *P. aeruginosa* were diluted with double strength media instead of single strength media used in the previous project. Therefore, the final concentration of the media was single strength. Secondly, dynamic conditions were used in this study in order to simulate the flushing of water and/or action of jets within the hot tub system whereas static conditions were used previously (Karagianni, 2022). Also, most microtiter plate assays are performed under static conditions and less is known about the influence of hydrodynamics on biofilm formation. Furthermore, experiments were only conducted on *E. coli* and *P. aeruginosa* at 37^{o}C based on manufacturer instructions which state that water should be at "operating temperatures of 35-40^{o}C." In addition, the previous project incorporated addition of products which were incubated for 24h. Due to time constraints, this time-frame was reduced to 1h based on manufacturer instructions that indicate that the biofilm removal product should be added to hot tub water and "run for at least 60 minutes where foaming occurs and dark coloured biofilm particulates are seen."

5.2.1 Efficacy of Product 1 (biofilm remover) against pre-formed biofilms

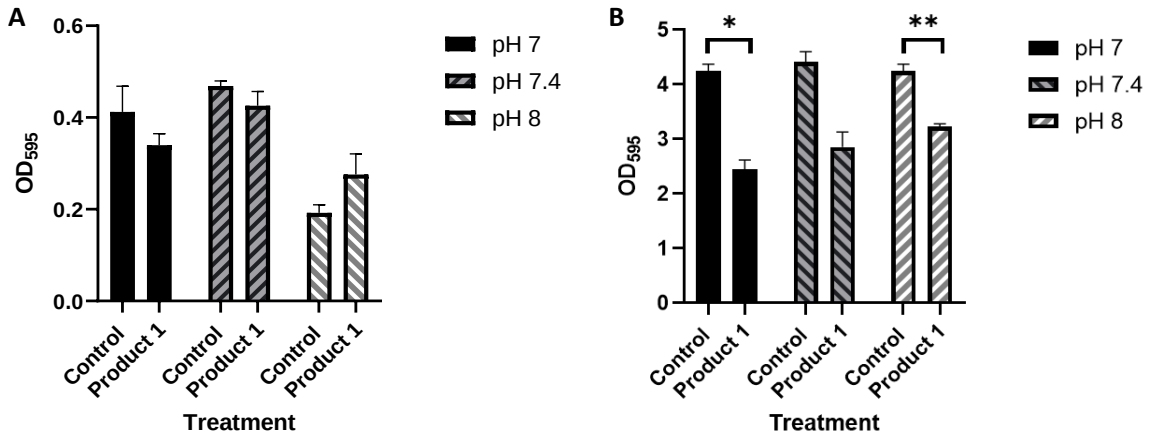

Figure 5.1. Quantification of *E. coli* K12 (A) and *P. aeruginosa* PA01 (B) biofilm formation in M9 minimal media at pH 7, 7.4 and 8 (indicated as OD_{595}) in the presence and absence of Product 1 (biofilm remover) at 37°C. N=3 for each data point and error bars represent standard error of the mean (SEM). Paired t-test was conducted and statistical significance is indicated by *p<0.05;**p<0.01.

In order to investigate the efficacy of Product 1 (biofilm remover), *E. coli and P. aeruginosa* biofilms were grown for 24h. Following the establishment of pre-formed biofilms, wells were treated with the biofilm remover at the SOP concentration before introducing dynamic conditions by shaking for 1h in a plate reader. The results of the biofilm removal assays are illustrated in figure 5.1. The presence of biofilm remover demonstrated minor effects on *E. coli* biofilm removal at pH 7 and 7.4 after 1h of treatment (Fig. 5.1A) which paired t-tests did not find significantly different to control wells ($p<0.05$). Also, at pH 8, addition of biofilm remover appeared to increase biofilm formation levels. Furthermore, the addition of the biofilm remover reduced *P. aeruginosa* biofilm formation at pH 7 and 7.4 by 42.2% and 35.3% (Fig. 5.1B). However, statistical analyses between treated and untreated controls showed that significant reductions were only observed at pH 7 and 8 ($p=0.0150$ and $p=0.0073$, paired t-test) which was not observed at pH 7.4 ($p=0.0525$, paired t-test).

5.2.2 Efficacy of Active Oxygen against pre-formed biofilms

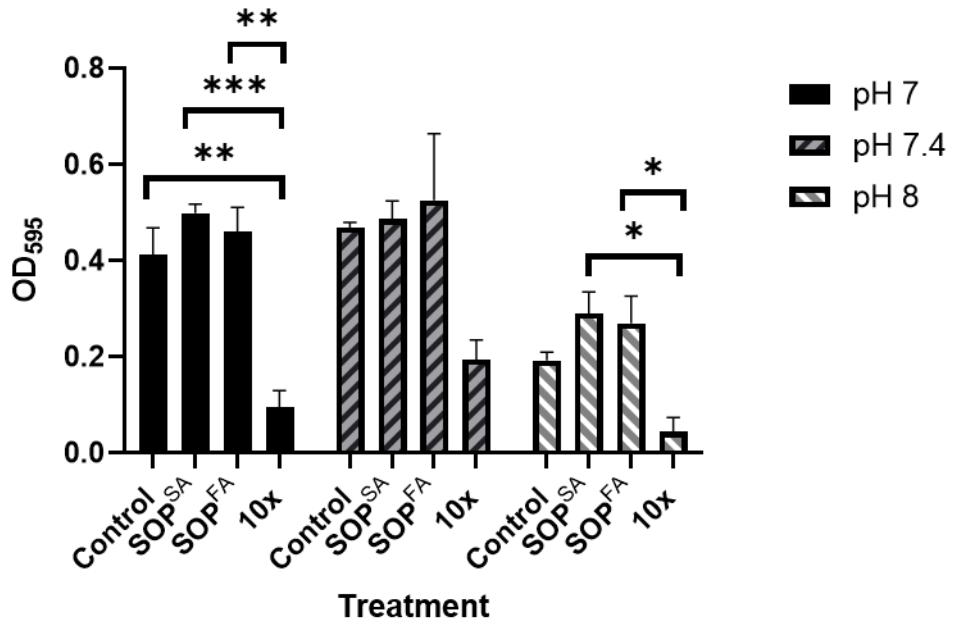

Figure 5.2. Quantification of *E. coli* K12 biofilm formation in M9 minimal media at pH 7, 7.4 and 8 (indicated as OD_{595}) in the presence and absence of Active Oxygen at 37°C. SOP^{FA} and SOP^{SA} indicate the initial dosage and follow on applications of Active Oxygen. N=3 for each data point and error bars represent standard error of the mean (SEM). One-way ANOVA with Tukey's post-hoc test for multiple comparisons was conducted and statistical significance is indicated by *p<0.05;**p<0.01;***p<0.001.

Figure 5.2 demonstrates the efficacy of Active Oxygen in removing *E. coli* biofilms after treatment with Active Oxygen at various dilutions. Following treatment with Active Oxygen, only the 10x concentrated concentration was able to cause a decrease in biofilm formation by 77%, 58.5% and 76.8% across all pHs tested. In contrast, at SOP^{FA} and SOP^{SA} concentrations both treatments caused biofilm formation levels to be higher than controls which was observed across all pHs tested. One-way ANOVA testing between treated and untreated controls returned significantly different outcomes at each pH (p=0.0006, 0.0492 and 0.0094). Tukey's post-hoc analysis revealed that comparisons between 10x concentrated Active Oxygen and control treatments returned statistically significant differences at pH 7 (p=0.0034, -0.5112 to -0.1238, 95% CI). In addition, statistically significant differences were also found at pH 7 between 10x concentrated Active Oxygen, SOP^{FA} (p=0.0014, -0.5588 to -0.1715, 95% CI) and SOP^{SA} (p=0.0007, -0.5983 to -0.2109, 95% CI). Similarly, statistically significant differences were observed from Tukey's post-hoc comparisons between the same treatments at pH 8 (p=0.0171, -0.4059 to -0.04405, 95% CI; p=0.0105, -0.4266 to -0.06479, 95% CI). No statistical difference was found between treatments conducted at pH 7.4 in Tukey's multiple comparisons tests.

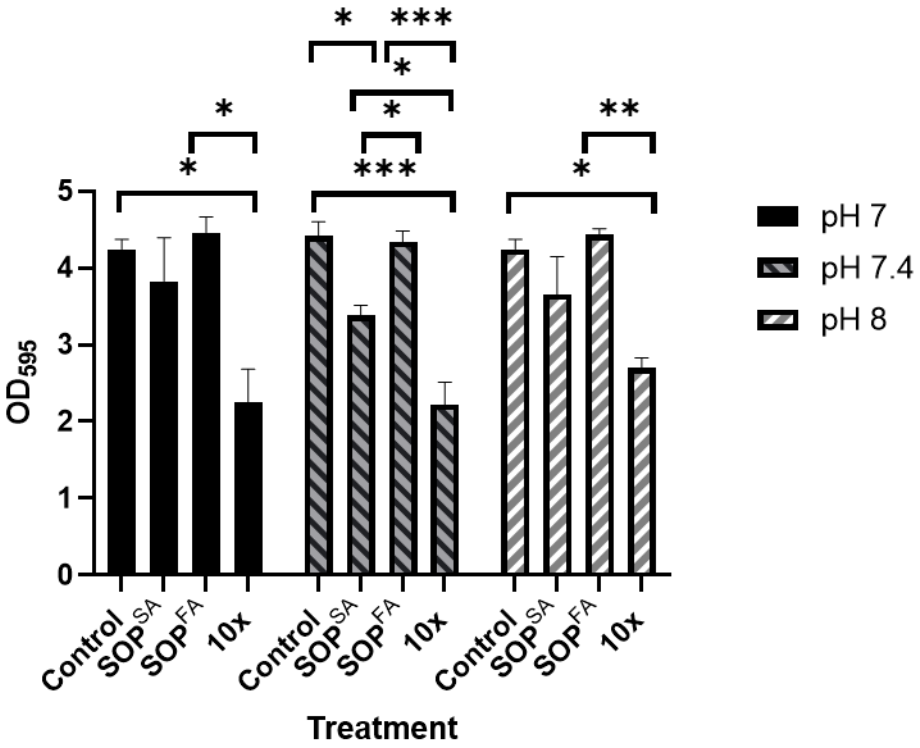

Figure 5.3. Quantification of *P. aeruginosa* PA01 biofilm formation in M9 minimal media at pH 7, 7.4 and 8 (indicated as OD_{595}) in the presence and absence of Active Oxygen at 37°C. SOP^{FA} and SOP^{SA} indicate the initial dosage and follow on applications of Active Oxygen. N=3 for each data point and error bars represent standard error of the mean (SEM). One-way ANOVA with Tukey's post-hoc test for multiple comparisons was conducted and statistical significance is indicated by *p<0.05;**p<0.01;***p<0.001.

Active oxygen at 10x concentration also reduced biofilm formation of *P. aeruginosa* by 46.8%, 49.6% and 36.4% across all pHs tested (Fig. 5.3). However, Active Oxygen at the SOP^{SA} concentration was able to remove biofilms formed in the wells whereas the SOP^{FA} concentration did not affect biofilm formation as OD readings were higher or equivalent to control wells. One-way ANOVA testing conducted between treated biofilms and untreated controls revealed that there were statistically significant differences in biofilm formation (p=0.0118, 0.0001 and 0.0069). Tukey's post-hoc comparison tests revealed statistically significant differences between 10x concentrated Active Oxygen and controls (p= 0.0225, -3.672 to -0.3030, 95% CI; p=0.0002, -3.079 to -1.301, 95% CI; p=0.0144, -2.748 to -0.3406, 95% CI). Also, statistically significant differences were seen at pH 7.4 between SOP^{SA} compared against untreated controls (p=0.0251, -1.916 to -0.1377, 95% CI). Several other comparisons showed statistically significant differences between 10x concentrated Active Oxygen and SOP^{FA} at all pHs (p=0.0129, -3.888 to -0.5193, 95% CI; p=0.0003, -3.005 to -1.227, 95% CI; p=0.0074, -2.940 to -0.5326, 95% CI), 10x concentrated Active oxygen and SOP^{SA} (p=0.0129, -2.052 to -0.2740, 95% CI) and SOP^{FA} and SOP^{SA} (p=0.0362, 0.06405 to 1.842, 95% CI) at pH 7.4.

5.2.3 Efficacy of Active Oxygen and Product 1 (biofilm remover) against pre-formed biofilms

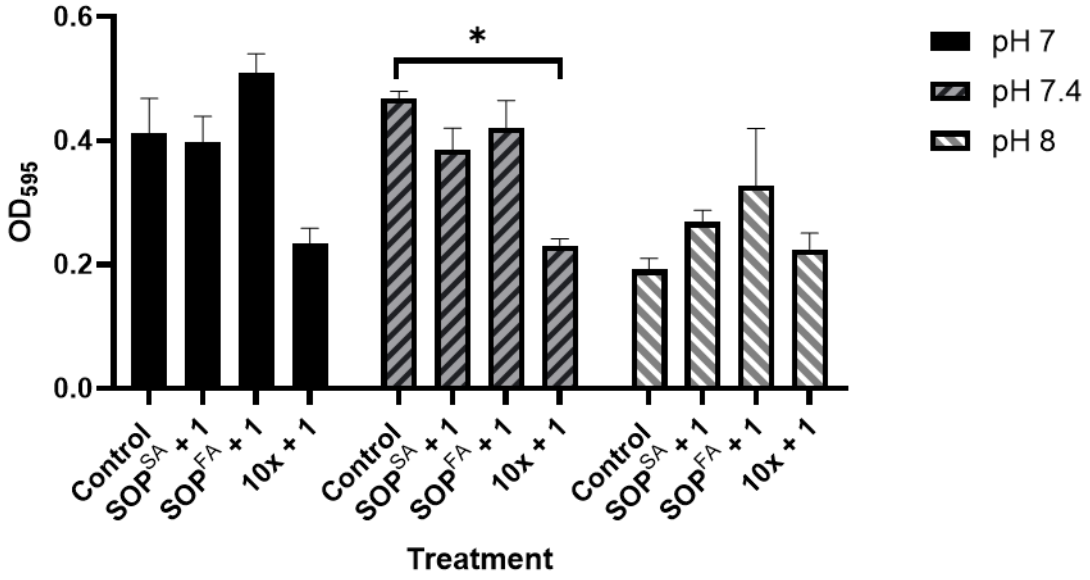

Figure 5.4. Quantification of *E. coli* K12 biofilm formation in M9 minimal media at pH 7, 7.4 and 8 (indicated as OD_{595}) in the presence and absence of Product 1 (biofilm remover) and Active Oxygen at 37°C. SOP^{FA} and SOP^{SA} indicate the initial dosage and follow on applications of Active Oxygen. N=3 for each data point and error bars represent standard error of the mean (SEM). Two-way ANOVA was conducted and statistical significance is indicated by *p<0.05.

The efficacy of product combinations (Product 1 and 3) against *E. coli* and *P. aeruginosa* biofilms is depicted in figures 5.4 and 5.5. The strongest efficacy against *E. coli* biofilms was observed at the 10x concentrated Active Oxygen in combination with biofilm remover where biofilm formation was reduced by 43.4% and 50.8% at pH 7 and 7.4. However, the same treatment did not appear to have any effect on biofilm formation at pH 8. In addition, biofilm formation levels were elevated at higher concentrations of Active Oxygen (SOP^{FA}) compared to SOP^{SA} in combination with biofilm remover. Two-way ANOVA testing revealed that at pH 7 and 8, only 10x concentrated Active Oxygen at 10x concentrated ($p<0.001$ and $p=0.0124$) or biofilm remover alone ($p=0.0259$ and $p=0.0028$) was able to cause statistically significant reductions in biofilm formation. However, comparisons between treatments at pH 7.4 showed statistically significant reductions in biofilms treated with 10x concentrated Active Oxygen and in combination with biofilm remover ($p<0.001$ and $p=0.0102$, two-way ANOVA).

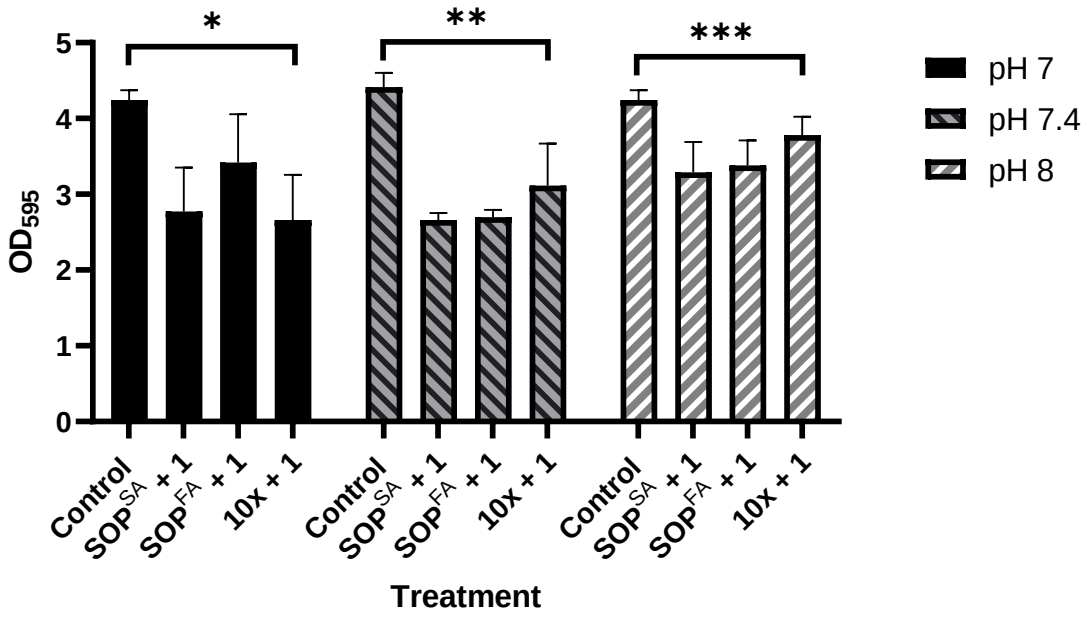

Figure 5.5. Quantification of *P. aeruginosa* PA01 biofilm formation in M9 minimal media at pH 7, 7.4 and 8 (indicated as OD_{595}) in the presence and absence of Product 1 (biofilm remover) and Active Oxygen at 37°C. SOP^{FA} and SOP^{SA} indicate the initial dosage and follow on applications of Active Oxygen. N=3 for each data point and error bars represent standard error of the mean (SEM). Two-way ANOVA was conducted and statistical significance is indicated by *p<0.05;**p<0.01;***p<0.001.

Across all product combinations and pH values tested, reductions in *P. aeruginosa* biofilm formation were observed after 1h. When *P. aeruginosa* biofilms were treated with Active Oxygen at 10x concentrated, biofilm formation was reduced by 37.3% at pH 7 whereas at pH 7.4 and 8, reductions were lower (29.4% and 10.9%). 10x concentrated Active Oxygen alone was found to cause significant reductions in biofilm formation across all pHs tested (p=0.0474, 0.0264 and p=0.0127, Two-way ANOVA). This was also seen when 10x concentrated Active Oxygen was added in combination with the biofilm remover (p=0.0203, 0.0087 and 0.000, Two-way ANOVA). Compared to the initial dosage and follow on applications of Active Oxygen (SOP^{FA} and SOP^{SA}) in combination with the biofilm remover, similar reductions in biofilm formation were observed at both concentrations of Active Oxygen pH 7.4 which were 38.9% and 39.7% respectively. Small differences in biofilm formation levels were also observed for both Active Oxygen concentrations in combination with biofilm remover at pH 8 which were 20.2% and 22.5%. However, the SOP^{SA} concentration of Active Oxygen in combination with the biofilm remover caused a 15% higher reduction in biofilm formation at pH 7 compared to the SOP^{FA} concentration of Active Oxygen. Statistical comparisons between treatments showed that across all pHs tested, only the biofilm remover caused significant reductions in biofilm formation (p=0.0037,

0.000 and 0.000, Two-way ANOVA). Further statistical analyses demonstrated that Active Oxygen at SOP^{SA} concentration alone caused significant reductions in biofilm formation levels at pH 7.4 (p=0.0108, Two-way ANOVA). Statistical significance was not observed in two-way ANOVAs conducted between product combinations using both Active Oxygen concentrations across all pHs tested (p>0.05).

5.3 Discussion

5.3.1 Anti-biofilm activity of Product 1 (biofilm remover)

The biofilm remover (Product 1) was able to successfully decrease biofilm of both *E. coli* and *P. aeruginosa* after 1h of treatment. However, the addition of the biofilm remover appeared to cause an increase in biofilm of *E. coli* at pH 8 which was unexpected. This suggested that the biofilm remover which had a pH of 7, could have modified the structure of *E. coli* biofilms. However, this was unlikely since all other treatments led to less biofilm reduction. Furthermore, the biofilm remover demonstrated much stronger efficacy against *P. aeruginosa* biofilms in comparison to *E. coli* biofilms. This is consistent with previous project results which found that the biofilm remover was more effective at eradicating *P. aeruginosa* biofilms than *E. coli* biofilms at 37°C (Karagianni, 2022). Statistical analyses returned statistically significant differences between treated and untreated controls at pH 7 and pH 8 demonstrating that the biofilm remover resulted in significant reductions in biofilm of *P. aeruginosa*. Statistically significant differences could not be found between treated *P. aeruginosa* biofilms and untreated controls at pH 7.4 despite the fact that a higher percentage of biofilm reduction was observed in comparison to pH 8. However, this could be attributed to the higher SEM bars plotted conveying a wider spread of OD readings obtained.

5.3.2 Anti-biofilm activity of Active Oxygen

Regarding the efficacy of Active Oxygen, the 10x concentrated Active Oxygen was the most effective concentration at eradicating pre-formed biofilms with percentage reductions of up to 77% for *P. aeruginosa* and 49.6% for *E. coli*. One-way ANOVA testing with Tukey's post-hoc analyses illustrated statistically significant differences between 10x concentrated Active Oxygen and control wells in both bacterial strains. Interestingly, there were distinct differences in the activity of Active Oxygen at SOP^{FA} and SOP^{SA} against *E. coli* and *P. aeruginosa* biofilms. Across all pHs tested, Active Oxygen at the SOP^{FA} and SOP^{SA} did not cause any reductions in biofilm formation of *E. coli* as OD readings were higher than control wells. In contrast, Active Oxygen at the SOP^{SA} concentration was more effective at eradicating *P. aeruginosa* biofilms compared to SOP^{FA} where biofilm formation levels were similar to control wells. These results demonstrate that the efficacy of Active Oxygen in eradicating biofilms may be strain dependent and that SOP^{FA} and SOP^{SA} concentrations are less effective at reducing biofilm formation

after 1h of treatment. In addition, Active Oxygen tablets which are recommended for usage in combination with water conditioner (Product 2) are recommended to be used at SOP^{FA} (initial dosage) and SOP^{SA} (follow on application) concentrations in hot tubs. These findings may indicate that although these Active Oxygen concentrations are effective at preventing biofilm formation, they may not necessarily be the optimal concentrations at eradicating *E. coli* and *P. aeruginosa* biofilms. According to the results shown, the 10x concentrated Active Oxygen would be more appropriate concentration for removal of biofilms in hot tubs. In addition, biofilm removal experiments in this project were only conducted at 37°C. Previous data demonstrates that *P. aeruginosa* retains its biofilm formation levels at 37°C compared with 25°C in the presence of Active Oxygen over a 24h incubation period (Karagianni, 2022). This gives insights that changes in temperature from normal operating temperatures (37°C) to maintenance temperatures (25°C) and repeated exposure over a 24h period does not enhance the biofilm removal properties of the biofilm remover product under static conditions.

5.3.3 Antibiofilm activity of Active Oxygen in combination with Product 1 (biofilm remover)

Regarding the efficacy of product combinations, potent anti-biofilm activity was observed at pH 7 and 7.4 when *E. coli* biofilms were treated with 10x concentrated Active Oxygen in combination with the biofilm remover. In contrast, this effect was not seen at pH 8 using the same treatment. In addition, as control wells showed low OD readings this suggests that *E. coli* did not form strong biofilms in the wells. Results from two-way ANOVA testing illustrated that at pH 7 and 8, addition of 10x concentrated Active Oxygen or biofilm remover alone led to statistically significant reductions in biofilm. This was different at pH 7.4 where 10x concentrated Active Oxygen alone and in combination with biofilm remover was able to result in significant reductions in biofilm formation.

All product combinations were effective at reducing levels of *P. aeruginosa* biofilm across all pHs tested. The highest anti-biofilm activity was observed at pH 7 with 10x concentrated Active Oxygen in combination with biofilm remover which declined as pH increased. Two-way ANOVA testing denoted that 10x concentrated Active Oxygen alone and in combination with biofilm remover exhibits potent anti-biofilm activity against *P. aeruginosa* biofilms. Furthermore, Active Oxygen at SOP^{FA} and SOP^{SA} behaved similarly in combination with biofilm remover at pH 7.4 and 8 as optimal densities were very similar. This suggests that both treatments resulted in the removal of *P. aeruginosa* biofilms to the same extent. Similar biofilm removal products have shown minor differences in levels of *P. aeruginosa* biofilm formation in M9 minimal media at various dilutions. Also, despite experiments not being conducted in LB media, biofilm removal products have also been found to display similar levels of *P. aeruginosa* biofilm reduction in LB and M9 minimal media suggesting that the biofilm remover could have eradicated *E. coli* and *P. aeruginosa* biofilms to the same extent regardless of the media used

(Delaney, 2018). Moreover, Active Oxygen at SOP^{FA} concentration in combination with biofilm remover at pH 7 led to greater levels of *P. aeruginosa* biofilm formation compared to SOP^{SA}. This effect was also observed across all pHs for *E. coli*. Hydrodynamic forces generated by shaking in a microplate reader is an important factor that could have resulted in these fluctuations in OD readings. This is concurrent with experiments conducted by Samad et al (2019). This study investigated the difference between levels of *P. aeruginosa* biofilm formation in 96-well plates under static and shaking conditions. Results demonstrated that *P. aeruginosa* formed strong biofilms in 60% of isolates and that hydrodynamic forces which aided the mixing of fluids in the microtiter plate caused increased biofilm formation levels. This is replicated in other literature which shows that biofilms formed by *Pseudomonas* spp. at higher flow rates lead to an increase in nutrient availability and exopolymer production which in turn promotes biofilm formation (Pereira and Vieira, 2001).

Chapter 6: Analytical assessment of components in Product 2 (Water conditioner), Product 3 (Active Oxygen tablets) and chlorine granules

6.1 Introduction

Product 2 (Water conditioner) is said to contain a mixture of glycosides, coconut fatty acids, citric acid, sodium chloride, sodium cocoate, the surfactant octyldimethylamine oxide and the hydrolytic enzymes protease, amylase and lipase. However, the enzymatic contribution to the function of the product was unclear. Therefore, analysis of protein concentration and amylase activity was performed alongside commercial enzyme preparations. An ultrasonic water bath was used to thoroughly mix the water conditioner. Ultrasonic sonic baths generate high frequency ultrasound waves causing formation of cavitation bubbles. These cavitation bubbles enable the material to be dissolved due to strong forces being exerted and suck dirt particles towards the bubble (Chahine et al., 2016). Therefore, ultrasonic water baths are typically used for regular cleaning of glassware and surgical instruments. It was also not well understood which chemical species were exactly present in Product 3 (Active Oxygen tablets). Therefore, chemical species analyses were undertaken using ion chromatography. The aim of this chapter was to investigate protein concentration and measure enzyme activity of amylase in Product 2 as well as characterise chlorine and Active Oxygen species present within the chlorine granules and Active Oxygen tablets.

6.2 Results

6.2.1 Protein quantitation by bicinchoninic acid (BCA) and Bradford assay

In order to assess the levels of protein present in Product 2 (Water conditioner), the BCA assay was performed. Working concentrations of bovine serum albumin (BSA) standards ranging from 25 to 2000 µg/ml were prepared in line with manufacturer instructions and incubated at 37°C for 30 min. Figure 6.1 shows the standard curve generated using BSA standards. The linear relationship between protein concentration and absorbance at OD_{595} denoted by the trendline equation was used to calculate protein concentration in samples of commercial enzymes (protease, amylase and lipase) and water conditioner. However, no protein in the water conditioner was detected. The concentrations of commercial enzymes calculated using the standard curve from the BCA assay are described in table 6.1.

Since no protein was detected in the water conditioner in the BCA assay, a Bradford assay was also conducted to determine protein concentration in the water conditioner. Working concentrations of BSA standards ranging from 125 to 2000 µg/ml were prepared in line with manufacturer instructions and incubated at room temperature for 10 min. The OD_{595} was plotted against BSA concentration which the Bradford assay also failed show the presence of any protein in Product 2. The correlation coefficient obtained from the standard curve for the Bradford assay was also lower than that seen in the BCA assay. Therefore, subsequent experiments for protein quantitation utilised the BCA assay only.

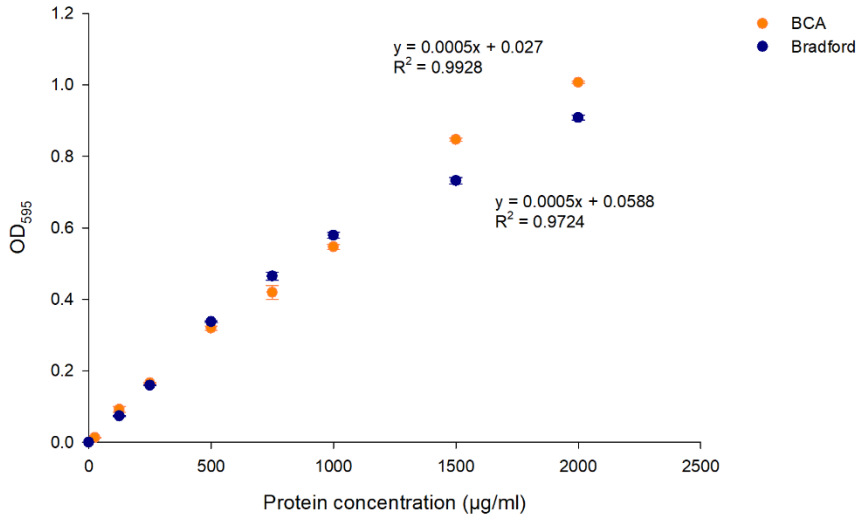

Figure 6.1. Protein standard curve for BCA and Bradford assay. OD_{595} is plotted against BSA concentrations. N=3 for each data point with error bars representing standard error of the mean (SEM).

Table 6.1. Protein concentration of commercial enzymes

Sample	Protein concentration (µg/ml)
Protease (1:10 diluted)	1866.6
Amylase (1:100 diluted)	1432.0
Lipase (1:10 diluted)	619.3

6.2.2 Use of ultrasonic water bath and protein precipitation

Previous attempts to precipitate proteins in the water conditioner to concentrate were conducted without shaking thoroughly before use as stated by manufacturer instructions (Karagianni, 2022). Therefore, the water conditioner was shaken vigorously before transferring an aliquot to an appropriate plastic container. Then, the water conditioner was placed in an ultrasonic bath to dissolve visible precipitates. Figure 6.2 illustrates the change in appearance of Product 2 before and after placing samples in an ultrasonic water bath.

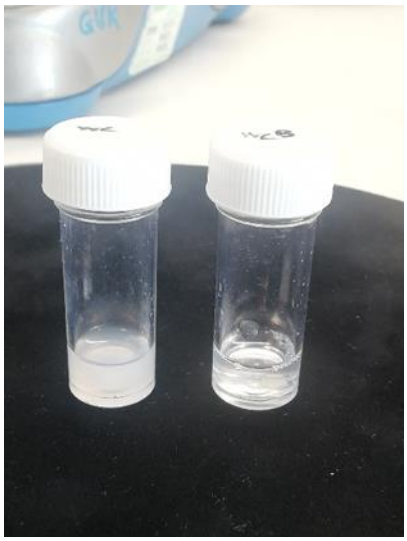

Figure 6.2. Appearance of water conditioner before and after being placed in an ultrasonic water bath at 30°C for 90 minutes. Abbreviations are as follows: WC (shaken water conditioner) and WC^B (water conditioner after being placed in ultrasonic water bath) labelled from left to right (Chau, 2022).

From initial observation, Product 2 is a white cloudy liquid which loses its colour and turns clear once samples of water conditioner were placed in an ultrasonic water bath for 90 minutes at 30°C. In addition, after leaving samples for several hours at room temperature, the appearance of the water conditioner reverted back to cloudy white liquid. However, less visible white clumps were seen following mixing in the ultrasonic water bath.

Prior to conducting protein assays on Product 2, acetone and trichloroacetic acid (TCA) protein precipitation procedures were performed in order to concentrate any protein in the sample. Any protein pellets which formed were resuspended in either ultrapure water or 5% SDS in 0.1M NaOH after which samples were used in protein assays.

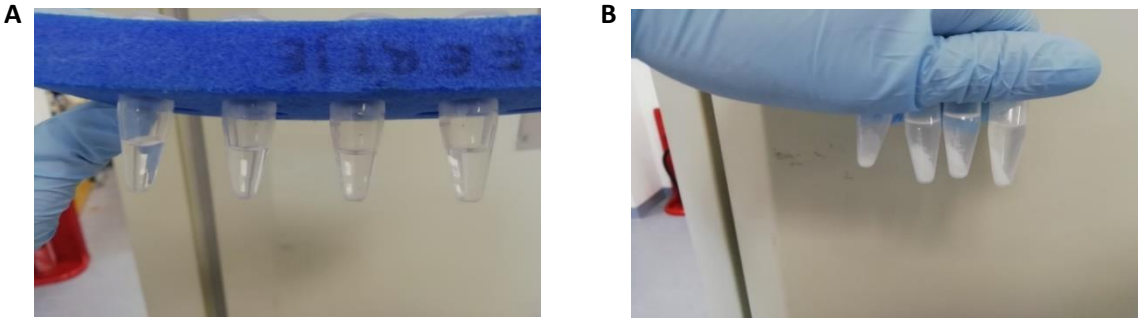

Figure 6.3. Appearance of tubes after acetone precipitation (A) and TCA precipitation (B) of Water conditioner samples following centrifugation. In both images, the first two tubes from left to right represent samples of shaken water conditioner and remaining tubes contain water conditioner following mixing in an ultrasonic bath (Chau, 2022).

Figure 6.3 shows the results of acetone and TCA precipitations on samples of water conditioner and samples placed in an ultrasonic water bath. Acetone precipitation did not allow the formation of protein pellets in any of the water conditioner samples (Fig. 6.3A) whereas successful pellet formation was observed with TCA precipitation in all samples (Fig. 6.3B). However, the BCA assay still failed to detect any protein in samples taken from TCA precipitation of the water conditioner.

6.2.3 Concentrating proteins using freeze-drying

Since no protein was detected in both protein assays using Product 2 taken from an ultrasonic bath and following acetone and TCA precipitation, it was decided to perform freeze-drying on samples of water conditioner. The freeze-drying process involves dehydration of products through the action of vacuum desiccation. Freeze-drying offers many advantages for concentrating proteins such as reductions in thermal inactivation and precipitation of proteins by the salting out effect including longer preservation of unstable materials (Adams, 2007). Samples of water conditioner (50ml) were subjected to freeze-drying for 2 days. Following this process, the freeze-dried material was powderised using a pestle and mortar and weighed in a universal to obtain the dry weight (N=3).

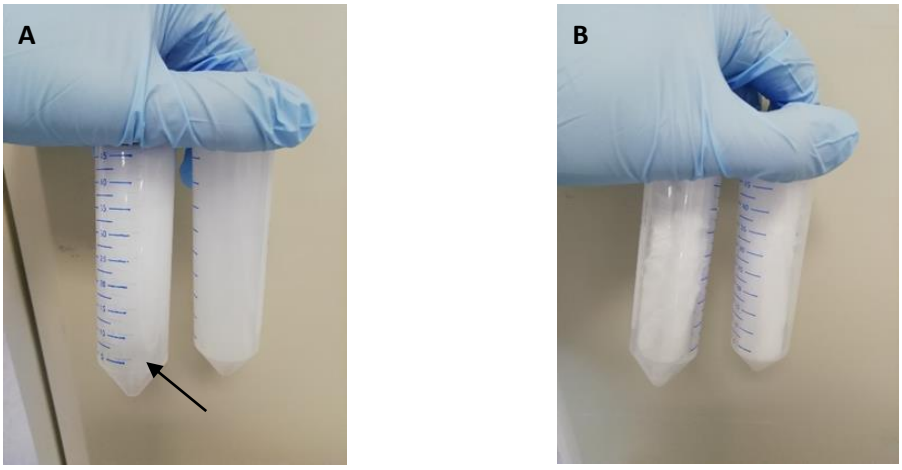

Figure 6.4. Comparison of Product 2 before (A) and after freeze drying for 2 days (B). The general appearance of Product 2 is a white solution consisting of floating material (arrow). After freeze drying samples for 2 days, a fluffy and soft white material is observed (Chau, 2022).

Figure 6.4 depicts the change in appearance of the water conditioner before and after subjection to freeze-drying procedures. Product 2 is a thick cloudy white liquid with clumps of floating material indicated by the black arrow (Fig. 6.4A). Following the freeze-drying process, the water conditioner adopts a fluffy white appearance (Fig. 6.4B). The dry weight of freeze-dried water conditioner and water conditioner placed in an ultrasonic water bath was found to be 0.1049g and 0.1140g respectively. The powder was dissolved in 1ml of dH_2O before being used in protein assays. From BCA assays, it was determined that the freeze-dried water conditioner and water conditioner after mixing

in an ultrasonic bath contained 865.45 µg/ml and 260.083 µg/ml of protein. Since the freeze-dried water conditioner contained higher levels of protein, the same sample was used in gel electrophoresis experiments.

6.2.4 Gel electrophoresis

To provide a visual representation of proteins within the water conditioner, gel electrophoresis procedures were conducted. This would give insights into protein size and distinguish between proteins in commercial enzyme solutions. Each lane was loaded with 10 µg of protein on a NuPage 10% Bis-Tris gel and stained with Coomassie blue (Fig. 6.5).

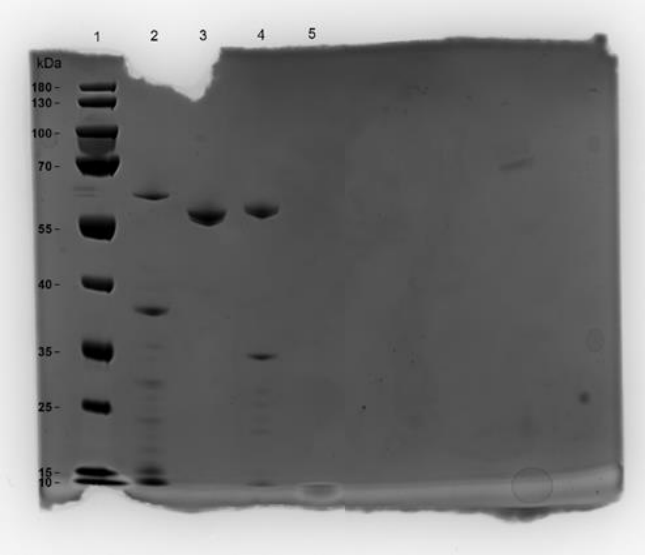

Figure 6.5. Separation of proteins on a NuPage 10% Bis-Tris gel stained with Coomassie. Numbers to the left of each band indicate protein molecular weight in kDa. (1) Prestained protein ladder, (2) 10 µg protease, (3) 10 µg amylase, (4) 10 µg lipase and (5) water conditioner containing 10 µg of protein.

Proteins bands were observed for protease at 38 and 60 kDa (lane 2) followed by a thick protein band for the amylase sample at 57 kDa (lane 3). The lipase sample contained protein bands at 34 and 58 kDa (lane 4). The lane with freeze-dried water conditioner product added (lane 5) did not show the presence of any protein bands which was supposed to contain 10 µg of protein.

6.2.5 Lugol iodine amylase assay

As protein electrophoresis could not detect the presence of protein, attempts were undertaken to assess enzyme activity within the water conditioner. Therefore, the Lugol-iodine amylase assay was set up in order to investigate amylase activity. Samples of water conditioner or amylase were added to 1% starch and thoroughly mixed before adding Lugol-iodine solution (N=3). If starch was absent, the Lugol-iodine remained amber-red whereas a colour change to blue-black was observed in the presence

of starch. An overview of the placement of samples and results from the Lugol-iodine amylase assay is shown in figure 6.6.

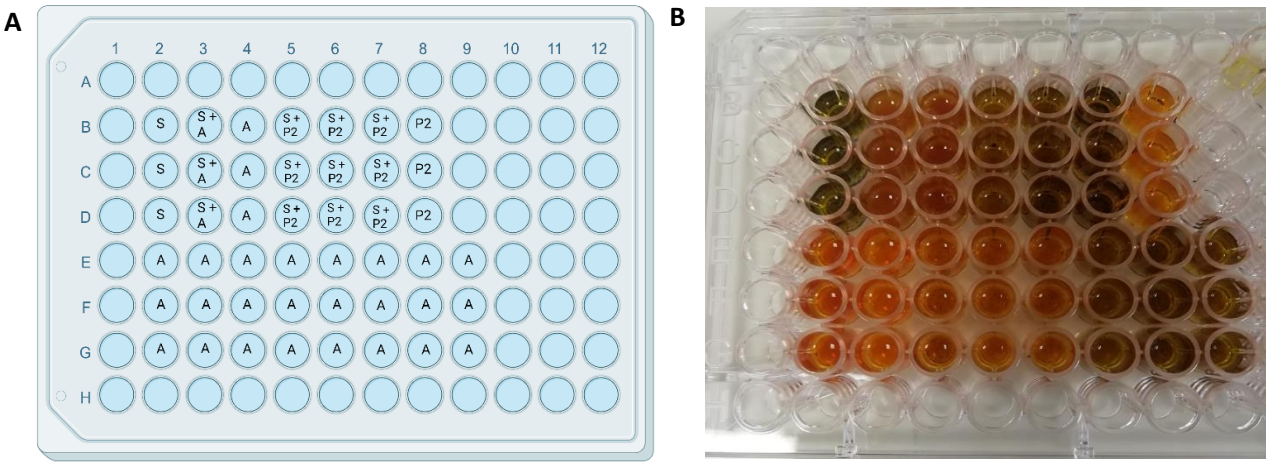

Figure 6.6. Microtiter plate layout of samples used in Lugol-iodine amylase assay (A) and results of Lugol iodine amylase assay for determining amylase activity in Product 2 (B). N=3 for each sample. S (Starch), S + A (Starch + amylase), A (Amylase), S + P2 (Starch + Product 2 following incubation times of 0, 1 and 24h at room temperature: B5-D5, B6-D6 and B7-D7) and P2 (Product 2). Rows E-G represent dilutions of amylase ranging from 10x diluted to 10^{11} times diluted added to 1% starch.

Wells containing only starch instantly turned an intense black colour while samples containing amylase added to starch or amylase alone gave a dark amber-red colour in the presence of iodine (Fig. 6.6B). A weak amber-red colour was observed in wells containing Product 2 added to starch at 0h which shifted to an intense black colour as incubation time increased up to 24h. In addition, a combination of Product 2 with iodine showed a bright amber-red colour indicating the absence of starch. Due to a cold room failure issue where the amylase was stored, it was also decided to confirm if the commercial amylase was still active after addition to starch. Rows E-G illustrate various dilutions of amylase added to starch which were stained with iodine. The results show that the enzyme activity of commercial amylase was maintained following the development of an amber-red colour which showed the absence of starch due to amylase-based degradation of starch.

6.3 Ion exchange chromatography

6.3.1 Preparation of calibration curves

In order to identify and quantify anions in the chlorine granules and Active Oxygen tablets, ion chromatography procedures were performed. Based on the dissociation products of sodium dichloroisocyanurate present within the chorine granules, chloride, chlorite and chlorate anions were selected as standards for quantitation in samples. Selection of an anion standard for Active Oxygen

tablets was based on the structure of KMPS which contains the following compounds: potassium sulphate, sulphuric acid and peroxymonosulphuric acid. Initially, it was decided to use a standard containing peroxymonosulphate but unavailability led to the exploration of other possible options. It is also important to note that potassium bisulfate was proposed as a standard to detect hydrogen sulphate ions in Active Oxygen samples but time constraints meant that these experiments could not be conducted. Standards were prepared separately either from powder or purchased stock solutions and run through the Dionex™ Integrion™ HPIC™ System with a flow rate of 0.5 mL/min and loop volume of 5µl for sample injection.

Calibration curves for each anion are given in Fig. 6.7. Peaks with high intensity were seen across all chloride standard chromatograms with a retention time of 3.1 min with the calibration curve having a correlation coefficient of 0.9947 (Fig. 6.7A). Strong signals were observed in chlorite standard chromatograms at retention times of 2.9 min and 3.1 min with high degree of linearity with correlation coefficient of 0.9919 (Fig. 6.7B). Standard chromatograms for chlorate and sulphate contained strong signals at retention times of 5.2 min and 6.9 min with correlation coefficients of 0.9977 and 0.9973 respectively (Fig. 6.7C and D).

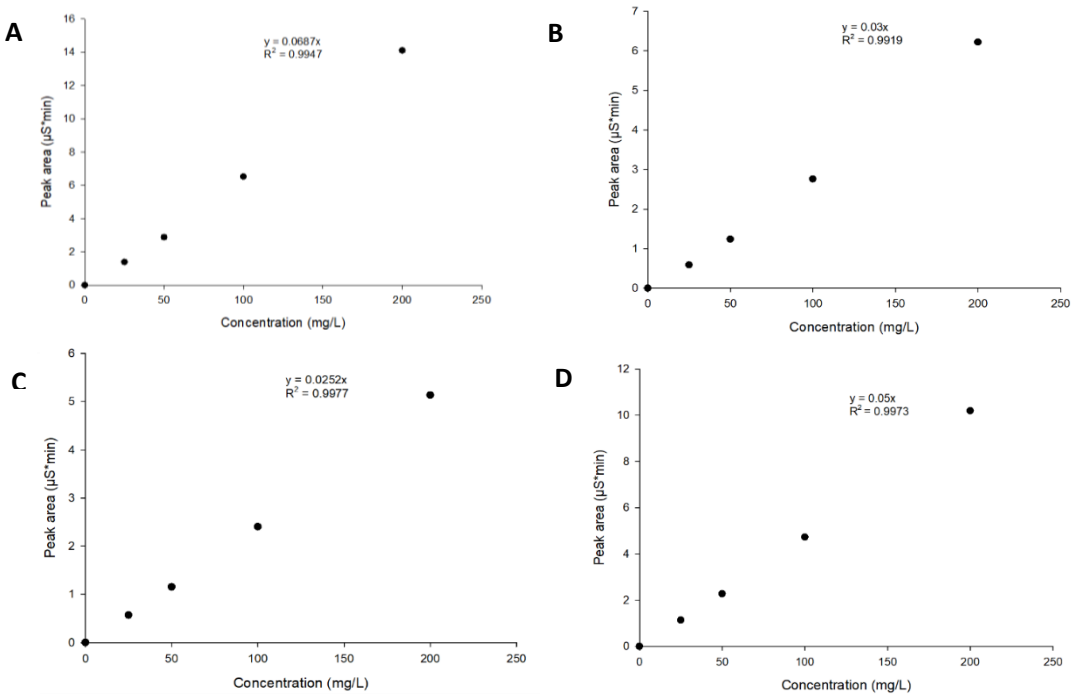

Figure 6.7. Calibration curves of chloride (A), chlorite (B), chlorate (C) and sulphate (D) measured by ion exchange chromatography with retention times of 3.1 min, 2.9 min, 5.2 min and 6.9 min. Each graph is plotted including the equation of the line and the corresponding correlation coefficient (R^2).

Data analysis of chlorite standard chromatograms showed that between each peak, the increase in conductivity did not occur from baseline levels of conductivity (Fig. 6.8). Following the identification of the chloride anion with a retention time of 3.1 minutes, it was determined that the peak observed at a retention time of 2.9 min was chlorite.

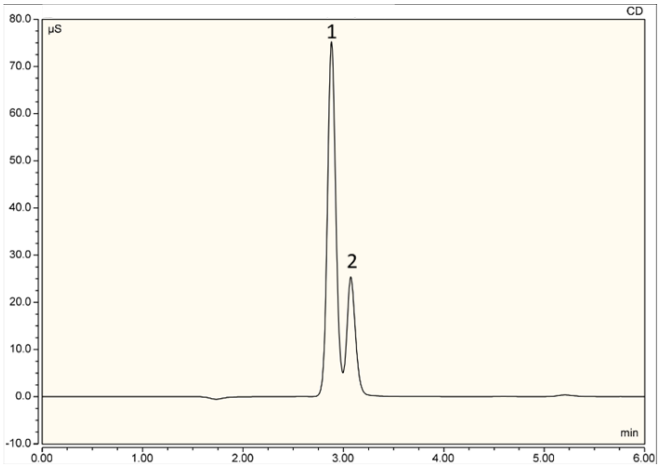

Figure 6.8. Chromatogram of a chlorite standard (200 mg/L). The column used was Dionex IonPac AS14A-5µm (3 x 150 mm) with the mobile phase as 8.0 mM sodium carbonate and 1.0 mM sodium bicarbonate (0.5 mL/min). Chlorite (1) and chloride (2) peaks are separated at retention times of 2.9 min and 3.1 min.

6.3.2 Chemical analysis of chlorine granules and Active Oxygen tablets

Samples prepared using chlorine granules and Active Oxygen tablets were run using the same operating conditions as stated previously. Figure 6.9 shows the chromatogram of a chlorine granule sample at 5 mg/L, the recommended concentration used in hot tubs. Peaks with high intensity were observed at 3.1 min which represents the chloride ion followed by a small peak at 6.9 min which relates to a sulphate ion. The concentrations of chloride in the chlorine granules calculated using the standard calibration curve are shown in table 8.1. At recommended concentrations and very dilute samples, there is very little chloride content ranging from 0.3697-1.523 mg/L. Only the stock solution at concentration of 100 mg/L contained chloride levels within the range of the standard curve at 28.923 mg/L.

Figure 6.9. Chromatogram of chlorine granules at 5 mg/L. The column used was Dionex IonPac AS14A-5µm (3 x 150 mm) with the mobile phase as 8.0 mM sodium carbonate and 1.0 mM sodium bicarbonate (0.5 mL/min). Peaks with high intensity are found at 3.1 min followed by a marginal increase in signal at 6.9 min which was identified as chloride (1) and sulphate ions (2).

The concentrations of chloride in the chlorine granules calculated using the standard calibration curve are shown in table 6.2. At recommended concentrations and very dilute samples, there is very little chloride content ranging from 0.3697-1.523 mg/L. Only the stock solution at concentration of 100 mg/L contained chloride levels within the range of the standard curve at 28.923 mg/L. However, since these experiments were conducted under N=1 conditions, repeats are required to confirm whether the same results are observed.

Table 6.2**.** Concentration of chloride ions present in chlorine granules

Concentration of chlorine granules (mg/L)	Concentration of chloride ion present (mg/L)
1	0.3697
3	0.9607
5	1.523
50	13.112
100	28.923

Samples of Active Oxygen at different concentrations (1:600, 1:400, SOP^{SA} and SOP^{FA}) were run in order to provide a chemical analysis of the active compound KMPS present in the tablets. Chromatogram results from an Active Oxygen sample at the SOP^{FA} concentration which relates to the first addition of the tablets are seen in figure 6.10. Several peaks were seen at retention times of 3.1 min, 5.7 min and 6.9 min. Based on the retention times obtained from running calibration standards, chloride and sulphate were identified at 3.1 min and 6.9 min. Of interest is the unidentified anion with a retention

time of 5.7 min which could possibly represent a peroxide, peroxymonosulphate or hydrogen sulphate ion based on the structure of KMPS.

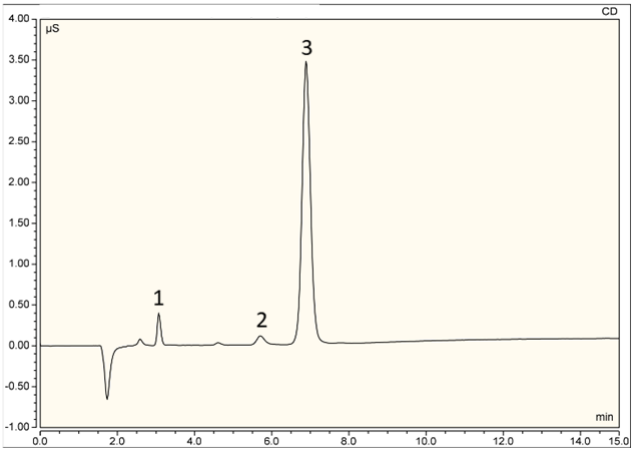

Figure 6.10. Chromatogram of Active Oxygen sample at the SOP^{FA} concentration (first application of Active Oxygen tablets). The column used was Dionex IonPac AS14A-5µm (3 x 150 mm) with the mobile phase as 8.0 mM sodium carbonate and 1.0 mM sodium bicarbonate (0.5 mL/min). Chloride (1) and sulphate (3) peaks are identified at retention times of 3.1 min and 6.9 min. The small peak (2) observed at retention time 5.7 min suggests the presence of a peroxide, peroxymonosulphate or hydrogen sulphate ion.

Table 6.3. Concentration of sulphate ions present in Active Oxygen tablets

Concentration of Active Oxygen tablets	Concentration of sulphate ion present (mg/L)
1:600	1.464
1:400	2.218
SOP^{SA}	8.626
SOP^{FA}	17.390

Table 6.3 contains the sulphate ion levels present in the Active Oxygen tablets at different dilutions. Very dilute solutions gave low concentrations of sulphate ion from 1.464-2.218 mg/L which was expected. However, the highest concentration of Active Oxygen tested only contained 17.390 mg/L of sulphate which fell below levels used in the standard calibration range. Therefore, concentrations of Active Oxygen which are not typical in hot tubs are required to obtain levels within the calibration standard range.

6.4 Discussion

6.4.1 Protein analyses of Product 2 (Water conditioner)

Both protein assays conducted on the water conditioner failed to detect any protein, even after mixing in an ultrasonic water bath. However, it was noticed that the temperature of the ultrasonic water bath after 90 minutes had risen to 60^{o}C which is known to reduce enzyme activity of protease, amylase and lipase (Ayansina et al., 2017; Kareem et al., 2014; Yossan et al., 2006). In addition, no pellet formation was observed following acetone precipitation which was apparent in TCA precipitation but despite this, protein assays did not show the presence of any protein. Since acetone precipitation could not form a protein pellet, it could be argued that several cycles of precipitation are required in order to obtain a protein pellet. An explanation for the absence of protein following TCA precipitation in the Bradford assay could be due to incompatible concentrations of SDS being used in the protein assay. According to the protein quantitation assay compatibility table, the maximum compatible concentration for SDS was 0.5% whereas in TCA precipitation procedures, protein pellets were resuspended in 5% SDS in 0.1M NaOH (Thermo Fisher Scientific, 2021). Freeze drying procedures provided more positive results with high levels of protein being detected for the freeze-dried water conditioner in the BCA assay. However, when samples of freeze-dried product were loaded onto a 10% Bis-Tris gel, no protein bands were detected. Higher volumes of product or adding the concentrated stock solution could possibly show the presence of protein bands. Lugol-iodine amylase assays failed to detect amylase activity upon addition of Product 2 to starch following incubation times of up to 24h since all wells remained dark brown or blue/black indicating the presence of starch. These observations lead to the conclusion that no active amylase was present which is consistent with previous results (Karagianni, 2022). Despite this, the freeze-dried product was able to react with the components used in the BCA assay which suggests that specific components present within Product 2 may be responsible for the protein detected in the protein assay.

6.4.2 Ion chromatography analysis of chlorine granules and Active Oxygen tablets

The calibration curves generated for each anion provide a good degree of linearity with correlation coefficients ranging from 0.9919 to 0.9978. This is in accordance with guidelines that state that for quantitation in instruments using suppressed conductivity, correlation coefficients are required to be greater than 0.99 (Nelson and Marbury, 2021). Chlorite standard chromatograms showed that each peak obtained did not originate from baseline levels of conductivity. This is consistent with chlorite standard chromatograms observed in other studies (Dillemuth, 2011). In addition, ion chromatography analysis of trace impurities provided in the certificate of analysis for the chlorite standard chromatogram state that the concentration of chloride ions is less than 200 mg/L which would explain the presence of chloride ions on chromatograms with chlorite standards. Based on the water chemistry

of sodium dichloroisocyanurate, dissociation into hypochlorite ions meant that chlorite ions were expected to be present in chlorine samples. However, ion chromatography experiments only showed the presence of chloride ions and failed to detect chlorite or chlorate species. Therefore, the stock solution at 100 mg/L and samples at 50 mg/L, 3 mg/L and 1 mg/L were also run to confirm if the same conclusions were made, which was conclusive. However, since these experiments were conducted under N=1 conditions, repeats are required to confirm whether the same results are observed. Chlorinated water and water taken from other sources are known to contain sulphate ions as contaminants in concentrations up to 55 mg/L (Dawood and Sanad, 2014; Mok, Prasadb and Li, 2000). However, only very dilute concentrations were investigated in this study which meant that levels of sulphate ions did not exceed 1 mg/L.

Chromatograms obtained for Active Oxygen at the initial dosage in hot tubs (SOP^{FA}) showed the presence of chloride and sulphate ions. The unidentified anion observed at a retention time of 5.7 min could represent a peroxide, peroxymonosulphate or hydrogen sulphate ion. This would confirm that KMPS was part of the product formulation. However, since calibration standards were not run for peroxide, peroxymonosulphate or hydrogen sulphate ions and retention times were not obtained, further experiments are required to clarify the identity of this peak. The appearance of sulphate ions in chlorine granules and chloride ions in Active Oxygen samples is most likely the result of residual sample from inefficient cleaning of the column or from trace anions present in the ultrapure water used to dilute samples which is known to contain chloride and sulphate (Lee et al., 2020).

Chapter 7: General Discussion and Conclusions

7.1 Introduction

The product used in this project was Eco3spa, one of the leading distributors of water sanitation products designed specifically for the hot tub sector with an emphasis on creating environmentally friendly products. Previous work on the project provided insights into the efficacy of Eco3spa's products in growth and biofilm prevention as well as biofilm removal properties against *E. coli* and *P. aeruginosa* over a hot tub relevant pH range from 7 to 8 (Karagianni, 2022). However, Eco3spa wishes to comprehend its scientific understanding of the efficacy of Eco3spa's products in support of the product claims made. Therefore, further experiments were conducted as previous work limited the number of experiments due to the COVID-19 pandemic.

This project aimed to extend the conclusions reached in the previous project by testing the efficacy of Eco3spa's products for growth and biofilm prevention over a wider pH range (5.2-8) as well as biofilm removal properties. Time-kill assays and decay experiments were also conducted in order to investigate the killing effect and chemical stability of Active Oxygen once added to hot tub water. Further experiments were also performed to detect the presence of enzymes in the Water conditioner and assess the effect in combination Active Oxygen on cell viability by carrying out fluorescent staining procedures.

7.2 Optimisation of studies

In this project, there were many factors which needed to be considered in order to replicate conditions found in a hot tub environment. The strains selected in this study were *Escherichia coli* K12 and *P. aeruginosa* PA01 based on their high prevalence in water systems and ability to form biofilms on pipe surfaces (Butler et al., 2021; Huhulescu et al., 2011; Liu et al., 2014; Lu et al., 2014; Lutz and Lee, 2011). Also, both bacterial strains are known to exhibit resistance to disinfectants which presents a challenge for biofilm prevention and removal (Guo et al., 2015; Sagripanti and Bonifacino, 2000). The two temperatures used in this project (25^{o}C and 37^{o}C) were chosen in order to simulate the operation of hot tubs at maintenance and normal operating temperatures. In addition, the media of choice needed to reflect conditions where biofilm formation could occur. LB media was chosen to mimic the nutrient rich environment of the hot tub piping. Also, M9 minimal media was used in this study in order to simulate the nutrient poor environment of the hot tub water. These parameters led to the development of a biofilm assay using 96-well plates (Chapters 3, 4 and 5).

Experimental conditions and plate design were also reviewed to ensure accurate results were obtained. Firstly, the edge effect which is associated with 96-well plates causes inaccuracies in OD readings between inner and outer wells (Delaney, 2018; Karagianni, 2022). Therefore, only the inner wells of the 96-well plate were utilised in this study. In addition, the number of PBS washes, drying and

staining times were chosen for each bacterial strain and an incubation period of 24 hours was required for biofilm formation to occur.

As biofilm removal assays were conducted under time constraints, it was decided that the experimental parameters needed to reflect the conditions in which the biofilm removal product would be used. Therefore, experiments were only conducted at 37°C under shaking conditions for 1 hour which is in accordance with product instructions which state that the temperature of the water should be between 35°C and 40°C and jets should be run for at least 60 minutes. Therefore, the conditions chosen for these experiments simulate the flushing of water or action of jets within the hot tub system and application of the biofilm removal product as described in the product instructions (Chapter 5).

Time-kill assays were conducted for the first time in this project in order to determine how quickly Active Oxygen takes to kill bacteria (Chapter 4). Therefore, it was important to decide on the incubation times of bacteria in the presence of Active Oxygen which were chosen based on available literature (Oliveira et al., 2022). Investigations into the chemical stability of Active Oxygen were tested over a period of 7 days based on product instructions which state that one tablet should be added every day if hot tub water becomes "dull or foamy" and prior to each hot tub use, customers should add "at least two tablets each week to keep the water sanitised."

Finally, the characterisation of chlorine and Active Oxygen species in the chlorine granules and Active Oxygen tablets was assessed using ion chromatography (Chapter 6). The anions chosen for detection were selected based on the structure of active components found within the chlorine granules (NaDCC) and Active Oxygen tablets (KMPS). Suitable standards such as chlorite, chlorate, chloride and sulphate were prepared in order to measure the concentration of anions in these products.

7.3 Effect of pH

Static growth and biofilm prevention assays demonstrated that Active Oxygen concentrations from 10x concentrated to SOP^{SA} successfully prevent planktonic growth and biofilm formation of *E. coli* K12 and *P. aeruginosa* PA01 across a pH range from 5.2-8. This was accompanied by sharp rises in planktonic growth and biofilm formation at concentrations 1:10 and lower. This demonstrates that pH adjustment is not required when Active Oxygen tablets are added to hot tubs as pH adjustment and alkalinity, a term used to describe the buffering capacity of water which neutralises acids and bases in order to retain a stable pH (Water Science School, 2018) is a common issue in hot tubs. Also, the results convey that the recommended concentrations of Active Oxygen used in hot tubs, the initial dosage of Active Oxygen (SOP^{FA}) and follow on applications (SOP^{SA}) are correct and do not need to be adjusted.

Higher levels of planktonic growth were exhibited by *E. coli* at pH 8 when 25°C which could be attributed to the upregulation of inner membrane proteins such as YqjA which lead to transport of sodium and potassium ions from the surrounding environment into the cell which promotes further growth (Kumar and Doerrler, 2015; Kumar, Tiwari and Doerrler, 2017).

Investigations into the effect of acidic pH environments (pH 5.2) revealed that both bacterial strains displayed the highest planktonic growth at 37°C. This gives interesting insights that acidic pH environments could be inducing acid tolerance mechanisms in *E. coli* K12 and *P. aeruginosa* PA01 which act as a survival strategy for their survival. In response to low pH environments, genes found in *E. coli* required for survival at low pH environments such as *fabB* have been shown to be upregulated which is also conserved in *P. aeruginosa* (Xu et al., 2020). This causes changes in lipid composition of the cell membrane and activity of proton pumps as a method to achieve a stable intracellular pH. Evidence also suggests that eDNA results in the activation of *cyoABCDE* genes and antibiotic resistance genes in *P. aeruginosa* which would explain the higher levels of planktonic growth leading to reduce susceptibility to disinfectants (Lewenza et al., 2020). pH microelectrode measurements of the culture media after addition of Active Oxygen demonstrated that the pH remains relatively consistent as the higher pH change was only a difference of 0.4 pH units.

7.4 Effect of temperature

Regarding the effect of temperature, *P. aeruginosa* exhibited the highest levels of planktonic and biofilm formation at 37°C compared to 25°C and *E. coli* grown at both temperatures. This makes sense as *P. aeruginosa* grows well in M9 media supplemented with glucose which is used as a carbon source required for further growth. Interestingly, at the lowest concentrations of Active Oxygen tested (1:400 and 1:600), planktonic growth of *E. coli* exceeded levels observed with *P. aeruginosa* at 25°C. These could be attributed to the upregulation of cold shock proteins which stimulate the cold shock response allowing further translation to occur or stress response genes which have been linked with cell growth at lower temperatures (Phadtare, 2012; White-Ziegler et al., 2008). In addition, the levels of biofilm formation shown by *P. aeruginosa* at 25°C appeared to be higher than seen at 37°C. Previous studies have demonstrated that lower temperature environments could increase levels of signalling molecules such as c-di-GMP which regulate the systems responsible for exopolysaccharide production in the biofilm process (Kim et al., 2020; Townsley and Yildiz, 2015). Upregulation of β-galactosidase activity contributes to the glucose rich environment found in the EPS matrix and identification of phage proteins shows that there is a link between low temperature environments and elevated levels of biofilm formation (Sakuragi and Kolter, 2007).

7.5 Effect on cell viability

Log reduction data derived from OD_{595}-CFU calibration curves indicated that Active Oxygen caused the highest reductions in cell viability of *E. coli* and *P. aeruginosa* at pH 5.2 when grown at 37°C which exceeded 1.4 and 2 for *E. coli* and *P. aeruginosa*. This makes sense as *P. aeruginosa* showed the maximum levels of planktonic growth and biofilm formation at the same experimental conditions. However, due to time constraints, the data obtained here reflects the difference in cell viability between control and treated samples calculated from OD^{595}-CFU calibration curves which is not as accurate as performing cell viability assays on agar plates (Karagianni, 2022). Time-kill assays which were CFU based demonstrated that Active Oxygen tablets are able to kill *E. coli* within five minutes and follows the trend shown by bactericidal antibiotics such as ampicillin. *E. coli* treated with chlorine at the recommended concentration in hot tubs (5ppm) led to no CFU formation. In addition, investigations into the chemical stability of Active Oxygen revealed that efficacy can be maintained for up to 7 days. The active compound within the Active Oxygen tablets is KMPS which once prepared has been reported to be stable for at least 7 days (Griffin, 2012; Sykes and Weese, 2014).

7.6 Benchmarking Active Oxygen against chlorine

In general, Active Oxygen at the SOP^{FA} concentration performed as well as chlorine at preventing planktonic growth and biofilm formation of *E. coli* and *P. aeruginosa* whereas the efficacy of chlorine was affected by pH values outside its optimum (pH 7 and 8). This is in line with previous literature which states that chlorine exhibits optimal activity at pH 7.4 but at pH values which are above and below, efficacy is affected as the distribution of chlorine species is highly dependent on pH (Deborde and Gunten, 2008). At 25°C, the efficacy of Active Oxygen to prevent planktonic growth and biofilm formation was slightly affected at pH 7 and 7.4 whereas at 37°C, Active Oxygen at SOP^{FA} maintained efficacy across all pHs tested and both temperature for both bacterial strains. These results suggest that the Active Oxygen tablets work optimally under normal operating temperatures compared to maintenance temperatures in hot tubs without loss of efficacy in comparison to chlorine. Since cell viability assays showed that treatment with chlorine at 5ppm resulted in no CFU formation, it may explain the extremely low levels of planktonic growth demonstrated by *E. coli* and *P. aeruginosa* which limits the extent to which these bacterial strains can form biofilms.

7.7 Efficacy of products alone and in combination

Overall, Active Oxygen in combination with Product 2 (water conditioner) led to increased planktonic growth and biofilm formation of *E. coli* across all pHs tested and both temperatures. This effect was less pronounced when tested against *P. aeruginosa* as elevated levels of planktonic growth and biofilm formation were only observed at the SOP^{SA} and 1:10 concentration in combination with Product 2 at

both temperatures. It is possible that certain components found within the water conditioner promote growth of *E. coli* and *P. aeruginosa*. However, it is uncertain which components are responsible for this effect which was observed at all pHs tested. The addition of Product 2 reduced planktonic growth and biofilm formation of *E. coli* across all pHs at both temperatures whereas it was only effective against planktonic growth of *P. aeruginosa* at 37^{o}C with low efficacy in preventing biofilm formation. The ability of *P. aeruginosa* to form strong biofilms as denoted in biofilm prevention assays may indicate that it could resist the effects of the water conditioner whereas biofilms formed by *E. coli* are more susceptible to components found within the water conditioner.

Light and fluorescent microscopy revealed that Active Oxygen in combination with Product 2 results in a high number of immotile cells which adopt a formation where clump-like structures are seen in a viable state. This is in accordance with results found in the previous project where the product combination could lead to cells entering the VBNC state. Further light microscopy experiments showed that Active Oxygen at the 1:10 concentration also generated clump-like structures. Therefore, this could suggest that Active Oxygen may interact with components present within the water conditioner product which have a synergistic effect in causing bacteria to revert to a VBNC state. Cell viability assays revealed that addition of the water conditioner led to no CFU formation which further suggests that it could play an important role in causing *E. coli* to enter the VBNC state as live cells were still observed in fluorescence microscopy experiments.

The efficacy of the biofilm removal product (Product 1), Active Oxygen and product combinations to eradicate biofilms formed by *E. coli* and *P. aeruginosa* was also assessed. The biofilm remover tested at the SOP concentration was able to remove biofilms formed by *E. coli* at pH 7 and 7.4 whereas the product performed better in the eradication of *P. aeruginosa* biofilms at all pHs tested. Active Oxygen at 10x concentrated showed the most efficacy in removal of biofilms formed by *E. coli* and *P. aeruginosa* whereas at the SOP^{FA} concentrations, this led to higher or similar levels of biofilm formation relative to control wells. Interestingly, the SOP^{SA} concentration of Active Oxygen showed efficacy in eradication of *P. aeruginosa* biofilms which was not observed at the SOP^{FA} concentration. It is possible that this could be an accidental experimental error or could suggest that dynamic conditions created by the action of jets in hot tubs or changes in pH could influence the efficacy of Active Oxygen. Active Oxygen was most effective at eradicating *E. coli* biofilms at the 10x concentrated and SOP^{SA} concentrations at pH 7 and 7.4 with loss of efficacy at pH 8. This agrees with the conclusions reached using the biofilm remover against *E. coli* biofilms at pH 8 which also led to increased biofilm formation. This suggests that the biofilm remover product is less effective at eradicating *E. coli* biofilms at pH 8. All product combinations led to the removal of *P. aeruginosa* biofilms which was present across all pHs tested. Therefore, it can be deduced that the biofilm remover alone and in combination with Active

Oxygen is most effective in eradicating *P. aeruginosa* biofilms which is of more significance due to its high prevalence in water systems (Lutz and Lee, 2011).

7.8 Protein analysis

From protein assays, the BCA and Bradford assay did not show the presence of any protein in samples of water conditioner despite carrying out procedures such as protein precipitation and use of an ultrasonic water bath. Performing freeze-drying procedures in order to concentrate proteins within the water conditioner provided better insights into the protein levels in the water conditioner which were detected in BCA and Bradford assays. However, no bands were observed on the protein gel which confirmed that there was no protein present in the product. The Lugol iodine assay also confirmed the absence of amylase activity within the water conditioner product, even after 24 hours in the presence of starch. This was unexpected as the addition of water conditioner was effective at preventing planktonic growth and biofilm formation of *E. coli* which could be attributed to the presence of enzymes. These results signify that enzymes may be present in conditioner but in such low concentrations that they are undetectable by gel electrophoresis and enzyme activity. In addition, if proteases, amylases and lipases were present together, it suggests that they would digest each other which would explain the inability to detect the presence of bands on protein gels and the lack of enzyme activity.

7.9 Characterisation of Active Oxygen and chlorine species

Chemical analysis of chlorine species in the chlorine granules failed to detect the presence of chlorite or chlorate anions as only chloride was observed in chromatograms. This was unexpected since chlorite and chlorate are the chlorine reactive oxygen species responsible for its biocidal activity. Therefore, other methods may be required in order to detect the presence of chlorite or chlorate. In addition, samples of Active Oxygen were found to contain sulphate as expected based on the structure of KMPS, the active compound within the Active Oxygen tablets. The chromatogram also showed the presence of another anion which is possibly a peroxymonosulphate, peroxide or hydrogen sulphate ion. However, in the absence of an appropriate standard, the identity of the anion is currently unknown and warrants further investigation.

7.10 List of conclusions

Following a literature review and the experiments addressed in this project, the results were critically analysed. Therefore, the questions asked at the start of the project as set out by the sponsoring company have been answered. The most important conclusions reached in this project are:

- Active Oxygen performs as well as chlorine in preventing planktonic growth and biofilm formation of *E. coli* and *P. aeruginosa* without the loss of efficacy (Chapter 3).
- Active Oxygen at the recommended concentrations used in hot tubs (SOP^{FA} and SOP^{SA}) are effective in preventing planktonic growth and biofilm formation of *E. coli* and *P. aeruginosa* at 25^{o}C and 37^{o}C over a pH range of 5.2 to 8 (Chapter 4).
- There is no requirement for pH balancing when Active Oxygen tablets are added to hot tubs.
- Active Oxygen kills bacteria within 5 minutes and chemical stability is maintained for up to 7 days (Chapter 4).
- The water conditioner in combination with Active Oxygen increases planktonic growth and may lead to cell clumping and VBNC (Chapter 4).
- Biochemical analysis of the water conditioner showed that enzymes could not be detected (Chapter 6).
- Chlorine species such as chlorite and chlorate could not be detected in chlorine granules but it is possible that peroxide, peroxymonosulphate or hydrogen sulphate ions could be identified in the Active Oxygen tablets using ion chromatography (Chapter 6).

7.11 Limitations

Biofilm removal experiments were conducted in the later stages of the project which were rectified only in the last two weeks of the project. In addition to this, limited accessibility to the plate reader between students meant that several adaptations such as shorter incubation times were implemented in order to obtain results within a shorter time frame. Also, due to time constraints, log reductions in cell viability from growth prevention assays were calculated from CFU calibration curves to OD at low to very low OD. Light and fluorescence microscopy experiments were conducted for the first time using different microscopes which showed some difficulty in obtaining optimal image capture. Furthermore, ion chromatography procedures were performed for the first time under N=1 conditions with not enough time to procure standards in time and optimise experimental parameters such as flow rate and choice of analytical column.

7.12 Future work

There are several ways in which the project could be improved based on the conclusions reached in this project. Firstly, as pH microelectrode measurements were only applied to samples where Active

Oxygen was added to M9 minimal media, the pH of *E. coli* and *P. aeruginosa* cultures could be measured following overnight incubation including after product addition to monitor the pH of samples as experiments progress. Since attempts to detect the presence of protein bands could not be achieved using the water conditioner product, the concentrated product of water conditioner i.e. stock solution of freeze-dried product prepared as described in section 2.3.6 should be tested on protein gels to further investigate if higher concentrations are required in order to be detected using gel electrophoresis. In addition, further experiments on the chemical stability of Active Oxygen should include a control which would be used to calculate reduction levels in cell viability. As there is a possibility that Active Oxygen in combination with the water conditioner may lead to cells adopting a VBNC state, components within the water conditioner could be tested in isolation and with Active Oxygen to determine if there is an interaction between them in causing cell clumping and VBNC states (Robben et al., 2018).

Further experiments using the ion chromatography apparatus are required to confirm if the Active Oxygen tablets contain KMPS. Therefore, a potassium bisulfate or peroxide containing standard should be used to detect the presence of hydrogen sulphate or peroxide ions which would conform with the structure of KMPS. In addition, column selection and flow rates which could not be optimized due to time constraints could be tested to find optimal conditions for experiments. Other methods of detection such as liquid chromatography – mass spectrometry may be useful in determining the concentration of radical species (Li et al., 2003; Popa et al., 2010). In addition, since results from IEC did not identify the presence of chlorite or chlorate in chlorine granules, other methods of detection and quantitation may be required. Testing samples of the chlorine granules at different pH could be implemented as the distribution of chlorine species is pH-dependent as previously discussed. Another option could be to carry out colorimetric biochemical assays in 96 well plates to measure levels of hypochlorite. Since ion exchange chromatography cannot measure levels of radicals and only anions in solution, fluorescent probes such as 2′,7′-dichlorofluorescin-diacetate, fluorescein or benzoic acid for detection of ·OH or $SO_4^{\bullet-}$ could be used to measure intracellular levels of Active Oxygen species in living cells (Huang et al., 2018; Jin et al., 2020; Zhang et al., 2016). Furthermore, radical scavenger assays using tert-butanol or isopropanol (radical scavenger for ·OH) and sodium chloride (radical scavenger for $SO_4^{\bullet-}$) could be implemented to confirm that the presence of Active Oxygen species is responsible for the loss of viability in biofilm formation assays. To determine the effects of Active Oxygen on metabolic activity in *E. coli* and *P. aeruginosa*, using metabolic dyes could be another option of interest. Metabolic dyes often referred to as tetrazolium salts are used to investigate metabolic activity within bacterial cells as a measure of cell viability. Several tetrazolium salts such as resazurin and 2,3-bis-(2-methoxy-4-nitro-5-sulfophenyl)-2H-tetrazolium-5-carboxanilide are dependent on

dehydrogenase enzymes in live cells which reduce cofactors such as nicotinamide adenine dinucleotide and nicotinamide adenine dinucleotide phosphate (Freeberg, Kallenbach and Awad, 2019; Pereira et al., 2023; Travnickova et al., 2019). This causes a precipitate known as a formazan to be formed which usually requires solubilisation steps before quantitation using spectrophotometers or plate readers. Furthermore, cationic tetrazolium salts which can permeate live cells such as 3-(4,5-dimethylthiazol-2-yl)-2,5 diphenyl tetrazolium bromide have been used to assess metabolic activity in *E. coli* and *P. aeruginosa* (Grela, Kozłowska and Grabowiecka, 2018).

References

Abidi, S. H., Ahmed, K., Sherwani, S. K., & Kazmi, S. U. (2014). Reduction and removal of Pseudomonas aeruginosa biofilm by natural agents. International Journal of Chemical and Pharmaceutical Sciences, 5(1). Retrieved from https://www.researchgate.net/publication/262300116_Reduction_and_removal_of_Pseudomonas_aeruginosa_biofilm_by_natural_agents#:~:text=Several%20of%20the%20plant%20extracts%20were%20identified%20as,efficient%20in%20reducing%20and%20removing%20Pseudomonas%20aeruginosa%20biofilms.

Abkar, L., Wilfart, F. M., Piercey, M., & Gagnon, G. A. (2022). Enhanced Reproducibility and Precision of High-Throughput Quantification of Bacterial Growth Data Using a Microplate Reader. JoVE, (185), e63849. https://doi.org/10.3791/63849

Aharoni, N., Mamane, H., Biran, D., Lakretz, A., & Ron, E. Z. (2018). Gene expression in Pseudomonas aeruginosa exposed to hydroxyl-radicals. Chemosphere, 199, 243–250. https://doi.org/10.1016/j.chemosphere.2018.02.012

Ajiboye, T. O., Habibu, R. S., Saidu, K., Haliru, F. Z., Ajiboye, H. O., Aliyu, N. O., … Bello, S. A. (2017). Involvement of oxidative stress in protocatechuic acid-mediated bacterial lethality. MicrobiologyOpen, 6(4), e00472. https://doi.org/10.1002/mbo3.472

Akinbobola, A. B., Sherry, L., Mckay, W. G., Ramage, G., & Williams, C. (2017). Tolerance of Pseudomonas aeruginosa in in-vitro biofilms to high-level peracetic acid disinfection. Journal of Hospital Infection, 97(2), 162–168. https://doi.org/10.1016/j.jhin.2017.06.024

Amsalu, A., Sapula, S. A., De Barros Lopes, M., Hart, B. J., Nguyen, A. H., Drigo, B., … Venter, H. (2020). Efflux Pump-Driven Antibiotic and Biocide Cross-Resistance in Pseudomonas aeruginosa Isolated from Different Ecological Niches: A Case Study in the Development of Multidrug Resistance in Environmental Hotspots. Microorganisms, 8(11), 1647. https://doi.org/10.3390/microorganisms8111647

Anipsitakis, G. P., Tufano, T. P., & Dionysiou, D. D. (2008). Chemical and microbial decontamination of pool water using activated potassium peroxymonosulfate. Water Research, 42(12), 2899–2910. https://doi.org/10.1016/j.watres.2008.03.002

Anversa, L., Arantes Stancari, R. C., Garbelotti, M., da Silva Ruiz, L., Pereira, V. B. R., Nogueira Nascentes, G. A., … Mores Rall, V. L. (2019). Pseudomonas aeruginosa in public water supply. Water Practice and Technology, 14(3), 732–737. https://doi.org/10.2166/wpt.2019.057

Aribisala, J. O., Nkosi, S., Idowu, K., Nurain, I. O., Makolomakwa, G. M., Shode, F. O., & Sabiu, S. (2021). Astaxanthin-Mediated Bacterial Lethality: Evidence from Oxidative Stress Contribution and Molecular Dynamics Simulation. Oxidative Medicine and Cellular Longevity, 2021, 7159652. https://doi.org/10.1155/2021/7159652

Arun, C., & Sivashanmugam, P. (2015). Investigation of biocatalytic potential of garbage enzyme and its influence on stabilization of industrial waste activated sludge. Process Safety and Environmental Protection, 94, 471–478. https://doi.org/10.1016/j.psep.2014.10.008

Arun, C., & Sivashanmugam, P. (2017). Study on optimization of process parameters for enhancing the multi-hydrolytic enzyme activity in garbage enzyme produced from preconsumer organic waste. Bioresource Technology, 226, 200–210. https://doi.org/10.1016/j.biortech.2016.12.029

Auty, M. A. E., Gardiner, G. E., McBrearty, S. J., O'Sullivan, E. O., Mulvihill, D. M., Collins, J. K., … Ross, R. P. (2001). Direct In Situ Viability Assessment of Bacteria in Probiotic Dairy Products Using Viability Staining in Conjunction with Confocal Scanning Laser Microscopy. Appl Environ Microbiol, 67(1), 420–425. https://doi.org/10.1128/aem.67.1.420-425.2001

Ayansina, A. D. V., Adelaja, A. O., & Mohammed, S. S. D. (2017). Characterization of Amylase from Some Aspergillus and Bacillus Species Associated with Cassava Waste Peels. Advances in Microbiology, 7(4), 280–292. https://doi.org/10.4236/aim.2017.74023

Badar, M., Hemmen, K., Nimtz, M., Stieve, M., Stiesch, M., Lenarz, T., … Schnabelrauch, M. (2010). Evaluation of Madurahydroxylactone as a Slow Release Antibacterial Implant Coating. The Open Biomedical Engineering Journal, 4(1), 263–270. https://doi.org/10.2174/1874120701004010263

Bakker, D. P., Busscher, H. J., van Zanten, J., de Vries, J., Klijnstra, J. W., & van der Mei, H. C. (2004). Multiple linear regression analysis of bacterial deposition to polyurethane coatings after conditioning film formation in the marine environment. Microbiology (Reading), 150(6), 1779–1784. https://doi.org/10.1099/mic.0.26983-0

Bapat, P., Nandy, S. K., Wangikar, P., & Venkatesh, K. V. (2006). Quantification of metabolically active biomass using Methylene Blue dye Reduction Test (MBRT): Measurement of CFU in about 200 s. Journal of Microbiological Methods, 65(1), 107–116. https://doi.org/10.1016/j.mimet.2005.06.010

Beena, A. K. (2014). Purification of an Alkaline Protease Suited for Ecofriendly Sanitation in Milk Processing Units. Indian Journal of Applied Research, 4(12). Retrieved from https://www.worldwidejournals.com/indian-journal-of-applied-research-(IJAR)/recent_issues_pdf/2014/December/December_2014_1417447429__141.pdf

Beena, A. K., Geevarghes, P. I., & Jayavardan, K. K. (2012). Detergent Potential of a Spoilage Protease Enzyme Liberated by a Psychrotrophic Spore Former Isolated from Sterilized Skim Milk. American J. of Food Technology, 7, 89–95. https://doi.org/10.3923/ajft.2012.89.95

Beeson, P. B. (1985). Alleged susceptibility of the elderly to infection. Yale J Biol Med, 58(2), 71–77. Retrieved from https://europepmc.org/article/PMC/PMC2589900

Behr, S., Fried, L., & Jung, K. (2014). Identification of a Novel Nutrient-Sensing Histidine Kinase/Response Regulator Network in Escherichia coli. Journal of Bacteriology, 196(11), 2023–2029. https://doi.org/10.1128/jb.01554-14

Benyoussef, W., Deforet, M., Monmeyran, A., & Henry, N. (2022). Flagellar Motility During E. Coli Biofilm Formation Provides a Competitive Disadvantage Which Recedes in the Presence of Co-Colonizers. Front Cell Infect Microbiol, 8, 896898. https://doi.org/10.3389/fcimb.2022.896898

Berg, J. M., Tymoczko, J. L., Gatto, G. J., & Stryer, L. (2015). Biochemistry (8th ed., p. 224). New York: WH Freeman.

Berruti, I., Nahim-Granados, S., Abeledo-Lameiro, M. J., Oller, I., & Polo-López, M. I. (2021). UV-C Peroxymonosulfate Activation for Wastewater Regeneration: Simultaneous Inactivation of Pathogens and Degradation of Contaminants of Emerging Concern. Molecules, 26(16), 4890. https://doi.org/10.3390/molecules26164890

Bhagirath, A., Li, Y., Somayajula, D., Dadashi, M., Badr, S., & Duan, K. (2016). Cystic fibrosis lung environment and Pseudomonas aeruginosa infection. BMC Pulm Med, 16(1), 174. https://doi.org/10.1186/s12890-016-0339-5

Bhosle, N. B., Garg, A., Fernandes, L., & Citon, P. (2005). Dynamics of amino acids in the conditioning film developed on glass panels immersed in the surface seawaters of Dona Paula Bay. Biofouling, 21(2), 99–107. https://doi.org/10.1080/08927010500097821

Bisht, K., Moore, J. L., Caprioli, R. M., Skaar, E. P., & Wakeman, C. A. (2021). Impact of temperature-dependent phage expression on Pseudomonas aeruginosa biofilm formation. Npj Biofilms and Microbiomes, 7(1), 22. https://doi.org/10.1038/s41522-021-00194-8

Bjarnsholt, T., Alhede, M., Jensen, P. Ø., Nielsen, A. K., Johansen, H. K., Homøe, P., … Kirketerp-Møller, K. (2015). Antibiofilm Properties of Acetic Acid. Advances in Wound Care, 4(7), 363–372. https://doi.org/10.1089/wound.2014.0554

Boateng, M. K., Price, S. L., Huddersman, K. D., & Walsh, S. E. (2011). Antimicrobial activities of hydrogen peroxide and its activation by a novel heterogeneous Fenton's-like modified PAN catalyst. J Appl Microbiol, 111(6), 1533–1543. https://doi.org/10.1111/j.1365-2672.2011.05158.x

Bove, G. E., Rogerson, P. A., & Vena, J. E. (2007). Case control study of the geographic variability of exposure to disinfectant byproducts and risk for rectal cancer. Int J Health Geogr, 6(1), 18. https://doi.org/10.1186/1476-072x-6-18

Brown, S., Santa Maria, J. P., & Walker, S. (2013). Wall Teichoic Acids of Gram-Positive Bacteria. Annu. Rev. Microbiol., 67(1), 313–336. https://doi.org/10.1146/annurev-micro-092412-155620

Brown, S., Xia, G., Luhachack, L. G., Campbell, J., Meredith, T. C., Chen, C., … Peschel, A. (2012). Methicillin resistance in Staphylococcus aureus requires glycosylated wall teichoic acids. Proc Natl Acad Sci USA, 109(46), 18909–18914. https://doi.org/10.1073/pnas.1209126109

Buck, L. D., Paladino, M. M., Nagashima, K., Brezel, E. R., Holtzman, J. S., Urso, S. J., & Ryno, L. M. (2021). Temperature-Dependent Influence of FliA Overexpression on PHL628 E. coli Biofilm Growth and Composition. Front. Cell. Infect. Microbiol., 11, 775270. https://doi.org/10.3389/fcimb.2021.775270

Butaitė, E., Kramer, J., Wyder, S., & Kümmerli, R. (2018). Environmental determinants of pyoverdine production, exploitation and competition in natural Pseudomonas communities. Environ Microbiol, 20(10), 3629–3642. https://doi.org/10.1111/1462-2920.14355

Butler, A. J., Pintar, K., Thomas, J. L., Fleury, M., Kadykalo, S., Ziebell, K., … Lapen, D. (2021). Microbial water quality at contrasting recreational areas in a mixed-use watershed in eastern Canada. J Water Health, 19(6), 975–989. https://doi.org/10.2166/wh.2021.021

Camper, A. K. (2014). Organic matter pipe materials disinfectants and biofilms in distribution systems. In Dirk van der Kooij & P. W. J. J. van der Wielen (Eds.), Microbial Growth in Drinking Water Supplies: Problems, Causes, Control and Research Needs (pp. 73–94). London: IWA Publishing.

Carfrae, L. A., MacNair, C. R., Brown, C. M., Tsai, C. N., Weber, B. S., Zlitni, S., … Coombes, B. K. (2020). Mimicking the human environment in mice reveals that inhibiting biotin biosynthesis is effective against antibiotic-resistant pathogens. Nat Microbiol, 5(1), 93–101. https://doi.org/10.1038/s41564-019-0595-2

Cartron, M. L., Maddocks, S., Gillingham, P., Craven, C. J., & Andrews, S. C. (2006). Feo – Transport of Ferrous Iron into Bacteria. Biometals, 19, 143–157. https://doi.org/10.1007/s10534-006-0003-2

Centers for Disease Control and Prevention. (2019, December). Pseudomonas Aeruginosa Infection | HAI | CDC. Retrieved September 30, 2022, from Centers for Disease Control and Prevention website: https://www.cdc.gov/hai/organisms/pseudomonas.html

Centers for Disease Control and Prevention (CDC). (2012). Pseudomonas aeruginosa Respiratory Tract Infections Associated With Contaminated Ultrasound Gel Used for Transesophageal Echocardiography—Michigan, December 2011–January 2012. MMWR Morb Mortal Wkly Rep , 61(15), 262–264. Retrieved from https://europepmc.org/article/MED/22513528

Chahine, G. L., Kapahi, A., Choi, J.-K., & Hsiao, C.-T. (2016). Modeling of surface cleaning by cavitation bubble dynamics and collapse. Ultrasonics Sonochemistry, 29, 528–549. https://doi.org/10.1016/j.ultsonch.2015.04.026

Chakraborty, B., Pal, N. K., Maiti, P. K., Patra, S. K., & Ray, R. (2014). ACTION OF NEWER DISINFECTANTS ON MULTIDRUG RESISTANT BACTERIA. Journal of Evolution of Medical and Dental Sciences, 3(11), 2797–2813. https://doi.org/10.14260/jemds/2014/2211

Chen, B., Han, J., Dai, H., & Jia, P. (2021). Biocide-tolerance and antibiotic-resistance in community environments and risk of direct transfers to humans: Unintended consequences of community-wide surface disinfecting during COVID-19? Environmental Pollution, 283, 117074. https://doi.org/10.1016/j.envpol.2021.117074

Chowdary, G. V., & Prapulla, S. G. (2002). The influence of water activity on the lipase catalyzed synthesis of butyl butyrate by transesterification. Process Biochemistry, 38(3), 393–397. https://doi.org/10.1016/s0032-9592(02)00096-1

Christofi, T., Panayidou, S., Dieronitou, I., Michael, C., & Apidianakis, Y. (2019). Metabolic output defines Escherichia coli as a health-promoting microbe against intestinal Pseudomonas aeruginosa. Sci Rep, 9(1), 14463. https://doi.org/10.1038/s41598-019-51058-3

Clasen, T., Saeed, T. F., Edmondson, P., Boisson, S., & Shipin, O. (2007). Household water treatment using sodium dichloroisocyanurate (NaDCC) tablets: a randomized, controlled trial to assess microbiological effectiveness in Bangladesh. The American Journal of Tropical Medicine and Hygiene , 76(1), 187–192. https://doi.org/10.4269/ajtmh.2007.76.187

Coates, D. (1987). Relative stability of sodium hypochlorite liquids and sodium dichloroisocyanurate effervescent disinfectant tablets. Journal of Hospital Infection, 10(1), 96–97. https://doi.org/10.1016/0195-6701(87)90041-7

Cochran, W. L., Suh, S.-J., McFeters, G. A., & Stewart, P. S. (2000). Role of RpoS and AlgT in Pseudomonas aeruginosa biofilm resistance to hydrogen peroxide and monochloramine. J Appl Microbiol, 88(3), 546–553. https://doi.org/10.1046/j.1365-2672.2000.00995.x

Cole, S. J., & Lee, V. T. (2016). Cyclic Di-GMP Signaling Contributes to Pseudomonas aeruginosa-Mediated Catheter-Associated Urinary Tract Infection. J Bacteriol, 198(1), 91–97. https://doi.org/10.1128/jb.00410-15

Cosgrove, W. J., & Loucks, D. P. (2015). Water management: Current and future challenges and research directions. Water Resour. Res., 51(6), 4823–4839. https://doi.org/10.1002/2014wr016869

Crnich, C. J., Gordon, B., & Andes, D. (2003). Hot Tub–Associated Necrotizing Pneumonia due to Pseudomonas aeruginosa. Clin Infect Dis, 36(3), e55–e57. https://doi.org/10.1086/345851

Daer, S., Rehmann, E., Rehmann, J., & Ikuma, K. (2022). Development of Resistance in Escherichia coli Against Repeated Water Disinfection. Front. Environ. Sci., 10, 855224. https://doi.org/10.3389/fenvs.2022.855224

Dawood, D. H., & Sanad, M. I. (2014). DETERMINATION OF IONS (ANION AND CATION) BY ION CHROMATOGRAPHY IN DRINKING WATER FROM TALKHA TERRITORY AND SOME ITS VILLAGES, DAKAHLIA, EGYPT. Journal of Agricultural Chemistry and Biotechnology, 5(9), 215–226. https://doi.org/10.21608/jacb.2014.49898

Deborde, M., & von Gunten, U. (2008). Reactions of chlorine with inorganic and organic compounds during water treatment—Kinetics and mechanisms: A critical review. Water Research, 42(1–2), 13–51. https://doi.org/10.1016/j.watres.2007.07.025

Delaney, R. J. (2018). Determining the efficacy of products for bacterial biofilm prevention and removal for the wet leisure industry.

Díaz-Pérez, S. P., Solis, C. S., López-Bucio, J. S., Valdez Alarcón, J. J., Villegas, J., Reyes-De la Cruz, H., & Campos-Garcia, J. (2022). Pathogenesis in Pseudomonas aeruginosa PAO1 Biofilm-Associated Is Dependent on the Pyoverdine and Pyocyanin Siderophores by Quorum Sensing Modulation. Microb Ecol. https://doi.org/10.1007/s00248-022-02095-5

Dillemuth, N. (2011). Determination of chloride, chlorite, chlorate and bromate in pool water samples by ion chromatography. Concordia College Journal of Analytical Chemistry 2, 23–30. Retrieved from https://dept.cord.edu/chemistry/CCJAC/2011_Vol_2/2011_2_23.pdf#:~:text=A%20more%20accurate%20and%20still%20fairly%20simple%20way,ions%20can%20be%20analyzed%20to%20create%20calibration%20curves.

Ding, T., Suo, Y., Xiang, Q., Zhao, X., Chen, S., Ye, X., & Liu, D. (2017). Significance of Viable but Nonculturable Escherichia coli: Induction, Detection, and Control. Journal of Microbiology and Biotechnology, 27(3), 417–428. https://doi.org/10.4014/jmb.1609.09063

Dogsa, I., Kriechbaum, M., Stopar, D., & Laggner, P. (2005). Structure of Bacterial Extracellular Polymeric Substances at Different pH Values as Determined by SAXS. Biophysical Journal, 89(4), 2711–2720. https://doi.org/10.1529/biophysj.105.061648

Dubois-Brissonnet, F., Trotier, E., & Briandet, R. (2016). The Biofilm Lifestyle Involves an Increase in Bacterial Membrane Saturated Fatty Acids. Front. Microbiol., 7, 1673. https://doi.org/10.3389/fmicb.2016.01673

Dumas, Z., Ross-Gillespie, A., & Kümmerli, R. (2013). Switching between apparently redundant iron-uptake mechanisms benefits bacteria in changeable environments. Proc. R. Soc. B., 280, 20131055. https://doi.org/10.1098/rspb.2013.1055

ECHA. (2022). Pentapotassium bis(peroxymonosulphate) bis(sulphate) - Registration Dossier - ECHA. Retrieved December 14, 2022, from ECHA website: https://echa.europa.eu/registration-dossier/-/registered-dossier/15990/5/2/3

eco3spa. (2023, March 21). Step 2 Water Conditioner. Retrieved March 21, 2023, from eco3spa website: https://www.eco3spa.com/step-2-condition

El-Bana, A. A., Barakat, N. M., Abdelghany, A. M., & Meikhail, M. S. (2022). Effect of surfactants addition on physical, structure and antimicrobial activity of (Na-CMC/Na–Alg) biofilms. Polym. Bull. https://doi.org/10.1007/s00289-022-04189-z

Farkas, A., Bocoș, B., Bularda, M. D., & Crăciunaș, C. (2014). EFFECT OF DIFFERENT DISINFECTANTS AGAINST BIOFILM BACTERIA. STUDIA UNIVERSITATIS BABEŞ-BOLYAI BIOLOGIA, 1, 5–20. Retrieved from https://www.researchgate.net/publication/265168052_EFFECT_OF_DIFFERENT_DISINFECTANTS_AGAINST_BIOFILM_BACTERIA

Fernández, L., & Hancock, R. E. W. (2012). Adaptive and Mutational Resistance: Role of Porins and Efflux Pumps in Drug Resistance. Clin Microbiol Rev, 25(4), 661–681. https://doi.org/10.1128/cmr.00043-12

Flemming, H.-C., & Wingender, J. (2010). The biofilm matrix. Nat Rev Microbiol, 8, 623–633. https://doi.org/10.1038/nrmicro2415

Freeberg, M. A. T., Kallenbach, J. G., & Awad, H. A. (2019). Assessment of Cellular Responses of Tissue Constructs in vitro in Regenerative Engineering. In Encyclopedia of Biomedical Engineering (Vol. 1, pp. 414–426). Retrieved from https://www.sciencedirect.com/science/article/pii/B9780128012383998982

Freschi, L., Vincent, A. T., Jeukens, J., Emond-Rheault, J.-G., Kukavica-Ibrulj, I., Dupont, M.-J., … Levesque, R. C. (2019). ThePseudomonas aeruginosaPan-Genome Provides New Insights on Its Population Structure, Horizontal Gene Transfer, and Pathogenicity. Genome Biol. Evol., 11(1), 109–120. https://doi.org/10.1093/gbe/evy259

Gabale, U., Peña Palomino, P. A., Kim, H., Chen, W., & Ressl, S. (2020). The essential inner membrane protein YejM is a metalloenzyme. Sci Rep, 10(1), 17794. https://doi.org/10.1038/s41598-020-73660-6

Gallandat, K., Wolfe, M. K., & Lantagne, D. (2017). Surface Cleaning and Disinfection: Efficacy Assessment of Four Chlorine Types UsingEscherichia coliand the Ebola Surrogate Phi6. Environ. Sci. Technol., 51(8), 4624–4631. https://doi.org/10.1021/acs.est.6b06014

Gast, P., Hemelrijk, P. W., Gorkom, H. J., & Hoff, A. J. (1996). The Association of Different Detergents with the Photosynthetic Reaction Center Protein of Rhodobacter sphaeroides R26 and the Effects on its Photochemistry. Eur J Biochem, 239(3), 805–809. https://doi.org/10.1111/j.1432-1033.1996.0805u.x

Gedge, L. M., Hollingsworth, A. L., & Suchmann, D. B. (2019). New disinfectants for inactivation and disinfection of Pseudomonas aeruginosa: comparison with market leaders. J Bacteriol Mycol Open Access, 7(3), 55–59. https://doi.org/10.15406/jbmoa.2019.07.00243

Gerlach, D., Guo, Y., De Castro, C., Kim, S.-H., Schlatterer, K., Xu, F.-F., … Codée, J. (2018). Methicillin-resistant Staphylococcus aureus alters cell wall glycosylation to evade immunity. Nature, 563(7733), 705–709. https://doi.org/10.1038/s41586-018-0730-x

Göing, S., & Jung, K. (2021). Viable but Nonculturable Gastrointestinal Bacteria and Their Resuscitation. Archives of Gastroenterology Research, 2(2), 55–62. https://doi.org/10.33696/gastroenterology.2.027

Goodarzi, R., Yousefimashouf, R., Taheri, M., Nouri, F., & Asghari, B. (2021). Susceptibility to biocides and the prevalence of biocides resistance genes in clinical multidrug-resistant Pseudomonas aeruginosa isolates from Hamadan, Iran. Mol Biol Rep, 48(6), 5275–5281. https://doi.org/10.1007/s11033-021-06533-4

Gottesman, S. (2018). Chilled in Translation: Adapting to Bacterial Climate Change. Molecular Cell, 70(2), 193–194. https://doi.org/10.1016/j.molcel.2018.04.003

Graciaa, D. S., Cope, J. R., Roberts, V. A., Cikesh, B. L., Kahler, A. M., Vigar, M., … Montgomery, S. P. (2018). Outbreaks Associated with Untreated Recreational Water - United States, 2000-2014. MMWR Morb Mortal Wkly Rep, 67(25), 701–706. https://doi.org/10.15585/mmwr.mm6725a1

Grela, E., Kozłowska, J., & Grabowiecka, A. (2018). Current methodology of MTT assay in bacteria – A review. Acta Histochemica, 120(4), 303–311. https://doi.org/10.1016/j.acthis.2018.03.007

Griffin, B. (2012). Population Wellness: Keeping Cats Physically and Behaviorally Healthy. In S. E. Little (Ed.), The Cat (pp. 1312–1356). Retrieved from https://www.sciencedirect.com/science/article/pii/B9781437706604000466

Guan, Y.-H., Ma, J., Li, X.-C., Fang, J.-Y., & Chen, L.-W. (2011). Influence of pH on the Formation of Sulfate and Hydroxyl Radicals in the UV/Peroxymonosulfate System. Environ. Sci. Technol., 45(21), 9308–9314. https://doi.org/10.1021/es2017363

Gundlach, J., & Winter, J. (2014). Evolution of Escherichia coli for maximum HOCl resistance through constitutive expression of the OxyR regulon. Microbiology, 160(8), 1690–1704. https://doi.org/10.1099/mic.0.074815-0

Guo, L., Long, M., Huang, Y., Wu, G., Deng, W., Yang, X., … Fan, L. (2015). Antimicrobial and disinfectant resistance of Escherichia coli isolated from giant pandas. J Appl Microbiol, 119(1), 55–64. https://doi.org/10.1111/jam.12820

Halliwell, B., Adhikary, A., Dingfelder, M., & Dizdaroglu, M. (2021). Hydroxyl radical is a significant player in oxidative DNA damage in vivo. Chem. Soc. Rev., 50(15), 8355–8360. https://doi.org/10.1039/d1cs00044f

Halstead, F. D., Rauf, M., Moiemen, N. S., Bamford, A., Wearn, C. M., Fraise, A. P., … Webber, M. A. (2015). The Antibacterial Activity of Acetic Acid against Biofilm-Producing Pathogens of Relevance to Burns Patients. PLoS ONE, 10(9), e0136190. https://doi.org/10.1371/journal.pone.0136190

Hambsch, B., Ashworth, J., & van der Kooij, D. (2014). Enhancement of microbial growth by materials in contact with drinking water: problems and test methods. In Dirk van der Kooij & P. W. J. J. van der Wielen (Eds.), Microbial Growth in Drinking Water Supplies: Problems, Causes, Control and Research Needs (pp. 339–361). London: IWA Publishing.

Hausner, M., & Wuertz, S. (1999). High Rates of Conjugation in Bacterial Biofilms as Determined by Quantitative In Situ Analysis. Appl Environ Microbiol, 65(8), 3710–3713. https://doi.org/10.1128/aem.65.8.3710-3713.1999

Hazan, R., Que, Y.-A., Maura, D., & Rahme, L. G. (2012). A method for high throughput determination of viable bacteria cell counts in 96-well plates. BMC Microbiol, 12(1), 259. https://doi.org/10.1186/1471-2180-12-259

Held, P. (2011). Monitoring of Algal Growth Using their Intrinsic Properties. Retrieved September 12, 2022, from Agilent website: https://www.agilent.com/cs/library/applications/monitoring-of-algal-growth-5994-3290EN-agilent.pdf

Hernlem, B. J., & Tsai, L.-S. (2000). Titration of Chlorine: Amperometric versus Potentiometric. Journal - American Water Works Association, 92(12), 101–107. https://doi.org/10.1002/j.1551-8833.2000.tb09075.x

Hernndez, A., Martró, E., Matas, L., Martín, M., & Ausina, V. (2000). Assessment of in-vitro efficacy of 1% Virkon® against bacteria, fungi, viruses and spores by means of AFNOR guidelines. Journal of Hospital Infection, 46(3), 203–209. https://doi.org/10.1053/jhin.2000.0818

Hsieh, C.-M., Huang, Y.-H., Chen, C.-P., Hsieh, B.-C., & Tsai, T. (2014). 5-Aminolevulinic acid induced photodynamic inactivation on Staphylococcus aureus and Pseudomonas aeruginosa. Journal of Food and Drug Analysis, 22(3), 350–355. https://doi.org/10.1016/j.jfda.2013.09.051

Huang, G.-X., Si, J.-Y., Qian, C., Wang, W.-K., Mei, S.-C., Wang, C.-Y., & Yu, H.-Q. (2018). Ultrasensitive Fluorescence Detection of Peroxymonosulfate Based on a Sulfate Radical-Mediated Aromatic Hydroxylation. Anal. Chem., 90(24), 14439–14446. https://doi.org/10.1021/acs.analchem.8b04047

Huang, J.-J., Hu, H.-Y., Wu, Y.-H., Wei, B., & Lu, Y. (2013). Effect of chlorination and ultraviolet disinfection on tetA-mediated tetracycline resistance of Escherichia coli. Chemosphere, 90(8), 2247–2253. https://doi.org/10.1016/j.chemosphere.2012.10.008

Huhulescu, S., Simon, M., Lubnow, M., Kaase, M., Wewalka, G., Pietzka, A. T., … Allerberger, F. (2011). Fatal Pseudomonas aeruginosa pneumonia in a previously healthy woman was most likely associated with a contaminated hot tub. Infection, 39(3), 265–269. https://doi.org/10.1007/s15010-011-0096-6

Hulshof, P. B. J. E., Veenstra, J., & van Zwieten, R. (2019). Severe hemolytic anemia due to transient acquired G6PD deficiency after ingestion of sodium chlorite. Clinical Toxicology, 57(1), 65–66. https://doi.org/10.1080/15563650.2018.1491984

Hung, C., Zhou, Y., Pinkner, J. S., Dodson, K. W., Crowley, J. R., Heuser, J., … Hultgren, S. J. (2013). Escherichia coli Biofilms Have an Organized and Complex Extracellular Matrix Structure. MBio, 4(5), e00645-13. https://doi.org/10.1128/mbio.00645-13

Hwang, H.-J., Choi, H., Hong, S., Moon, H. R., & Lee, J.-H. (2021). Antipathogenic Compounds That Are Effective at Very Low Concentrations and Have Both Antibiofilm and Antivirulence Effects against Pseudomonas aeruginosa. Microbiol Spectr, 9(2), e00249-21. https://doi.org/10.1128/spectrum.00249-21

Ishikawa, S., Matsumura, Y., Yoshizako, F., & Tsuchido, T. (2002). Characterization of a cationic surfactant-resistant mutant isolated spontaneously from Escherichia coli. J Appl Microbiol, 92(2), 261–268. https://doi.org/10.1046/j.1365-2672.2002.01526.x

Jabeen, S., Farag, M., Malek, B., Choudhury, R., & Greer, A. (2020). A Singlet Oxygen Priming Mechanism: Disentangling of Photooxidative and Downstream Dark Effects. J. Org. Chem., 85(19), 12505–12513. https://doi.org/10.1021/acs.joc.0c01712

Jee, S.-C., Kim, M., Sung, J.-S., & Kadam, A. A. (2020). Efficient Biofilms Eradication by Enzymatic-Cocktail of Pancreatic Protease Type-I and Bacterial α-Amylase. Polymers, 12(12), 3032. https://doi.org/10.3390/polym12123032

Ji, Y., Shi, Y., Dong, W., Wen, X., Jiang, M., & Lu, J. (2016). Thermo-activated persulfate oxidation system for tetracycline antibiotics degradation in aqueous solution. Chemical Engineering Journal, 298, 225–233. https://doi.org/10.1016/j.cej.2016.04.028

Jin, M., Liu, L., Wang, D., Yang, D., Liu, W., Yin, J., … Shen, Z. (2020). Chlorine disinfection promotes the exchange of antibiotic resistance genes across bacterial genera by natural transformation. ISME J, 14(7), 1847–1856. https://doi.org/10.1038/s41396-020-0656-9

Johnson, L., Mulcahy, H., Kanevets, U., Shi, Y., & Lewenza, S. (2012). Surface-Localized Spermidine Protects the Pseudomonas aeruginosa Outer Membrane from Antibiotic Treatment and Oxidative Stress. J Bacteriol, 194(4), 813–826. https://doi.org/10.1128/jb.05230-11

Kalpana, B. J., Aarthy, S., & Pandian, S. K. (2012). Antibiofilm Activity of α-Amylase from Bacillus subtilis S8-18 Against Biofilm Forming Human Bacterial Pathogens. Appl Biochem Biotechnol, 167(6), 1778–1794. https://doi.org/10.1007/s12010-011-9526-2

Kamal, M. A., Khalaf, M. A., Ahmed, Z. A. M., & El Jakee, J. (2019). Evaluation of the efficacy of commonly used disinfectants against isolated chlorine-resistant strains from drinking water used in Egyptian cattle farms. Vet World, 12(12), 2025–2035. https://doi.org/10.14202/vetworld.2019.2025-2035

Kannan, A., & Gautam, P. (2015). A quantitative study on the formation of Pseudomonas aeruginosa biofilm. SpringerPlus, 4(1), 379. https://doi.org/10.1186/s40064-015-1029-0

Karagianni, K. (2022). Sanitizing efficacy of an environmentally friendly combination hot tub product – eco3spa. Retrieved from https://cronfa.swan.ac.uk/Record/cronfa59100

Karbasi, M., Karimzadeh, F., Raeissi, K., Giannakis, S., & Pulgarin, C. (2020). Improving visible light photocatalytic inactivation of E. coli by inducing highly efficient radical pathways through peroxymonosulfate activation using 3-D, surface-enhanced, reduced graphene oxide (rGO) aerogels. Chemical Engineering Journal, 396, 125189. https://doi.org/10.1016/j.cej.2020.125189

Kareem, S. O., Adio, O. Q., & Osho, M. B. (2014). Immobilization of Aspergillus niger F7-02 Lipase in Polysaccharide Hydrogel Beads of Irvingia gabonensis Matrix. Enzyme Research, 2014, 967056. https://doi.org/10.1155/2014/967056

Kaya, E., Grassi, L., Benedetti, A., Maisetta, G., Pileggi, C., Di Luca, M., … Esin, S. (2020). In vitro Interaction of Pseudomonas aeruginosa Biofilms With Human Peripheral Blood Mononuclear Cells. Front. Cell. Infect. Microbiol., 10(1), 187. https://doi.org/10.3389/fcimb.2020.00187

Kennedy, R. J., & Stock, A. M. (1960). The Oxidation of Organic Substances by Potassium Peroxymonosulfate. J. Org. Chem., 25, 1901–1906. https://doi.org/10.1021/JO01081A019

Khurshid, H., Rafiq, M., Nazir, F., Ali, I., Ahmed, M., Akbar, B., & Ahmed, M. (2019). Antimicrobial properties of hydrogen peroxide and potash alum alone and in combination against clinical bacterial isolates. Pure Appl. Biol, 8(4). https://doi.org/10.19045/bspab.2019.80169

Kim, D., Chung, S., Lee, S., & Choi, J. (2012). Relation of microbial biomass to counting units for Pseudomonas aeruginosa. Afr. J. Microbiol. Res., 6(21), 4620–4622. https://doi.org/10.5897/ajmr10.902

Kim, M., Hatt, J. K., Weigand, M. R., Krishnan, R., Pavlostathis, S. G., & Konstantinidis, K. T. (2018). Genomic and Transcriptomic Insights into How Bacteria Withstand High Concentrations of Benzalkonium Chloride Biocides. Appl Environ Microbiol, 84(12), e00197-18. https://doi.org/10.1128/aem.00197-18

Kim, Sunghwan, Chen, J., Cheng, T., Gindulyte, A., He, J., He, S., … Yu, B. (2021). PubChem in 2021: new data content and improved web interfaces. Nucleic Acids, 49(D1), D1388–D1395. https://doi.org/10.1093/nar/gkaa971

Kim, Suran, Li, X.-H., Hwang, H.-J., & Lee, J.-H. (2020). Thermoregulation of Pseudomonas aeruginosa Biofilm Formation. Appl Environ Microbiol, 86(22), e01584-20. https://doi.org/10.1128/AEM.01584-20

Klausen, M., Heydorn, A., Ragas, P., Lambertsen, L., Aaes-Jørgensen, A., Molin, S., & Tolker-Nielsen, T. (2003). Biofilm formation by Pseudomonas aeruginosa wild type, flagella and type IV pili mutants. Molecular Microbiology, 48(6), 1511–1524. https://doi.org/10.1046/j.1365-2958.2003.03525.x

Kohanski, M. A., Dwyer, D. J., Hayete, B., Lawrence, C. A., & Collins, J. J. (2007). A Common Mechanism of Cellular Death Induced by Bactericidal Antibiotics. Cell, 130(5), 797–810. https://doi.org/10.1016/j.cell.2007.06.049

Kristensen, G. H., Klausen, M. M., Hansen, V. A., & Lauritsen, F. R. (2010). On-line monitoring of the dynamics of trihalomethane concentrations in a warm public swimming pool using an unsupervised membrane inlet mass spectrometry system with off-site real-time surveillance. Rapid Commun. Mass Spectrom., 24(1), 30–34. https://doi.org/10.1002/rcm.4360

Kumar, S., & Doerrler, W. T. (2015). Escherichia coli YqjA, a Member of the Conserved DedA/Tvp38 Membrane Protein Family, Is a Putative Osmosensing Transporter Required for Growth at Alkaline pH. J Bacteriol, 197(14), 2292–2300. https://doi.org/10.1128/jb.00175-15

Kumar, S., Tiwari, V., & Doerrler, W. T. (2017). Cpx-dependent expression of YqjA requires cations at elevated pH. FEMS Microbiology Letters, 364(12). https://doi.org/10.1093/femsle/fnx115

Kunanusont, N., Punyadarsaniya, D., Jantafong, T., Pojprasath, T., Takehara, K., & Ruenphet, S. (2020). Bactericidal efficacy of potassium peroxymonosulfate under various concentrations, organic material conditions, exposure timing and its application on various surface carriers. The Journal of Veterinary Medical Science, 82(3), 320–324. https://doi.org/10.1292/jvms.19-0562

Kundukad, B., Schussman, M., Yang, K., Seviour, T., Yang, L., Rice, S. A., … Doyle, P. S. (2017). Mechanistic action of weak acid drugs on biofilms. Sci Rep, 7(1), 4783. https://doi.org/10.1038/s41598-017-05178-3

Kuznesof, P. M. (2004). SODIUM DICHLOROISOCYANURATE (NaDCC – anhydrous and dihydrate). Retrieved October 1, 2022, from Food and Agriculture Organization of the United Nations website: https://www.fao.org/fileadmin/templates/agns/pdf/jecfa/cta/61/NaDCC.pdf

Lappann, M., Claus, H., van Alen, T., Harmsen, M., Elias, J., Molin, S., & Vogel, U. (2010). A dual role of extracellular DNA during biofilm formation of Neisseria meningitidis. Molecular Microbiology, 75(6), 1355–1371. https://doi.org/10.1111/j.1365-2958.2010.07054.x

Lee, S. F., Rose, A., Christison, T., & Rohrer, J. (2020). Determination of trace anions in basic solutions by single pass AutoNeutralization and ion chromatography. Retrieved October 2, 2022, from Thermo Fisher Scientific website: https://assets.thermofisher.com/TFS-Assets/CMD/Application-Notes/an-72481-ic-trace-anions-concentrated-bases-an72481-en.pdf

Leoni, E., Catalani, F., Marini, S., & Dallolio, L. (2018). Legionellosis Associated with Recreational Waters: A Systematic Review of Cases and Outbreaks in Swimming Pools, Spa Pools, and Similar Environments. Int J Environ Res Public Health, 15(8), 1612. https://doi.org/10.3390/ijerph15081612

Lewenza, S., Johnson, L., Charron-Mazenod, L., Hong, M., & Mulcahy-O'Grady, H. (2020). Extracellular DNA controls expression of Pseudomonas aeruginosa genes involved in nutrient utilization, metal homeostasis, acid pH tolerance and virulence. Journal of Medical Microbiology, 69, 895–905. https://doi.org/10.1099/jmm.0.001184

Li, M., Carlson, S., Kinzer, J. A., & Perpall, H. J. (2003). HPLC and LC-MS studies of hydroxylation of phenylalanine as an assay for hydroxyl radicals generated from Udenfriend's reagent. Biochemical and Biophysical Research Communications, 312(2), 316–322. https://doi.org/10.1016/j.bbrc.2003.10.116

Li, X., Yan, Z., & Xu, J. (2003). Quantitative variation of biofilms among strains in natural populations of Candida albicans. Microbiology, 149(2), 353–362. https://doi.org/10.1099/mic.0.25932-0

Lim, E. S., Koo, O. K., Kim, M.-J., & Kim, J.-S. (2019). Bio-enzymes for inhibition and elimination of Escherichia coli O157:H7 biofilm and their synergistic effect with sodium hypochlorite. Sci Rep, 9(1), 9920. https://doi.org/10.1038/s41598-019-46363-w

Liu, G., Bakker, G. L., Li, S., Vreeburg, J. H. G., Verberk, J. Q. J. C., Medema, G. J., … Van Dijk, J. C. (2014). Pyrosequencing Reveals Bacterial Communities in Unchlorinated Drinking Water Distribution System: An Integral Study of Bulk Water, Suspended Solids, Loose Deposits, and Pipe Wall Biofilm. Environ. Sci. Technol., 48(10), 5467–5476. https://doi.org/10.1021/es5009467

Liu, Y., Zhang, J., & Ji, Y. (2020). Environmental factors modulate biofilm formation by Staphylococcus aureus. Science Progress, 103(1), 1–14. https://doi.org/10.1177/0036850419898659

Lonza Ltd. (2013). PROXELTM GXL Preservative. Retrieved March 22, 2023, from Lonza website: https://azelisamericascase.com/wp-content/uploads/2018/09/Proxel-GXL-Preservative.pdf

Lorite, G. S., Rodrigues, C. M., de Souza, A. A., Kranz, C., Mizaikoff, B., & Cotta, M. A. (2011). The role of conditioning film formation and surface chemical changes on Xylella fastidiosa adhesion and biofilm evolution. Journal of Colloid and Interface Science, 359(1), 289–295. https://doi.org/10.1016/j.jcis.2011.03.066

Lu, J., Gerke, T. L., Buse, H. Y., & Ashbolt, N. J. (2014). Development of an Escherichia coli K12-specific quantitative polymerase chain reaction assay and DNA isolation suited to biofilms associated with iron drinking water pipe corrosion products. J Water Health, 12(4), 763–771. https://doi.org/10.2166/wh.2014.203

Lugo, J. L., Lugo, E. R., & Puente, M. de la. (2021). A systematic review of microorganisms as indicators of recreational water quality in natural and drinking water systems. J Water Health, 19(1), 20–28. https://doi.org/10.2166/wh.2020.179

Lutz, J., & Lee, J. (2011). Prevalence and Antimicrobial-Resistance of Pseudomonas aeruginosa in Swimming Pools and Hot Tubs. Int. J. Environ. Res. Public Health, 8, 554–564. https://doi.org/10.3390/ijerph8020554

Ma, Q., Yang, Z., Pu, M., Peti, W., & Wood, T. K. (2011). Engineering a novel c-di-GMP-binding protein for biofilm dispersal. Environmental Microbiology, 13(3), 631–642. https://doi.org/10.1111/j.1462-2920.2010.02368.x

Ma, Q., Zhang, G., & Wood, T. K. (2011). Escherichia coli BdcA controls biofilm dispersal in Pseudomonas aeruginosa and Rhizobium meliloti. BMC Res Notes, 4(1), 447. https://doi.org/10.1186/1756-0500-4-447

Madsen, J. S., Burmølle, M., Hansen, L. H., & Sørensen, S. J. (2012). The interconnection between biofilm formation and horizontal gene transfer. FEMS Immunol Med Microbiol, 65(2), 183–195. https://doi.org/10.1111/j.1574-695x.2012.00960.x

Mahayothee, B., Koomyart, I., Khuwijitjaru, P., Siriwongwilaichat, P., Nagle, M., & Müller, J. (2016). Phenolic Compounds, Antioxidant Activity, and Medium Chain Fatty Acids Profiles of Coconut Water and Meat at Different Maturity Stages. International Journal of Food Properties, 19(9), 2041–2051. https://doi.org/10.1080/10942912.2015.1099042

Mansoury, M., Hamed, M., Karmustaji, R., Al Hannan, F., & Safrany, S. T. (2021). The edge effect: A global problem. The trouble with culturing cells in 96-well plates. Biochemistry and Biophysics Reports, 26, 100987. https://doi.org/10.1016/j.bbrep.2021.100987

Marjanovic, M., Giannakis, S., Grandjean, D., de Alencastro, L. F., & Pulgarin, C. (2018). Effect of µM Fe addition, mild heat and solar UV on sulfate radical-mediated inactivation of bacteria, viruses, and micropollutant degradation in water. Water Research, 140, 220–231. https://doi.org/10.1016/j.watres.2018.04.054

Mathlouthi, A., Pennacchietti, E., & Biase, D. D. (2018). Effect of Temperature, pH and Plasmids on In Vitro Biofilm Formation in Escherichia coli. Acta Naturae, 10(4), 129–132. https://doi.org/10.32607/20758251-2018-10-4-129-132

May, T., Ito, A., & Okabe, S. (2010). Characterization and global gene expression of F− phenocopies during Escherichia coli biofilm formation. Mol Genet Genomics, 284(5), 333–342. https://doi.org/10.1007/s00438-010-0571-2

McBride, S. M., & Sonenshein, A. L. (2011). The dlt operon confers resistance to cationic antimicrobial peptides in Clostridium difficile. Microbiology, 157(5), 1457–1465. https://doi.org/10.1099/mic.0.045997-0

Merritt, J. H., Kadouri, D. E., & O'Toole, G. A. (2005). Growing and Analyzing Static Biofilms. CP Microbiology, (1), Unit 1B.1. https://doi.org/10.1002/9780471729259.mc01b01s00

Meyer, K. J., Appletoft, C. M., Schwemm, A. K., Uzoigwe, J. C., & Brown, E. J. (2005). Determining the source of fecal contamination in recreational waters. Journal of Environmental Health, 68(1), 25–30. Retrieved from https://www.researchgate.net/publication/7640154_Determining_the_source_of_fecal_contamination_in_recreational_waters

Mistretta, N., Brossaud, M., Telles, F., Sanchez, V., Talaga, P., & Rokbi, B. (2019). Glycosylation of Staphylococcus aureus cell wall teichoic acid is influenced by environmental conditions. Sci Rep, 9(1), 3212. https://doi.org/10.1038/s41598-019-39929-1

Moberg, L., & Karlberg, B. (2000). An improved N,N'-diethyl-p-phenylenediamine (DPD) method for the determination of free chlorine based on multiple wavelength detection. Analytica Chimica Acta, 407(1–2), 127–133. https://doi.org/10.1016/s0003-2670(99)00780-1

Mok, W. F., Prasad, R., & Li, P. (2000). Ion chromatographic analysis of swimming pool water disinfected by ozone and sodium hypochlorite. Science Direct, S1574-0331(04), 70385–70389. Retrieved from https://ssrn.com/abstract=2969408

Montagnin, C., Cawthraw, S., Ring, I., Ostanello, F., Smith, R. P., Davies, R., & Martelli, F. (2022). Efficacy of Five Disinfectant Products Commonly Used in Pig Herds against a Panel of Bacteria Sensitive and Resistant to Selected Antimicrobials. Animals, 12(20), 2780. https://doi.org/10.3390/ani12202780

Moslehifard, E., Lotfipour, F., Anaraki, M. R., Shafee, E., Tamjid-Shabestari, S., & Ghaffari, T. (2015). Efficacy of Disinfection of Dental Stone Casts: Virkon versus Sodium Hypochlorite. J Dent (Tehran), 12(3), 206–215. Retrieved from https://europepmc.org/article/MED/26622274

Murphy, M. P., Bayir, H., Belousov, V., Chang, C. J., Davies, K. J. A., Davies, M. J., … Janssen-Heininger, Y. (2022). Guidelines for measuring reactive oxygen species and oxidative damage in cells and in vivo. Nat Metab , 4(6), 651–662. Retrieved from https://doi.org/10.1038/s42255-022-00591-z

Murray, A., & Lantagne, D. (2015). Accuracy, precision, usability, and cost of free chlorine residual testing methods. Journal of Water and Health, 13(1), 79–90. https://doi.org/10.2166/wh.2014.195

Nascimento, M. S., Silva, N., Catanozi, M. P. L. M., & Silva, K. C. (2003). Effects of Different Disinfection Treatments on the Natural Microbiota of Lettuce. Journal of Food Protection, 66(9), 1697–1700. https://doi.org/10.4315/0362-028x-66.9.1697

Nelson, D. J., & Marbury, G. D. (2021). A risk-based approach to validation of ion chromatography methods using suppressed conductivity. AAPS Open, 7(1), 10. https://doi.org/10.1186/s41120-021-00044-z

Newman, J., Floyd, R., & Fothergill, J. (2022). Invasion and diversity in Pseudomonas aeruginosa urinary tract infections. J Med Microbiol, 71(3), 001458. https://doi.org/10.1099/jmm.0.001458

Nguyen, N.-Y. T., Grelling, N., Wetteland, C. L., Rosario, R., & Liu, H. (2018). Antimicrobial Activities and Mechanisms of Magnesium Oxide Nanoparticles (nMgO) against Pathogenic Bacteria, Yeasts, and Biofilms. Sci Rep, 8(1), 16260. https://doi.org/10.1038/s41598-018-34567-5

Nickerson, K. P., & McDonald, C. (2012). Crohn's Disease-Associated Adherent-Invasive Escherichia coli Adhesion Is Enhanced by Exposure to the Ubiquitous Dietary Polysaccharide Maltodextrin. PLoS ONE, 7(12), e52132. https://doi.org/10.1371/journal.pone.0052132

Niu, C., & Gilbert, E. S. (2004). Colorimetric Method for Identifying Plant Essential Oil Components That Affect Biofilm Formation and Structure. Appl Environ Microbiol, 70(12), 6951–6956. https://doi.org/10.1128/aem.70.12.6951-6956.2004

Nontaleerak, B., Duang-nkern, J., Wongsaroj, L., Trinachartvanit, W., Romsang, A., & Mongkolsuk, S. (2020). Roles of RcsA, an AhpD Family Protein, in Reactive Chlorine Stress Resistance and Virulence in Pseudomonas aeruginosa. Appl Environ Microbiol, 86(20), e01480-20. https://doi.org/10.1128/aem.01480-20

Ochsner, U. A., Johnson, Z., & Vasil, M. L. (2000). Genetics and regulation of two distinct haem-uptake systems, phu and has, in Pseudomonas aeruginosa. Microbiology, 146(1), 185–198. https://doi.org/10.1099/00221287-146-1-185

Oliveira, I. M., Gomes, I. B., Simões, L. C., & Simões, M. (2022). Chlorinated cyanurates and potassium salt of peroxymonosulphate as antimicrobial and antibiofilm agents for drinking water disinfection. Science of The Total Environment, 811, 152355. https://doi.org/10.1016/j.scitotenv.2021.152355

O'Neill, J. (2016, May 19). Tackling Drug-Resistant Infections Globally: final report and recommendations. Retrieved April 8, 2023, from Review on Antimicrobial Resistance website: https://amr-review.org/sites/default/files/160525_Final%20paper_with%20cover.pdf

Orlandi, V. T., Chiodaroli, L., Tolker-Nielsen, T., Bolognese, F., & Barbieri, P. (2015). Pigments influence the tolerance of Pseudomonas aeruginosa PAO1 to photodynamically induced oxidative stress. Microbiology (Reading), 161(12), 2298–2309. https://doi.org/10.1099/mic.0.000193

Osborne, E., Bilalian, C., Cussans, A., & Ostlere, L. (2021). Pseudomonas folliculitis: a complication of the lockdown hot tub boom? Lessons from a patient. Br J Gen Pract, 71(702), 43–44. https://doi.org/10.3399/bjgp21x714605

O'Toole, G. A. (2011). Microtiter Dish Biofilm Formation Assay. JoVE, (47), 2437. https://doi.org/10.3791/2437

Owoseni, M., Olaniran, A., & Okoh, A. (2017). Chlorine Tolerance and Inactivation of Escherichia coli recovered from Wastewater Treatment Plants in the Eastern Cape, South Africa. Applied Sciences, 7(8), 810. https://doi.org/10.3390/app7080810

Paliy, O., & Gunasekera, T. S. (2007). Growth of E. coli BL21 in minimal media with different gluconeogenic carbon sources and salt contents. Appl Microbiol Biotechnol, 73(5), 1169–1172. https://doi.org/10.1007/s00253-006-0554-8

Pape-Bub, M. (2020). Effect Of Microplate Materials on UV Absorbance Measurements. Retrieved September 12, 2022, from Molecular Devices website: https://www.moleculardevices.com/en/assets/app-note/br/effect-of-microplate-materials-on-uv-absorbance-measurements#:~:text=Both%20COC%20microplates%2C%20the%20%CE%BCCLEAR%20UV%20STAR%2096-,nm%2C%20decreasing%20to%200.2%20OD%20at%20230%20nm.

Patterson, R. (2019, November 22). Bromine Vs. Chlorine: What's The Difference? Retrieved December 16, 2022, from Poolonomics website: https://poolonomics.com/bromine-vs-chlorine/#:~:text=Bromine%20and%20chlorine%20will%20sanitize%20and%20oxidize%20pool,ultraviolet%20light%2C%20especially%20when%20coupled%20with%20cyanuric%20acid.

Patterson, R. (2020, August 25). Free Chlorine Vs Combined & Total Chlorine (Explained). Retrieved March 17, 2023, from Poolonomics website: https://poolonomics.com/free-chlorine-vs-combined-total/

Paun, I., Iancu, V.-I., Chiriac, F. L., Vasilache, N., Pirvu, F., Niculescu, M., & Galaon, T. (2020). New ion-chromatography method for detection of chlorite, chlorate, and bromate in drinking water. Romanian Journal of Ecology & Environmental Chemistry, 2(2). https://doi.org/10.21698/rjeec.2020.207

Peeters, E., Nelis, H. J., & Coenye, T. (2008). Comparison of multiple methods for quantification of microbial biofilms grown in microtiter plates. Journal of Microbiological Methods, 72(2), 157–165. https://doi.org/10.1016/j.mimet.2007.11.010

Pereira, A. L., Vasconcelos, M. A., Andrade, A. L., Martins, I. M., Holanda, A. K. M., Gondim, A. C. S., … Teixeira, E. H. (2023). Antimicrobial and Antibiofilm Activity of Copper-Based Metallic Compounds Against Bacteria Related with Healthcare-Associated Infections. Curr Microbiol, 80(4), 133. https://doi.org/10.1007/s00284-023-03232-0

Pereira, M. O., & Vieira, M. J. (2001). Effects of the interactions between glutaraldehyde and the polymeric matrix on the efficacy of the biocide againstpseudomonas fluorescensbiofilms. Biofouling, 17(2), 93–101. https://doi.org/10.1080/08927010109378469

Peschel, A., Vuong, C., Otto, M., & Götz, F. (2000). The d-alanine residues of Staphylococcus aureus teichoic acids alter the susceptibility to vancomycin and the activity of autolytic enzymes. Antimicrob Agents Chemother, 44(10), 2845–2847. https://doi.org/10.1128/aac.44.10.2845-2847.2000

Phadtare, S. (2012). Escherichia coli cold-shock gene profiles in response to over-expression/deletion of CsdA, RNase R and PNPase and relevance to low-temperature RNA metabolism. Genes to Cells , 17(10), 850–874. https://doi.org/10.1111/gtc.12002

Piecuch, A., Lamch, Ł., Paluch, E., Obłąk, E., & Wilk, K. A. (2016). Biofilm prevention by dicephalic cationic surfactants and their interactions with DNA. J Appl Microbiol, 121(3), 682–692. https://doi.org/10.1111/jam.13204

Pierson, L. S., & Pierson, E. A. (2010). Metabolism and function of phenazines in bacteria: impacts on the behavior of bacteria in the environment and biotechnological processes. Appl Microbiol Biotechnol, 86(6), 1659–1670. https://doi.org/10.1007/s00253-010-2509-3

Pinto, G., & Rohrig, B. (2003). Use of Chloroisocyanuarates for Disinfection of Water: Application of Miscellaneous General Chemistry Topics. J. Chem. Educ., 80(1), 41. https://doi.org/10.1021/ed080p41

Poirel, L., Madec, J.-Y., Lupo, A., Schink, A.-K., Kieffer, N., Nordmann, P., & Schwarz, S. (2018). Antimicrobial Resistance in Escherichia coli. Microbiol Spectr, 6(4). https://doi.org/10.1128/microbiolspec.ARBA-0026-2017

Popa, D.-S., Vlase, L., Daciana, C., & Loghin, F. (2010). Rapid LC-MS/MS assay for the evaluation of hydroxyl radical generation and oxidative stress induction in vivo in rats. Revista Romana de Medicina de Laborator, 18(4), 37–45. Retrieved from https://www.researchgate.net/publication/230996986_Rapid_LC-MSMS_assay_for_the_evaluation_of_hydroxyl_radical_generation_and_oxidative_stress_induction_in_vivo_in_rats

Prabhawathi, V., Boobalan, T., Sivakumar, P. M., & Doble, M. (2014). Antibiofilm Properties of Interfacially Active Lipase Immobilized Porous Polycaprolactam Prepared by LB Technique. PLoS ONE, 9(5), e96152. https://doi.org/10.1371/journal.pone.0096152

Puspitasari, V. L., Rattier, M., Le-Clech, P., & Chen, V. (2010). Performances of protease and amylase cleaning for microporous membranes used in wastewater applications. Desalination and Water Treatment, 13, 441–449. https://doi.org/10.5004/dwt.2010.1003

Puthia, M., Marzinek, J. K., Petruk, G., Ertürk Bergdahl, G., Bond, P. J., & Petrlova, J. (2022). Antibacterial and Anti-Inflammatory Effects of Apolipoprotein E. Biomedicines, 10, 1430. https://doi.org/10.3390/biomedicines10061430

Raffellini, S., Guerrero, S., & Alzamora, S. M. (2008). Effect of hydrogen peroxide concentration and pH on inactivation kinetics of Escherichia coli. Journal of Food Safety, 28(4), 514–533. https://doi.org/10.1111/j.1745-4565.2008.00128.x

Rahman, M., Uddin, M. S., Zaman, S., Saleh, M., Ekram, A., Farhana, P., & Razu, M. (2012). Comparative study on growth and morphological characteristics of a wild type strain Rhizobium spp. (RCA-220) and a genetically engineered E. coli BL21. J Bio-Sci., 20, 75–82. https://doi.org/10.3329/jbs.v20i0.17718

Rajachar, P. B., Vidhya, M. S., Karale, R., Govindaraju, V. K., & Shetty, N. K. (2021). Evaluation of Free Available Chlorine of Sodium Hypochlorite When Admixed with 0.2% Chitosan: A Preliminary Study. The Journal of Contemporary Dental Practice, 22(10), 1171–1174. https://doi.org/10.5005/jp-journals-10024-3207

Rasamiravaka, T., Vandeputte, O. M., Pottier, L., Huet, J., Rabemanantsoa, C., Kiendrebeogo, M., … Duez, P. (2015). Pseudomonas aeruginosa Biofilm Formation and Persistence, along with the Production of Quorum Sensing-Dependent Virulence Factors, Are Disrupted by a Triterpenoid Coumarate Ester Isolated from Dalbergia trichocarpa, a Tropical Legume. PLoS ONE, 10(7), e0132791. https://doi.org/10.1371/journal.pone.0132791

Robben, C., Fister, S., Witte, A. K., Schoder, D., Rossmanith, P., & Mester, P. (2018). Induction of the viable but non-culturable state in bacterial pathogens by household cleaners and inorganic salts. Sci Rep, 8(1), 15132. https://doi.org/10.1038/s41598-018-33595-5

Robinson, P. K. (2015). Enzymes: principles and biotechnological applications. Essays Biochem, 59, 1–41. https://doi.org/10.1042/bse0590001

Saberi, E. A., Farhad-Mollashahi, N., & Saberi, M. (2019). Difference between the Actual and Labeled Concentrations of Several Domestic Brands of Sodium Hypochlorite. Iranian Endodontic Journal, 14(2), 139–143. Retrieved from https://journals.sbmu.ac.ir/iej/article/view/23120/18065

Sagripanti, J.-L., & Bonifacino, A. (2000). Resistance of Pseudomonas aeruginosa to Liquid Disinfectants on Contaminated Surfaces before Formation of Biofilms. J AOAC Int, 83(6), 1415–1422. https://doi.org/10.1093/jaoac/83.6.1415

Sakuragi, Y., & Kolter, R. (2007). Quorum-Sensing Regulation of the Biofilm Matrix Genes (pel) of Pseudomonas aeruginosa. J Bacteriol, 189(14), 5383–5386. https://doi.org/10.1128/jb.00137-07

Samad, A., Khan, A. A., Sajid, M., & Zahra, R. (2019). Assessment of biofilm formation by pseudomonas aeruginosa and hydrodynamic evaluation of microtiter plate assay. J Pak Med Assoc , 69(5), 666–671. Retrieved from https://jpma.org.pk/article-details/9151?article_id=9151

Santos, D. M. S. dos, Pires, J. G., Braga, A. S., Salomão, P. M. A., & Magalhães, A. C. (2019). Comparison between static and semi-dynamic models for microcosm biofilm formation on dentin. J. Appl. Oral Sci., 27, e20180163. https://doi.org/10.1590/1678-7757-2018-0163

Saur, T., Morin, E., Habouzit, F., Bernet, N., & Escudié, R. (2017). Impact of wall shear stress on initial bacterial adhesion in rotating annular reactor. PLoS ONE, 12(2), e0172113. https://doi.org/10.1371/journal.pone.0172113

Schlafer, S., Meyer, R. L., Dige, I., & Regina, V. R. (2017). Extracellular DNA Contributes to Dental Biofilm Stability. Caries Res, 51(4), 436–442. https://doi.org/10.1159/000477447

Schneider, E. L. (1983). Infectious diseases in the elderly. Annals of Internal Medicine, 98(3), 395–400. https://doi.org/10.7326/0003-4819-98-3-395

Sezonov, G., Joseleau-Petit, D., & D'Ari, R. (2007). Escherichia coli Physiology in Luria-Bertani Broth. J Bacteriol, 189(23), 8746–8749. https://doi.org/10.1128/jb.01368-07

Sheraton, M. V., Yam, J. K. H., Tan, C. H., Oh, H. S., Mancini, E., Yang, L., … Sloot, P. M. A. (2018). Mesoscopic Energy Minimization Drives Pseudomonas aeruginosa Biofilm Morphologies and Consequent Stratification of Antibiotic Activity Based on Cell Metabolism. Antimicrob Agents Chemother, 62(5), e02544-17. https://doi.org/10.1128/aac.02544-17

Shukla, S. K., & Rao, T. S. (2017). An Improved Crystal Violet Assay for Biofilm Quantification in 96-Well Microtitre Plate. BioRxiv. https://doi.org/10.1101/100214

Sivaraman, S., Zwahlen, J., Bell, A. F., Hedstrom, L., & Tonge, P. J. (2003). Structure−Activity Studies of the Inhibition of FabI, the Enoyl Reductase from Escherichia coli, by Triclosan: Kinetic Analysis of Mutant FabIs. Biochemistry, 42(15), 4406–4413. https://doi.org/10.1021/bi0300229

Skandamis, P., Stopforth, J., Ashton, L., Geornaras, I., Kendall, P., & Sofos, J. (2009). Escherichia coli O157:H7 survival, biofilm formation and acid tolerance under simulated slaughter plant moist and dry conditions. Food Microbiology, 26(1), 112–119. https://doi.org/10.1016/j.fm.2008.09.001

Slipski, C. J., Zhanel, G. G., & Bay, D. C. (2018). Biocide Selective TolC-Independent Efflux Pumps in Enterobacteriaceae. J Membrane Biol, 251(1), 15–33. https://doi.org/10.1007/s00232-017-9992-8

Sobhanifar, S., Worrall, L. J., King, D. T., Wasney, G. A., Baumann, L., Gale, R. T., … Strynadka, N. C. J. (2016). Structure and Mechanism of Staphylococcus aureus TarS, the Wall Teichoic Acid β-glycosyltransferase Involved in Methicillin Resistance. PLoS Pathog, 12(12), e1006067. https://doi.org/10.1371/journal.ppat.1006067

Sohbatzadeh, F., Hosseinzadeh Colagar, A., Mirzanejhad, S., & Mahmodi, S. (2010). E. coli, P. aeruginosa, and B. cereus Bacteria Sterilization Using Afterglow of Non-Thermal Plasma at Atmospheric Pressure. Appl Biochem Biotechnol, 160(7), 1978–1984. https://doi.org/10.1007/s12010-009-8817-3

Stack, M. A., Fitzgerald, G., O'Connell, S., & James, K. J. (2000). Measurement of trihalomethanes in potable and recreational waters using solid phase micro extraction with gas chromatography-mass spectrometry. Chemosphere, 41(11), 1821–1826. https://doi.org/10.1016/s0045-6535(00)00047-3

Stevenson, K., McVey, A. F., Clark, I. B. N., Swain, P. S., & Pilizota, T. (2016). General calibration of microbial growth in microplate readers. Scientific Reports, 6, 38828. https://doi.org/10.1101/061861

String, G. M., Gutiérrez, E. V., & Lantagne, D. S. (2020). Laboratory efficacy of surface disinfection using chlorine against Vibrio cholerae. Journal of Water and Health, 18(6), 1009–1019. https://doi.org/10.2166/wh.2020.199

Sun, P., Tyree, C., & Huang, C.-H. (2016). Inactivation of Escherichia coli, Bacteriophage MS2, and Bacillus Spores under UV/H2O2 and UV/Peroxydisulfate Advanced Disinfection Conditions. Environ. Sci. Technol., 50(8), 4448–4458. https://doi.org/10.1021/acs.est.5b06097

Sviridova, D. A., Machigov, E. A., Igonina, E. V., Zhoshibekova, B. S., & Abilev, S. K. (2021). Studying the Mechanism of Dioxidine Genotoxicity Using Lux Biosensors of Escherichia coli. Biology Bulletin, 48(12), 2174–2180. https://doi.org/10.1134/s1062359021120098

Sykes, J. E., & Weese, J. S. (2014). Infection Control Programs for Dogs and Cats. In Canine and Feline Infectious Diseases (pp. 105–118). Retrieved from https:sciencedirect.com/science/article/pii/B9781437707953000119

Taghadosi, R., Shakibaie, M. R., Ghanbarpour, R., & Hosseini-Nave, H. (2017). Role of antigen-43 on biofilm formation and horizontal antibiotic resistance gene transfer in non-O157 Shiga toxin producing Escherichia coli strains. 9(2), 89–96. Retrieved from https://europepmc.org/article/PMC/5715282

Tamber, S., Maier, E., Benz, R., & Hancock, R. E. W. (2007). Characterization of OpdH, a Pseudomonas aeruginosa Porin Involved in the Uptake of Tricarboxylates. J Bacteriol, 189(3), 929–939. https://doi.org/10.1128/jb.01296-06

Tawfik, A., Knight, P., Duckworth, C. A., Pritchard, D. M., Rhodes, J. M., & Campbell, B. J. (2019). Replication of Crohn's Disease Mucosal E. coli Isolates inside Macrophages Correlates with Resistance to Superoxide and Is Dependent on Macrophage NF-kappa B Activation. Pathogens, 8, 74. https://doi.org/10.3390/pathogens8020074

Taylor, P. K., Zhang, L., & Mah, T.-F. (2019). Loss of the Two-Component System TctD-TctE in Pseudomonas aeruginosa Affects Biofilm Formation and Aminoglycoside Susceptibility in Response to Citric Acid. MSphere, 4(2), e00102-19. https://doi.org/10.1128/msphere.00102-19

Thermo Fisher Scientific. (2021). Protein quantitation assay compatibility table. Retrieved October 5, 2022, from Thermo Fisher Scientific website: https://assets.thermofisher.com/TFS-Assets/LSG/Application-Notes/TR0068-Protein-assay-compatibility.pdf

Thermo Scientific. (2016, August). Dionex Integrion HPIC System Operator's Manual. Retrieved December 13, 2022, from ThermoFisher Scientific website: https://www.thermofisher.com/document-connect/document-connect.html?url=https://assets.thermofisher.com/TFS-Assets%2FCMD%2Fmanuals%2FMan-22153-97003-IC-Integrion-Man2215397003-EN.pdf

Thomen, P., Robert, J., Monmeyran, A., Bitbol, A.-F., Douarche, C., & Henry, N. (2017). Bacterial biofilm under flow: First a physical struggle to stay, then a matter of breathing. PLoS ONE, 12(4), e0175197. https://doi.org/10.1371/journal.pone.0175197

Thorolfsdottir, B., & Marteinsson, V. (2013). Microbiological Analysis in Three Diverse Natural Geothermal Bathing Pools in Iceland. Int J Environ Res Public Health, 10(3), 1085–1099. https://doi.org/10.3390/ijerph10031085

Tirodimos, I., Christoforidou, E. P., Nikolaidou, S., & Arvanitidou, M. (2018). Bacteriological quality of swimming pool and spa water in northern Greece during 2011–2016: is it time for Pseudomonas aeruginosa to be included in Greek regulation? Water Supply, 18(6), 1937–1945. https://doi.org/10.2166/ws.2018.015

Tocut, M., Zohar, I., Schwartz, O., Yossepowitch, O., & Maor, Y. (2022). Short- and long-term mortality in patients with urosepsis caused by Escherichia coli susceptible and resistant to 3rd generation cephalosporins. BMC Infect Dis, 22(1), 571. https://doi.org/10.1186/s12879-022-07538-5

Tong, C., Hu, H., Chen, G., Li, Z., Li, A., & Zhang, J. (2021). Chlorine disinfectants promote microbial resistance in Pseudomonas sp. Environmental Research, 199, 111296. https://doi.org/10.1016/j.envres.2021.111296

Townsley, L., & Yildiz, F. H. (2015). Temperature affects c-di-GMP signaling and biofilm formation inVibrio cholerae. Environ Microbiol, 17(11), 4290–4305. https://doi.org/10.1111/1462-2920.12799

Travnickova, E., Mikula, P., Oprsal, J., Bohacova, M., Kubac, L., Kimmer, D., … Bittner, M. (2019). Resazurin assay for assessment of antimicrobial properties of electrospun nanofiber filtration membranes. AMB Expr, 9(1), 183. https://doi.org/10.1186/s13568-019-0909-z

Unamuno, V. R., van de Plassche, E., & van der Wal, L. (2022). Biocides . In Biomedical Sciences. Retrieved from https://doi.org/10.1016/B978-0-12-824315-2.00115-9

van Dalen, R., Peschel, A., & van Sorge, N. M. (2020). Wall Teichoic Acid in Staphylococcus aureus Host Interaction. Trends in Microbiology, 28(12), 869. https://doi.org/10.1016/j.tim.2020.05.017

van der Kooij, D., Vrouwenvelder, J. S., & Veenendaal, H. R. (2003). Elucidation and control of biofilm formation processes in water treatment and distribution using the unified biofilm approach. Water Sci Technol, 47(5), 83–90. https://doi.org/10.2166/wst.2003.0287

Vanden Esschert, K. L., Mattioli, M. C., Hilborn, E. D., Roberts, V. A., Yu, A. T., Lamba, K., … Combes, S. M. (2020). Outbreaks Associated with Untreated Recreational Water — California, Maine, and Minnesota, 2018–2019. MMWR Morb. Mortal. Wkly. Rep., 69(25), 781–783. https://doi.org/10.15585/mmwr.mm6925a3

Veschetti, E., Cittadini, B., Maresca, D., Citti, G., & Ottaviani, M. (2005). Inorganic by-products in waters disinfected with chlorine dioxide. Microchemical Journal, 79(1–2), 165–170. https://doi.org/10.1016/j.microc.2004.10.017

Vilhena, C., Kaganovitch, E., Grünberger, A., Motz, M., Forné, I., Kohlheyer, D., & Jung, K. (2019). Importance of Pyruvate Sensing and Transport for the Resuscitation of Viable but Nonculturable Escherichia coli K-12. J Bacteriol, 201(3), e00610-18. https://doi.org/10.1128/jb.00610-18

Villanueva, C. M., Cantor, K. P., Cordier, S., Jaakkola, J. J. K., King, W. D., Lynch, C. F., … Kogevinas, M. (2004). Disinfection byproducts and bladder cancer: a pooled analysis. Epidemiology, 15(3), 357–367. https://doi.org/10.1097/01.ede.0000121380.02594.fc

Wahman, D. G. (2018). Chlorinated Cyanurates: Review of Water Chemistry and Associated Drinking Water Implications. J Am Water Works Assoc, 110(9), E1–E15. https://doi.org/10.1002/awwa.1086

Wahman, D. G., Alexander, M. T., & Dugan, A. G. (2019). Chlorinated cyanurates in drinking water: Measurement bias, stability, and disinfectant byproduct formation. AWWA Wat Sci, 1(2). https://doi.org/10.1002/aws2.1133

Waldow, F., Kohler, T. P., Hess, N., Schwudke, D., Hammerschmidt, S., & Gisch, N. (2018). Attachment of phosphorylcholine residues to pneumococcal teichoic acids and modification of substitution patterns by the phosphorylcholine esterase. Journal of Biological Chemistry, 293(27), 10620–10629. https://doi.org/10.1074/jbc.ra118.003360

Wandersman, C., & Delepelaire, P. (2012). Haemophore functions revisited. Molecular Microbiology, 85(4), 618–631. https://doi.org/10.1111/j.1365-2958.2012.08136.x

Wang, F., & Li, D. (2022). Role of bacterial flagella in bacterial adhesion of Escherichia coli to glass surface. Journal of Emerging Investigators. Retrieved from https://emerginginvestigators.org/articles/role-of-bacterial-flagella-in-bacterial-adhesion-of-em-escherichia-coli-em-to-glass-surface

Wang, H., Hasani, M., Wu, F., Prosser, R., MacHado, G. B., & Warriner, K. (2022). Hydroxyl-radical activated water for inactivation of Escherichia coli O157:H7, Salmonella and Listeria monocytogenes on germinating mung beans. International Journal of Food Microbiology, 367, 109587. https://doi.org/10.1016/j.ijfoodmicro.2022.109587

Wang, W., Wang, H., Li, G., An, T., Zhao, H., & Wong, P. K. (2019). Catalyst-free activation of persulfate by visible light for water disinfection: Efficiency and mechanisms. Water Research, 157, 106–118. https://doi.org/10.1016/j.watres.2019.03.071

Wang, X., & Zhao, X. (2009). Contribution of Oxidative Damage to Antimicrobial Lethality. Antimicrob Agents Chemother, 53(4), 1395–1402. https://doi.org/10.1128/aac.01087-08

Warren, C. R. (2008). Rapid Measurement of Chlorophylls with a Microplate Reader. Journal of Plant Nutrition, 31(7), 1321–1332. https://doi.org/10.1080/01904160802135092

Water Science School. (2018, August 7). Alkalinity And Water. Retrieved December 13, 2022, from U.S. Geological Survey website: https://www.usgs.gov/special-topics/water-science-school/science/alkalinity-and-water

Weisel, C. P., Richardson, S. D., Nemery, B., Aggazzotti, G., Baraldi, E., Blatchley, E. R., … Frimmel, F. H. (2009). Childhood Asthma and Environmental Exposures at Swimming Pools: State of the Science and Research Recommendations. Environ Health Perspect, 117(4), 500–507. https://doi.org/10.1289/ehp.11513

White-Ziegler, C. A., Um, S., Pérez, N. M., Berns, A. L., Malhowski, A. J., & Young, S. (2008). Low temperature (23 °C) increases expression of biofilm-, cold-shock- and RpoS-dependent genes in Escherichia coli K-12. Microbiology, 154(1), 148–166. https://doi.org/10.1099/mic.0.2007/012021-0

Wilton, M., Charron-Mazenod, L., Moore, R., & Lewenza, S. (2016). Extracellular DNA Acidifies Biofilms and Induces Aminoglycoside Resistance in Pseudomonas aeruginosa. Antimicrobial Agents and Chemotherapy, 60(1), 544–553. https://doi.org/10.1128/aac.01650-15

Wordofa, D. N., Walker, S. L., & Liu, H. (2017). Sulfate Radical-Induced Disinfection of Pathogenic Escherichia coli O157:H7 via Iron-Activated Persulfate. Environ. Sci. Technol. Lett., 4(4), 154–160. https://doi.org/10.1021/acs.estlett.7b00035

Wu, C., Lim, J. Y., Fuller, G. G., & Cegelski, L. (2013). Disruption of Escherichia coli Amyloid-Integrated Biofilm Formation at the Air–Liquid Interface by a Polysorbate Surfactant. Langmuir, 29(3), 920–926. https://doi.org/10.1021/la304710k

Xu, H., Qu, F., Xu, H., Lai, W., Andrew Wang, Y., Aguilar, Z. P., & Wei, H. (2012). Role of reactive oxygen species in the antibacterial mechanism of silver nanoparticles on Escherichia coli O157:H7. Biometals, 25(1), 45–53. https://doi.org/10.1007/s10534-011-9482-x

Xu, X., Ran, Z., Wen, G., Liang, Z., Wan, Q., Chen, Z., … Huang, T. (2020). Efficient inactivation of bacteria in ballast water by adding potassium peroxymonosulfate alone: Role of halide ions. Chemosphere, 253, 126656. https://doi.org/10.1016/j.chemosphere.2020.126656

Xu, Y., Zhao, Z., Tong, W., Ding, Y., Liu, B., Shi, Y., … Wang, Y. (2020). An acid-tolerance response system protecting exponentially growing Escherichia coli. Nat Commun, 11(1), 1496. https://doi.org/10.1038/s41467-020-15350-5

Yang, J., Zhang, J., Zhu, Z., Jiang, X., Zheng, T., & Du, G. (2022). Revealing novel synergistic defense and acid tolerant performance of Escherichia coli in response to organic acid stimulation. Appl Microbiol Biotechnol, 106, 7577–7594. https://doi.org/10.1007/s00253-022-12241-1

Yang, Q., Schultz, G. S., & Gibson, D. J. (2018). A Surfactant-Based Dressing to Treat and Prevent Acinetobacter baumannii Biofilms. Journal of Burn Care & Research, 39(5), 766–770. https://doi.org/10.1093/jbcr/irx041

Yoshikawa, T. T., Norman, D. C., & Grahn, D. (1985). Infections in the Aging Population. J Am Geriatr Soc, 33(7), 496–503. https://doi.org/10.1111/j.1532-5415.1985.tb05463.x

Yossan, S., Reungsang, A., & Yasuda, M. (2006). Purification and Characterization of Alkaline Protease from Bacillus megaterium Isolated from Thai Fish Sauce Fermentation Process. ScienceAsia, 32, 377–383. https://doi.org/10.2306/scienceasia1513-1874.2006.32.377

Yu, K., Zhang, Y., Xu, W., Zhang, X., Xu, Y., Sun, Y., … Cao, J. (2020). Hyper-expression of the efflux pump gene adeB was found in Acinetobacter baumannii with decreased triclosan susceptibility. Journal of Global Antimicrobial Resistance, 22, 367–373. https://doi.org/10.1016/j.jgar.2020.02.027

Yu, S., Su, T., Wu, H., Liu, S., Wang, D., Zhao, T., … Chua, S. L. (2015). PslG, a self-produced glycosyl hydrolase, triggers biofilm disassembly by disrupting exopolysaccharide matrix. Cell Res, 25(12), 1352–1367. https://doi.org/10.1038/cr.2015.129

Yu, Y., Cheng, A. S., Wang, L., Dunne, W. M., & Bayliss, S. J. (2007). Hot tub folliculitis or hot hand–foot syndrome caused by Pseudomonas aeruginosa. Journal of the American Academy of Dermatology, 57(4), 596–600. https://doi.org/10.1016/j.jaad.2007.04.004

Zeng, Q., Zhou, B., He, D.-L., Wang, Y.-X., Wang, M., Yang, P., … Lu, W.-Q. (2016). Joint effects of trihalomethanes and trichloroacetic acid on semen quality: A population-based cross-sectional study in China. Environmental Pollution, 212, 544–549. https://doi.org/10.1016/j.envpol.2016.02.032

Zeng, W., Xu, W., Xu, Y., Liao, W., Zhao, Y., Zheng, X., … Cao, J. (2020). Overexpression of target enzyme gene fabI and efflux pump decrease triclosan susceptibility in Escherichia coli. Research Square. https://doi.org/10.21203/rs.2.21275/v1

Zhang, D.-F., Li, H., Lin, X.-M., Wang, S.-Y., & Peng, X.-X. (2011). Characterization of Outer Membrane Proteins of Escherichia Coli in Response to Phenol Stress. Curr Microbiol, 62(3), 777–783. https://doi.org/10.1007/s00284-010-9786-z

Zhang, L., Li, J., Liang, J., Zhang, Z., Wei, Q., & Wang, K. (2020). The effect of Cyclic-di-GMP on biofilm formation by Pseudomonas aeruginosa in a novel empyema model. Ann Transl Med, 8(18), 1146. https://doi.org/10.21037/atm-20-6022

Zhang, R., Zhao, J., Han, G., Liu, Z., Liu, C., Zhang, C., … Zhao, T. (2016). Real-Time Discrimination and Versatile Profiling of Spontaneous Reactive Oxygen Species in Living Organisms with a Single Fluorescent Probe. J. Am. Chem. Soc., 138(11), 3769–3778. https://doi.org/10.1021/jacs.5b12848

Zhang, W., Wu, J., Xiao, J., Zhu, M., & Yang, H. (2022). Compatibility and Washing Performance of Compound Protease Detergent. Applied Sciences, 12(1), 150. https://doi.org/10.3390/app12010150

Zhao, T., Zhang, Y., Wu, H., Wang, D., Chen, Y., Zhu, M.-J., & Ma, L. Z. (2018). Extracellular aminopeptidase modulates biofilm development ofPseudomonas aeruginosaby affecting matrix exopolysaccharide and bacterial cell death. Environmental Microbiology Reports, 10(5), 583–593. https://doi.org/10.1111/1758-2229.12682

Zhao, Y., Lin, Q., Liu, L., Ma, R., Chen, J., Shen, Y., … Han, M. (2020). Risk Factors and Outcomes of Antibiotic-resistant Pseudomonas aeruginosa Bloodstream Infection in Adult Patients With Acute Leukemia. Clin Infect Dis, 71(Supplement_4), S386–S393. https://doi.org/10.1093/cid/ciaa1522

Zhou, F., Wang, D., Hu, J., Zhang, Y., Tan, B. K., & Lin, S. (2022). Control Measurements of Escherichia coli Biofilm: A Review. Foods, 11(16), 2469. https://doi.org/10.3390/foods11162469

Zhou, L., Yang, X., Ji, Y., & Wei, J. (2019). Sulfate radical-based oxidation of the antibiotics sulfamethoxazole, sulfisoxazole, sulfathiazole, and sulfamethizole: The role of five-membered heterocyclic rings. Science of The Total Environment, 692, 201–208. https://doi.org/10.1016/j.scitotenv.2019.07.259